December 2020

The Role of Cerebellar Structural Plasticity and Astrocytic Activity in Motor-Skill Learning

Morgan Stevenson
University of Wisconsin-Milwaukee

THE ROLE OF CEREBELLAR STRUCTURAL PLASTICITY AND ASTROCYTIC ACTIVITY IN MOTOR-SKILL LEARNING

by

Morgan E. Stevenson

A Dissertation Submitted in

Partial Fulfillment of the

Requirements for the Degree of

Doctor of Philosophy

in Psychology

at

The University of Wisconsin-Milwaukee

December 2020

ABSTRACT

THE ROLE OF CEREBELLAR STRUCTRAL PLASTICITY AND ASTROCYTIC ACTIVITY IN MOTOR-SKILL LEARNING

by

Morgan Stevenson

The University of Wisconsin-Milwaukee, 2020
Under the Supervision of Rodney Swain

Motor-skill learning is associated with cerebellar synaptogenesis and astrocytic hypertrophy, but most of these assessments of cerebellar ultrastructure have been completed after one month of training. After one month of training, the motor-skills necessary to complete these tasks have been acquired for weeks. Furthermore, the contributions of cerebellar astrocytes to motor-skill learning remains largely unexamined. The first experiment of this dissertation aimed to characterize cerebellar ultrastructure during the acquisition phase of motor-skill learning, at a point when motor performance is still improving. The second experiment aimed to examine the contributions of cerebellar astrocytes to motor-skill learning by activating astrocytic Gi-signaling during acrobatic training and then assessing its impact on behavior and cerebellar ultrastructure. In both experiments, male and female rats trained for four days on the acrobatic motor learning task, which involved traversing challenging obstacles such as narrow beams and ladders. Concurrently, rats in the motor control condition walked a flat alleyway requiring no skilled movements. After training was complete, all rats were euthanized, and tissue was prepared for electron microscopy. Unbiased stereology techniques were used to assess synaptic and astrocytic plasticity. The first experiment revealed that female rats made fewer errors and had shorter

latencies on the acrobatic course compared to male rats. Male and female rats that completed four days of acrobatic training both displayed an increase in the density of parallel fiber-Purkinje cell synapses per Purkinje cell and an increase in astrocytic volume, relative to rats in the motor control group. The second experiment where the rats that trained on the acrobatic course expressed either an astrocytic mCherry control virus or hM4Di DREADD virus revealed that activation of Gi-signaling during acrobatic training increased the number of missteps per trial and the latency to complete trials on the acrobatic course. Further motor performance testing indicated a motor coordination, rather than a motor learning deficit, is likely driving this behavioral effect. In addition, activation of astrocytic hM4Di DREADDs increased synaptogenesis and astrocyte volume independent of motor-skill learning. These experiments find that cerebellar plasticity happens rapidly following motor-skill learning and highlight the role of cerebellar astrocytes, a relatively understudied cell population, in motor behavior.

TABLE OF CONTENTS

LIST OF FIGURES

ACKNOWLEDGEMENTS

I want to express gratitude to my advisor, Dr. Rodney Swain, for his mentorship. I thank him for his guidance and for fostering independence during my time in his lab. I also thank my dissertation committee members: Drs. Karyn Frick, Fred Helmstetter, Shama Mizra, and Heather Owen. I appreciate the time my advisor and committee members invested in helping me become a better scientist. The time spent with all of them discussing presentations, writing, methodology, and data interpretation was invaluable. I thank Drs. Shama Mirza and Heather Owen for teaching me MALDI mass spectrometry and electron microscopy, respectively. It was a privilege to work closely and learn from both of them.

I next thank the members of the UWM Psychology Department for their scientific discussions and friendship. Work lunches with Lisa Taxier, Hanna Yousuf, Sydney Trask, and Amanda Nazario were a joy and morale booster. I am grateful to Lisa Taxier for sharing her technical expertise and for her enthusiastic discussions about astrocytes and this dissertation. I also recognize Hanna Yousuf for the hours she spent helping with sample preparation for a related calcium imaging experiment. I thank Amanda Nazario and the Swain lab undergraduate research assistants, Alicja Czyz, Brittany Larson, Elpiniki Tianis, and Yael Greenberg, for their help with behavioral training. I especially want to thank research assistant Alicja Czyz for her leadership and dedication to data collection and quantification for this dissertation. I am also grateful to the attendees of Glia Journal Group. I enjoyed our stimulating monthly discussions about the latest glial research. I also acknowledge Pat Reilly for his technical assistance and speedy repairs of equipment that malfunctioned.

I also thank my family and friends for their support throughout this graduate program. My parents and grandparents showed me the value of determination, service, and kindness. I

thank my husband Michael for his constant love and encouragement, and for always keeping me grounded. I am also grateful to Mickey, Nick, Meredith, and Ryan, for their years of friendship and good humor.

Chapter One: Introduction

The cerebellum has been traditionally viewed as a structure important for motor coordination, but in recent decades its contributions to numerous non-motor tasks, ranging from spatial learning to social behavior, have been demonstrated (Koziol et al., 2014; Stoodley, 2012; Stoodley et al., 2017). The simple, repetitive anatomical organization of the cerebellum makes it easy to presume the structure is functionally homogenous. However, vast functional differences exist within and between cerebellar lobules, with different zones of the cerebellum receiving input from unique forebrain regions such as the primary motor cortex, somatosensory cortex, hippocampus, and basal ganglia. Consecutively, the cerebellum sends output, via the deep cerebellar nuclei, back to these same regions of the forebrain forming closed-loop circuits (Bostan et al., 2013; Clower et al., 2001; Coffman et al., 2011; Middleton & Strick, 1997). Recent chemogenetic and optogenetic techniques have been used to reveal that the cerebellum is a crucial hub in many of these circuits, and the manipulation of cerebellar activity disrupts motor and non-motor functions (Carta et al., 2019; Deverett et al., 2019; Sasaki et al., 2012; Shipman & Green, 2019; Stoodley et al., 2017). Nevertheless, a longstanding view is that the cerebellum supports motor learning— the acquisition of new motor-skills through repetition or experience. One lobule particularly implicated in motor-skill learning is the cerebellar paramedian lobule (PML). The PML displays robust structural plasticity that includes synaptogenesis and astrocytic hypertrophy following the acquisition of new motor-skills (Black et al., 1990; Federmeier et al., 2002; Isaacs et al., 1992; Kleim et al., 1997; Kleim et al., 2007). However, how rapidly these structural changes occur and whether this plasticity contributes to task performance is unknown. Of particular interest is the contribution of cerebellar astrocytes to motor-skill learning, as the

role of cerebellar astrocytes in any behavior remains largely uninvestigated. This dissertation aimed to address these deficits by 1) characterizing structural plasticity in the PML during the early phases of motor-skill learning and 2) using chemogenetic techniques to determine how disruption of astrocytic activity in the PML during motor-skill learning affects task performance and the structural plasticity that typically accompanies motor-skill learning.

Cerebellar Anatomy and Circuitry

Since examined by anatomist Vesalius in the 1500's, the cerebellum has been viewed as a distinct subregion of the brain, with the name cerebellum itself meaning "little brain" in Latin. The cerebellum, sitting dorsal to the brainstem, makes up a sizable portion of the hindbrain and is linked to the brainstem by three peduncles: superior, middle, and inferior (Glickstein & Doron, 2008; Glickstein et al., 2009). The middle and inferior cerebellar peduncles are afferent channels to the cerebellum, and the superior peduncle is the primary efferent channel from the cerebellum (Glickstein & Doron, 2008; Palay & Chan-Palay, 1974).

The cerebellum has been anatomically characterized at differing levels of detail. Grossly, the outer, gray matter, region of the cerebellum is the cerebellar cortex. The cerebellar cortex is composed of ten lobules, delineated I-X, and is the site where the largest source of cerebellar inputs terminate (Schmahmann, 2000; Stoodley & Schmahmann, 2010). These lobules have been further categorized into three lobes: anterior (lobules I-V), posterior (lobules VI-IX), and flocculonodular (lobule X; flocculus; Stoodley & Schmahmann, 2010). Structurally separate from the rest of the cerebellum, the flocculonodular lobe is phylogenetically the oldest lobe of the cerebellum. It serves as a key node in the vestibular system, receiving input from the vestibular nerve, and sending direct projections to synapse with the vestibular nuclear complex in

the brainstem. Functionally, the flocculonodular lobe is considered part of the vestibulocerebellum (Voogd et al., 1996).

With the exception of the flocculus, all other lobules of the cerebellar cortex send white matter tracts to the deep cerebellar nuclei, and the deep nuclei operate as the sole cerebellar output (Zhang, et al., 2016). The cerebellum has medial, intermediate, and lateral longitudinal zones, and the lobules within these zones primarily send projections to one of these three deep cerebellar nuclei (Coffman et al., 2011; Jansen & Brodal, 1940). The medial zone, the area of the cerebellum nearest the midline, consists of the cerebellar vermis. Vermal lobules project to the fastigial nucleus. The intermediate zone, which flanks the cerebellar vermis, contains the paravermal cortex. The paravermis innervates the interpositus nucleus. Traditionally, the vermis and paravermis were functionally classified as the spinocerebellum, because they largely receive somatosensory input from the ascending spinal cord (Piergiorgio Strata, Provini, & Redman, 2012). However, in recent decades, it has become clear that the vermis also receives cortical input, and the strict spinocerebellum classification has been questioned (Coffman et al., 2011; Piergiorgio Strata et al., 2012; Zhang et al., 2016). The lateral zone of the cerebellum consists of the larger cerebellar hemispheres, which predominantly send projections to the dentate nucleus (Schmahmann, 2000; Stoodley & Schmahmann, 2010). Functionally, the cerebellar hemispheres are considered part of the cerebrocerebellum, because their major source of input is from the cerebral cortex. The lateral cerebellar hemispheres are also referred to as the neocerebellum, because, evolutionarily, the cerebellar hemispheres expanded massively in humans, paralleling the enlargement of the cerebral cortex (Larsell & Jansen, 1972; Whiting & Barton, 2003).

The cells of the cerebellar cortex are arranged in a simple, monotonous scheme, which is repeated throughout all of the cerebellar lobules. Golgi and Cajal are credited for first defining

the cellular network of the cerebellar cortex (Glickstein et al., 2009; Palay & Chan-Palay, 1974). Cells are arranged in three layers: granule, Purkinje, and molecular. The innermost granule cell layer contains densely packed granule cells, which are the most numerous type of neuron in the central nervous system (Harvey & Napper, 1988). Granule cells are glutamatergic and they are innervated by excitatory mossy fibers. These mossy fibers provide sensory information to the cerebellar cortex and originate mainly from nuclei in the brainstem, including the pontine nuclei, and the spinal cord (Glickstein & Doron, 2008). The second type of neuron in the granule cell layer is the more sparsely distributed Golgi cell. Golgi cells are GABAergic interneurons that modulate granule cell activity (D'Angelo et al., 2013). Astrocytes are also numerous in the granule cell layer and have been classified as standard protoplasmic astrocytes, similar to those present in the gray matter of the cerebral cortex (Hoogland & Kuhn, 2010). The middle layer of the cerebellar cortex is the Purkinje cell layer. Purkinje cells, one of the largest neurons in the brain, serve as the lone output of the cerebellar cortex. They innervate the deep cerebellar nuclei, providing GABAergic input that inhibits deep cerebellar nuclei activity. The soma of the Purkinje cells form a single layer, but these cells have long, extensive, spiny dendrites that extend through the molecular layer and reach the surface of the cerebellar cortex (De Camilli et al., 1984; Voogd & Glickstein, 1998). The molecular layer is the outermost layer of the cerebellar cortex. Bergmann glia, a specialized form of radial astrocyte, have long, unipolar radial processes that also extend through the entire molecular layer. These processes are closely entwined with the Purkinje cell dendrites. Like Purkinje cells, Bergmann glial cell bodies are contained in the Purkinje cell layer (Hoogland & Kuhn, 2010). In the molecular layer, Purkinje cell dendrites are predominantly innervated by two fibers: parallel fibers and climbing fibers. Parallel fiber input comes from granule cell axons that ascend into the molecular layer. They

relay excitatory, mossy fiber input to the Purkinje cells. They are termed parallel fibers because when the granule cell axons reach the molecular layer, they bifurcate and form two fibers that run perpendicular to the distal Purkinje cell dendrites (Bloedel & Bracha, 1998; Hansel et al., 2001; Jörntell & Hansel, 2006). It is estimated that a single mossy fiber innervates approximately 150,000 Purkinje cells, and that each Purkinje cell receives input from about 175,000 parallel fibers in the rat cerebellum (Harvey & Napper, 1988; Hoxha et al., 2016). Parallel fibers innervate inhibitory interneurons, including the Golgi cells in the granule cell layer, and stellate and basket cells in the molecular cell layer. Basket and stellate cells terminate on Purkinje cell dendritic spines, modulating Purkinje cell activity (Barmack & Yakhnitsa, 2008; Consalez & Hawkes, 2013; Leto et al., 2006; Sotelo, 2015). The second major source of input to the Purkinje cell comes from excitatory climbing fibers, which originate in the inferior olive (Llinas et al., 1975). In stark contrast to parallel fiber input, the Purkinje cell only receives input from one climbing fiber. However, each climbing fiber wraps around the entire Purkinje cell dendritic tree, making more than 1,000 synaptic connections per Purkinje cell (Palay & Chan-Palay, 1974). Climbing fiber input is also more direct, relative to parallel fibers whose input first requires excitation of granule cells (Palay & Chan-Palay, 1974; Strata & Rossi, 1998). The Purkinje cell is consistently highlighted within the cerebellar cortex circuit, because it is the site where inputs converge, are integrated, and then relayed to the deep cerebellar nuclei. The deep cerebellar nuclei incorporate information from Purkinje cell projections and send cerebellar output mainly to the red nucleus or the thalamus (Baumel et al., 2009).

Cerebellar projections to the nuclei of the thalamus form disynaptic connections with areas of the cerebral cortex, including the primary motor cortex, premotor cortex, prefrontal cortex, and parietal cortex (Bostan et al., 2013; Clower et al., 2001; Middleton & Strick, 1994,

1997, 1998, 2001). Closed loop, cortico-cerebellar circuits are formed by these cortical regions sending projections back to the cerebellar cortex, largely via the pontine nuclei (Ishikawa et al., 2016). Thus far, of all the regions that have been investigated, all areas of the cerebral cortex that send projections to the cerebellum are also the targets of cerebellar efferents (Bostan et al., 2013). The cerebellum also sends projections to the basal ganglia, via discrete thalamic nuclei, and the basal ganglia sends information back to the cerebellum through the pontine nuclei (Bostan et al., 2010; Bostan et al., 2013; Clower et al., 2001; Hoshi et al., 2005). Cerebellar input terminating in the red nucleus is relayed down the spinal cord, through the rubrospinal tract, and information from the red nucleus is transmitted back to the cerebellum via the inferior olive and climbing fiber pathway (Burman, Darian-Smith, & Darian-Smith, 2000; Zeeuw et al., 1998; Eccles et al., 1967; Flumerfelt et al., 1973).

It should also be noted that, in addition to the broad medial, intermediate, and lateral zones described previously, additional, longitudinal, Purkinje cell modules, or zones, have been identified (Voogd & Ruigrok, 1997). Although the significance of these zones has not been entirely determined, Voogd and Ruigrok (1997) suggest that these longitudinal zones can be used to further describe the function and organization of the cerebellar cortex, and initially classified these zones as A, B, C, and D (Voogd, 1969; Voogd, 2014; Voogd & Bigare, 1980; Voogd & Ruigrok, 1997). These classifications have been further divided into microzones, totaling seven modular Purkinje cell microzones: A, B, C1, C2, C3, D1, D2, and Y in each hemisphere of the rat cerebellum (Voogd, 2014). Microzones A and B are vermal and project to the fastigial nucleus, microzones C1-C3 and Y terminate in the interpositus nucleus, and D1 and D2 microzones send afferents to the dentate nucleus (Apps et al., 2018). Furthermore, each of these Purkinje cell microzones projects to distinct regions within the deep cerebellar nuclei (Apps et

al., 2018). Regarding input, these Purkinje cell microzones receive climbing fiber projections from specific areas of the inferior olive (Courville et al., 1974; Voogd, 1969), and mossy fiber input shows a similar pattern, although clear zonal organization is less apparent (Pijpers et al., 2006). Therefore, to some degree, all input and output of the cerebellar cortex follows this modular, zonal patterning.

These Purkinje cell microzones are either zebrin-positive or zebrin-negative. Zebrin-II, also named aldolase C, is a glycolytic enzyme expressed by a subset of Purkinje cells in the vertebrate cerebellum (Albergaria & Carey, 2014; De Camilli et al., 1984). When immunohistochemical labeling for zebrin-II is completed, clear parasagittal stripes are apparent throughout the cerebellar cortex, indicating biochemical differences between the microzones (Hawkes & Herrup, 1995; Voogd et al., 2003). In the cerebellar cortex, microzones C1, C3, and Y zones are zebrin-negative, and zones C2, D1, and D2 are zebrin-positive. Despite the fact that clear physiological differences exist between the zebrin-positive and negative microzones (Albergaria & Carey, 2014; Graham & Wylie, 2012; Hawkes & Herrup, 1995; Pijpers et al., 2006; Voogd, 2014; Voogd & Glickstein, 1998; Voogd et al., 2003; Zhou et al., 2014), zebrin enzymatic activity itself has not yet been related to the zonal differences in physiology (Zhou et al., 2014). Purkinje cells show different firing patterns within zebrin-positive and negative microzones, with Purkinje cells in zebrin-negative zones firing more simple and complex spikes than those in zebrin-positive zones (Zhou et al., 2014). Zhou et al. (2014) suggest that this difference may be due to the intrinsic properties of the Purkinje cells themselves, rather than related to differences in the input sources between the microzones. The role of these different microzones in governing aspects of behavior is generally unknown.

Cerebellar Involvement in Motor and Cognitive Functions

Historically, the cerebellum was viewed as a motor structure, supporting coordinated movement through the integration of sensory information from the external environment and motor commands from higher cortical regions (Mauk, Medina, Nores, & Ohyama, 2000; Zang & De Schutter, 2019). This theory was based on observations that cerebellar damage produced pronounced motor impairments. Patients with cerebellar damage could still execute movements, but these movements were often uncoordinated and temporally erratic (Ito, 2002; Ito, 1984; Strata, 2009). In addition to its broad involvement in motor control, a cerebellar model for motor-skill learning was established in the 1960s. Based on Hebbian principles, Marr (1969) and Albus (1971) generated the first theory of cerebellar motor learning, which stated learning occurred through long-term potentiation (LTP; Marr, 1969) or long-term depression (LTD; Albus, 1971) of parallel fiber-Purkinje cell synapses. Albus (1971) hypothesized that LTD, or the weakening of the parallel fiber-Purkinje cell synapses, was caused by strong, concurrent activation of climbing fibers. The strong climbing fiber input was thought to provide performance error signals that eventually led to motor learning. Ito and Kano (1982) later demonstrated this theory experimentally by stimulating both parallel and climbing fibers, at the same time, in the rabbit cerebellar cortex. This conjunctive stimulation produced LTD of parallel fiber-Purkinje cell synapses and supported the Marr-Albus theory of cerebellar motor learning.

Although the Marr-Albus theory is the dominant cerebellar learning theory, it has been both challenged and expanded upon since its inception. In addition to LTD identification at parallel fiber-Purkinje cell synapses, LTP has also been induced at these synapses (Coesmans et al., 2004; Hansel et al., 2001; Lev-Ram et al., 2002). Interestingly, a blockade of Purkinje cell LTP disrupts motor learning (Schonewille et al., 2010), but a blockade of Purkinje cell LTD does

not impact motor-skill acquisition on an array of motor tasks (Martijn Schonewille et al., 2011). Silencing cerebellar granule cells, which provide major input to the Purkinje cells, impairs parallel fiber- Purkinje cell LTP and LTD without affecting overall motor performance. However, motor learning and memory consolidation were impaired on demanding motor tasks such as running on a rotarod that was accelerated at an extremely rapid rate (Galliano et al., 2013).These findings counter the original Marr-Albus model only emphasizing LTD, and has shifted focus towards also understanding the importance of LTP in cerebellar motor learning (Grasselli & Hansel, 2014). It was recently found that the default response to parallel fiber stimulation is LTP, regardless of whether or not the parallel fiber is stimulated alone or with a climbing fiber. However, when internal Purkinje cell calcium increases to a level that activates Ca^{2+}/calmodulin-dependent protein kinase II (CaMKII), an extracellular signal-regulated kinase (ERK)-based feedback loop is activated that instead produces LTD (Gallimore et al., 2018).

There are a number of theories, with no general consensus, describing the contributions of cerebellar circuitry and processing to motor learning, control, and coordination (Manto et al., 2012). Briefly, one theory is that the cerebellum regulates movement timing, making temporally predictive computations that are essential for the production of coordinated movements (Ivry, 1997; Ivry & Keele, 1989). It has also been hypothesized that the cerebellum is an area that synchronizes sensorimotor information, and this results in the precise temporal execution of movements (van der Steen et al., 2015). Another leading theory is that the cerebellum generates forward models, used to predict the sensory outcomes of voluntary movements (Ishikawa et al., 2016; Kawato, 1999; Miall & Wolpert, 1996; Stein, 2009). This internal model can be used to rapidly and accurately predict whether a movement will achieve the intended goal, prior to the generation of the movement. Once the movement has occurred, the model is updated by

comparing predictions with outcomes (Stein, 2009). Others instead view the cerebellum as a structure essential for monitoring and modulating sensory data acquisition. They posit the cerebellum itself is not directly responsible for any particular behavioral function, but rather ensures other regions of the brain receive the most accurate sensory information, allowing for optimal task performance (Bower, 1997; Gao et al., 1996).

The many theories of cerebellar function have been expanded to apply not only to motor behavior, but also to cognition. Originally, the cerebellum was thought to receive input from an array of cortical regions, which included projections from all lobes of the cerebral cortex. The cerebellum processed this input, and cerebellar output to the cerebral cortex was directed to the primary motor cortex exclusively, where this information facilitated movement production (Bostan et al., 2013). This view was modified after it became clear that the cerebellar dentate nucleus sends disynaptic efferents to numerous areas of the cerebral cortex, including non-motor regions like the prefrontal cortex (Middleton & Strick, 2001). Strick and colleagues are credited for this discovery, which they made using transneuronal, antero- and retrograde tracing methods to explore cerebro-cerebellar circuitry in primates (Bostan et al., 2013; Clower et al., 2001; Kelly & Strick, 2003; Lynch et al., 1994; Middleton & Strick, 1994, 1997, 1998, 2001; Strick et al., 2009). The dentate nucleus has been the main focus of efforts to understand cerebellar motor and non-motor circuits, and Strick and colleagues have found that the dentate nucleus is structurally organized into a dorsal motor portion and ventral non-motor portion that comprises nearly 40% of the structure (Dum et al., 2002). Based on the large area of the dentate nucleus dedicated to non-motor projections, the role of the dentate nucleus in non-motor behavior likely equates to its contribution to motor behavior (Bostan et al., 2013).

The cortical targets of the dentate nucleus have been most examined but are still not fully characterized. However, it is known that projections from the dentate nucleus form closed-loop, cerebello-thalamo-cerebro-cortical circuits (CTCCs) with the parietal, prefrontal, and oculomotor regions, in addition to subcortical circuits with the basal ganglia (Bostan et al., 2013; Clower et al., 2001; Middleton & Strick, 1994, 1997, 1998, 2001). This vast cortical and subcortical circuitry suggests that the dentate nucleus modulates more than movement. Cortical targets of the interpositus and fastigial nuclei are not well established, but preliminary studies support a role of these deep nuclei in cognitive functions. Using tracing methods, it was found that the posterior interpositus nucleus is disynaptically connected with area 46 of the prefrontal cortex, in addition to the primary motor cortex. The anterior portion of the interpositus nucleus had only motor channels that formed circuits with the primary motor cortex (Lu et al., 2012). This anatomical organization appears to be similar to that of the dentate nucleus, where somewhat discrete motor and non-motor domains exist within the nucleus (Dum et al., 2002; Lu et al., 2012). Both the interpositus and fastigial nuclei project to the basal ganglia, but connectivity was less substantial compared to the dentate nucleus (Hoshi et al., 2005). Beyond the primary motor cortex, few cortical CTCCs that involve the fastigial nucleus have been identified. However, the fastigial nucleus provides disynpatic input to the limbic system, including the hippocampus, amygdala, and septum (Harper & Heath, 1973; Heath & Harper, 1974). Connectivity with these non-motor areas suggests that the fastigial nucleus may modulate emotion (Zhang et al., 2016).

The examination of the role of cerebellum in higher-order cognition is rapidly growing. Beyond anatomical descriptions, there is experimental and clinical evidence that the cerebellum contributes to non-motor functions. Some of the earliest proponents for a cerebellar role in cognition were Schmahmann (1991; 1997) and Andreason (1998). The basis for this concept lies

in their work with cerebellar pathology patients and neuroimaging. Schmahmann (1991) devised the dysmetria of thought theory, which states that the movement deficits that occur due to cerebellar damage similarly impact cognitive and emotional processing, producing erratic thoughts, emotions, and behaviors. Patients with cerebellar damage can exhibit cognitive impairments, in addition to, or instead of, motor deficits. This condition has been termed cerebellar cognitive affective syndrome, and symptoms include impaired language, working memory, and spatial navigation, in addition to emotional dysfunction (Schmahmann et al., 2009; Schmahmann & Sherman, 1998; Schmahmann, 1998, 2000; Stoodley & Schmahmann, 2010; Stoodley et al., 2012). Similarly, Andreason and Pierson (2008) postulate that the cerebellum synchronizes sequences of thoughts, providing feedback to the cerebral cortex through the CTCC pathways through mechanisms that mirror its contributions to movement coordination. By studying patients with schizophrenia, Andreason and colleagues find this disease produces dysmetria of both movement and cognition, characterized by difficulties organizing movements and thoughts (Andreasen et al.,1998; Andreasen & Pierson, 2008; Parker et al., 2014). Furthermore, patients with schizophrenia show volume decreases in the cerebellum (Nopoulos et al., 1999; Okugawa et al., 2003), decreased cerebellar blood flow during semantic and episodic memory tasks (Andreasen et al., 1999; Andreasen et al., 1995a; Andreasen et al., 1995b), and diffusor tensor imaging (DTI) revealed white matter tracts between the cerebellum and thalamus have decreased fiber anisotropy (Magnotta et al., 2008). It should be noted that autism, another condition depicted by disrupted motor control and cognition, is also associated with cerebellar anatomical malformations, including decreased Purkinje cell size (Fatemi et al., 2002), Purkinje cell counts (Ciesielski et al., 1997; Ritvo et al., 1986), and overall cerebellar volume (Courchesne et al., 1988; D'Mello et al., 2015). Although causal relationships cannot be gleaned

from much of this evidence, cerebellar anatomical abnormalities or damage are present in states that disrupt both movement and cognition.

Neuroimaging experiments reveal that areas of the cerebellum are engaged in higher-order cognitive tasks that involve spatial processing, task switching, language, and working memory, even when the motor aspects of the task are controlled for (Schmahmann et al., 2009; Stoodley, 2012; Stoodley et al., 2012). A recent experiment showed that resting cerebellar activity consistently lagged behind cortical activity by hundreds of milliseconds, especially in association networks like the default mode and frontoparietal networks (Marek et al., 2018). This not only suggests cerebellar involvement in motion and cognition, but also speaks to what may generally be the function of the cerebellum: providing final corrections, or quality control, over all brain functions through its widespread networks with the cerebral cortex (Marek et al., 2018). Overall, there has been support for moving towards a network view of cerebellar function, naming the cerebellum as a key hub in a plethora of brain circuits that modulate movement and higher-order cognition (Buckner, 2013; Koziol et al., 2014; Schmahmann, 2019; Stoodley, 2012). Schmahmann (2019) has also expanded his theory on cerebellar function, proposing the human cerebellum has discrete motor and non-motor components, which form unique circuits with motor and cognitive regions of the cerebral cortex. Briefly, the anterior lobe and lobule VIII in the posterior lobe are primarily sensorimotor, linked solely with the motor cortex and spinal cord. Lobules engaged during higher-order cognition, tasks involving language and verbal memory, planning, working memory, and task flexibility, include hemispheric lobules VI, Crus I, Crus II, and VIIB. Vermal lobules VI and VII are engaged during emotional processing. The deep cerebellar nuclei that receive input from these lobules are also respectively organized into

motor and non-motor domains (Koziol et al., 2014; Schmahmann et al., 2009; Schmahmann, 2019; Stoodley, 2012; Stoodley & Schmahmann, 2010; Stoodley et al., 2012).

Experiments using rodent and rabbit models also support a cerebellar role in cognition. One of the earliest cognitive behaviors examined in the rabbit cerebellum is associative learning. Using the classically conditioned eyeblink response, the cerebellar interpositus nucleus was found to be critical for both the acquisition and retention of this behavior (Krupa & Thompson, 1997; Pakaprot et al., 2009; Park et al., 2006; Swain et al., 2011). Manipulation of rodent cerebellar function in recent years using optogenetic and chemogenetic techniques has built on this foundation, disrupting a range of cognitive behaviors independent of interference with movement (Shipman & Green, 2019). Several experiments suggest the lateral cerebellum contributes to spatial navigation (Lee et al., 2018; Leggio et al., 2000; Noblett & Swain, 2003; Rochefort et al., 2013) and working memory (Deverett et al., 2019; Lalonde & Strazielle, 2003; Mandolesi et al., 2001; Shipman & Green, 2019). Recently, optogenetic methods were used to inhibit Purkinje cells in mouse lobule Crus I (part of lobule VII with input primarily to the dentate nucleus) at various stages of a decision-making task. Inhibiting Purkinje cell activity in Crus I decreased the accuracy of memory-guided decisions. Specifically, optogenetic inhibition disrupted the compilation of sensory information into working memory (Deverett et al., 2019). The lateral cerebellum, especially Crus I, may have a key role in ensuring working memory is accurately maintained (Deverett et al., 2019). Furthermore, chemogenetic inhibition of Crus 1 in mice produced social behavior deficits, in addition to behaviors that were both repetitive and inflexible, including impaired reversal learning on the Y-maze (Stoodley et al., 2017). Pharmacological inhibition of the rat fastigial nucleus also disrupts social behavior, exhibited by experimental rats avoiding contact with a confederate rat (Behnke et al., 2018). Cerebellar

projections to the ventral tegmental area (VTA) from all three deep cerebellar nuclei of mice were also recently identified. Interestingly, these glutamatergic projections were monosynaptic and activated reward circuits. Optogenetic stimulation of these cerebellar projections increased VTA activity, and this activity was rewarding, as indicated by voluntary self-stimulation by the mice (Carta et al., 2019). This input also modulated social behavior, where silencing these projections led animals to no longer prefer spending time in a social chamber with a confederate mouse, as they did in previous baseline conditions (Carta et al., 2019). In the context of reward, particular populations of mouse cerebellar granule cells respond to reward, reward omission, or reward anticipation, as revealed by *in vivo* two-photon calcium imaging. These reward signals were present in all lobules imaged, which included VI and Crus I (in lobule VII), and suggest these granule cells provide contributions that go beyond sensorimotor encoding (Wagner et al., 2017) . In summary, there is ample support for cerebellar contributions to motor and non-motor behavior in rodents, and human and non-human primates, although the precise mechanism by which the cerebellum modulates these behaviors is under active debate and investigation. This dissertation focused on one lobule, the paramedian lobule of VII, which has been implicated in both motor and non-motor functions.

Paramedian Lobule and Motor Learning

The paramedian lobule (PML; lobule VIIB; Gracile lobule) is a bilateral, hemispheric lobule, located in the posterior lobe of the cerebellum that contains face and ipsilateral and contralateral forelimb representations (Atkins & Apps, 1997). The PML includes both zebrin-positive (C1, C3) and zebrin-negative (C2, D2) zones (Atkins & Apps, 1997; Haines & Patrick, 1981; Voogd et al., 2003). The major sources of cortical input to the PML, via the pontine nucleus, come from the anterior and posterior sigmoid gyrus (motor cortex), premotor cortex,

parietal areas 5 and 7, and somatosensory cortex (Enger & Brodal, 1985; Hoddevik, 1975; Suzuki et al., 2012). Damage to the PML produces degeneration of axons in the dentate and both anterior and posterior regions of the interpositus deep cerebellar nuclei, indicating these are the primary sites of PML Purkinje cell output (Haines & Patrick, 1981). As a general rule, all lobules with C1 and C3 zones mainly send projections to the anterior interpositus nucleus and those with C2 zones to the posterior interpositus nucleus. D zones largely terminate in the dentate nucleus (Lu et al., 2012). Injections of transneuronal retrograde tracers into the forelimb region of the motor cortex labeled Purkinje cells in the PML, and granule cells were labeled in the PML by an anterograde tracer injection in the motor cortex (Kelly & Strick, 2003). Like other lobules of the cerebellum, the PML forms multi-synaptic, closed-loop circuits with the cerebral cortex. This means that, generally, the PML receives input from areas to which it provides output (Kelly & Strick, 2003). Within the cerebellar cortex, electrical stimulation of nearby lobules Crus I (medial portion), Crus II (posteromedial portion), and lobulus simplex (hemispheric portion) produced the largest response in the PML, demonstrating functional connections also exist between the PML and other lobules of the cerebellar cortex (Combs & Thomas, 1970).

The PML has been implicated in motor and non-motor functions, with projections to motor and non-motor domains of the interpositus and dentate nucleus and its closed-loop circuitry that encompasses an array of cortical regions such as the primary motor, parietal, and prefrontal cortex (Lu et al., 2012). Stimulation of the lobule produces limb movements in humans (Mottolese et al., 2013) and rats (Pardoe & Apps, 2002), and, based on connectivity, the PML likely helps code the parameters for forelimb movements, synthesizing incoming proprioceptive information with motor plans (Prevosto et al., 2017). The PML, in addition to Crus II, is theorized to be an important locus for the integration of sensory and motor

information (Rondi-Reig et al., 2014). Populations of PML Purkinje cells display single spike activity that increases in frequency just before rats handled food pellets (Heck et al., 2007), and high frequency oscillations were observed in the rat PML before and after lever pressing (Groth & Sahin, 2015). Synchrony decreased when the lever was pressed (Groth & Sahin, 2015). These high frequency oscillations are likely related to forelimb movements based on the reproducible, temporal coherence observed between the oscillatory activity and behavior. Easily detectable as a field potential, these oscillatory changes were robust. The precise aspect by which these high frequency oscillations contribute to forelimb movement is unclear, but the authors speculate they relate to more global brain states, such as attention or planning movements, rather than the encoding of a particular motor behavior (Groth & Sahin, 2015). In humans, the lobule has also been grouped in the posterior, cognitive, region of the cerebellum, in part because lesions to the PML, Crus I, or Crus II (all included in lobule VII) disrupts cerebellar communication with association areas in the cerebral cortex (Stoodley & Schmahmann, 2010). The PML has been activated during verbal working memory tasks (Desmond et al, 1997; Ng et al., 2016) and may specifically regulate the late stages of verbal encoding through its interactions with the posterior partial cortex (Macher et al., 2014). It is also active during executive function tasks, which includes complex decision-making (Stoodley & Schmahmann, 2009).

Founded on its sizable limb representations, the most recognized utility of the PML is modulating motor-skill learning: the ability to acquire new motor skills through repetition (González-Tapi et al., 2017). Plasticity in the PML following motor-skill learning has been extensively examined in the rat, with one of the most well replicated form of plasticity being synaptogenesis (Black et al., 1990; Isaacs et al., 1992; Kleim et al., 1997; Kleim et al., 1998). This was first demonstrated by Black et al. (1990), where researchers found that training adult

female rats for 30 days on an acrobatic course containing obstacles such as ladders, narrow beams, and ropes increased the number of Purkinje cell synapses in the PML by approximately 25%, relative to animals that were inactive or completed treadmill or wheel running exercise for the same duration. It was concluded that learning new complex movements required the addition of synapses in the PML, but repetitive, learned movements, like running, only required increases in the activity of existing synapses. This claim was substantiated by observations of increased blood vessel density in the PML in rats that exercised, but not those that completed the motor-skill learning acrobatic task. Increased blood vessel density may provide increased oxygen and glucose delivery to this area, compensating for the elevated motor activity (Black et al., 1990), and it was later found that, following exercise, blood vessel density increased with no change in neuropil volume (Isaacs et al., 1992). In contrast, the motor-skill learning group showed a 20% increase in the volume of the molecular layer of the PML and any increases in vessel density in this group served only to maintain the diffusion distance that existed pre-training (Isaacs et al., 1992). Changes in Purkinje cell size were not observed following motor-skill learning, but Isaacs et al. (1992) did find there was an increase in the number of mitochondria per Purkinje cell in the female rats that completed the motor-skill learning tasks. This shows motor-skill learning also induces mitochondrial plasticity in the PML. The formation of new synapses and expanded volume of the molecular layer likely requires the addition of mitochondria to maintain an adequate mitochondrial volume that corresponds to the increased neuropil volume (Isaacs et al., 1992).

Next, the type of Purkinje cell synapse increase in the PML following motor-skill learning was identified. Although 90% of Purkinje cell synapses are formed with parallel fibers, they also receive input from climbing fibers and local molecular layer interneurons such as

stellate and basket cells (Palay & Chan-Palay, 1974). Although stellate cells displayed increased dendritic arborization following acrobatic training, relative to exercised and sedentary controls female rats (Kleim et al., 1997), the only type of synapse that increased in number following 30 days of acrobatic training employing female rats was the parallel fiber-Purkinje cell synapse (Kleim et al., 1998). It was later demonstrated that, per Purkinje cell, there was an increase in the formation of multiple synapses between two Purkinje cell spines and one parallel fiber varicosity (Federmeier et al., 2002). This increase in parallel fiber-Purkinje cell synapses supports the notion that patterns of experience-dependent learning in the cerebellar cortex may occur through the strengthening of particular parallel fiber-Purkinje cell synapses, rather than through LTD mediated weakening alone as described in the original Marr-Albus model. Federmeier et al. (2002) also speculate that this addition of multiple synapses between parallel fibers and Purkinje cell spines could increase the bidirectional range of synaptic plasticity. After training male rats on the task for 20 days, the origin of these multi-synapses was further characterized and found to arise from the same Purkinje cell dendrite. This suggests the strength of the local synapses was increased, as opposed to a reorganization of the network, which may have been more likely had different dendrites been recruited to form the multi-synapses. Intriguingly, synapses surrounding the multi-synapse boutons (< 2 μm in distance from the multi-synapses) had smaller post-synaptic densities compared to those that were 2-5 μm from the multi-synapses (Lee et al., 2013). This indicates the synapses near those that are strengthened may be depressed. The strengthening and weakening of particular synapses may be a mechanism for encoding information in the cerebellum, and changes in synaptic weight may be necessary to maintain stable activity within affected Purkinje dendritic segments (Lee et al., 2013). Plasticity in the dentate nucleus following acrobatic training has also been assessed, but no synaptogenesis was

detected in that area after 30 days of motor-skill learning on the acrobatic task (Kleim et al., 1998) . This indicates the deep nuclei may be structurally stable following motor learning, with plasticity largely occurring in the cerebellar cortex. However, it should be noted that the PML also projects to the interpositus nucleus, and no structural plasticity measurements have been quantified in this deep cerebellar nucleus following acrobatic motor-skill training.

Also examined was whether or not this increase in parallel fiber-Purkinje cell synapse number persists after the discontinuation of acrobatic training (Kleim et al., 1997). In this experiment, there were three different acrobatic training groups and all employed female rats. The "early" acrobatic group trained for 10 days on the acrobatic course and was then immediately euthanized. The "delay" acrobatic group was also trained for 10 days, but then discontinued training on the acrobatic course for 28 days. After this 28 day delay, these rats completed two trials on the acrobatic course to examine whether or not motor-skill learning was maintained over the course of the delay. The "continuous" acrobatic group trained on the acrobatic course for all 38 days before being euthanized. Instead of having an aerobic exercise or sedentary control group, experimenters used what was termed a motor control group instead. This motor control group traversed an alleyway that matched the distance of the acrobatic course but was free of obstacles that required skilled movements. While the acrobatic rats completed training on the course, the motor control animal simultaneously traversed this alleyway, receiving similar levels of handling and activity. In all three acrobatic conditions (early, delay, continuous), parallel fiber-Purkinje cell synapses were increased, relative to the motor control group. There were no significant differences in synapse number between any of the three acrobatic groups, indicating synapse number is increased by 10 days of acrobatic training and is maintained regardless of whether or not training is continued or discontinued for the next 28

days. This finding correlates with behavioral performance, which was assessed by recording the number of errors per trial and the latency to complete each trial. Asymptotic performance has already been reached after 10 days of acrobatic training, so, if these new synapses do underlie motor-skill learning, conceivably, it is not necessary to continue to add more synapses after the task is mastered. Additionally, animals that were tested on the same acrobatic course after the 28 day delay exhibited behavioral performances similar to animals that never discontinued training for the full 38 days. Taken together, these results advocate that parallel fiber-Purkinje cell synaptogenesis in the PML contributes to motor-skill learning (Kleim et al., 1997).

In addition to synapse quantifications, plasticity of Purkinje cell dendritic spines following acrobatic learning has also been investigated in adult male rats using Golgi impregnation techniques. After 26 days of acrobatic training, there was a significant increase in the overall density of dendritic spines following acrobatic training, with the density of thin, mushroom, and stubby shaped spines all being elevated relative to inactive and motor control groups. There was no change in the density of wide spines between the groups (González-Tapia et al., 2015). Rats rapidly learn the acrobatic course, with behavioral data indicating the acquisition phase occurs on Days 1-5 of training and the maintenance phase, exhibited by stable task performance, is already reached by Day 6 (Kleim et al., 1996). Therefore, in this experiment, spine density was measured after the task was well mastered. To assess spine plasticity during task acquisition, male rats were also trained on the task for only six days, and spine density and shape were characterized on all six days of training. On Days 2 and 6, there was an overall increase in spine density, and this was interpreted as a general increase in presynaptic activity induced by the motor-skill learning. When quantifying densities of specific spine types, the number of thin spines tended to be elevated on all days of acrobatic training with

increases reaching statistical significance on Days 1, 3, and 6. Thin spines are associated with LTP induction and high-efficacy synaptic transmission, and these events are related to cerebellar motor learning as previously described. Mushroom spines, which support memory consolidation, were significantly decreased in the acrobatic training group on Day 3. Fewer stubby spines were also found on Day 1 and more thick spines were found on Days 4 and 6; both stubby and wide spines can regulate the excitability of postsynaptic neurons (González-Tapia et al., 2017). The consistently high density of thin spines during the early, acquisition phases of motor-skill training suggests an emphasis on information acquisition, rather than storage. However, when the task is mastered after 26 days of training there is an increase in mushroom spines, implying the task relevant information has been consolidated (González-Tapia et al., 2015; González-Tapia et al., 2017).

Instead of analyzing plasticity in postsynaptic Purkinje cell spines, the presynaptic structural plasticity of parallel fiber terminals in the PML was investigated by completing repeated *in vivo* two-photon microscopy in adolescent male mice for the duration of acrobatic training. Parallel fiber terminals were examined six times within the same animal two weeks prior to and throughout the eight-week duration of acrobatic training. Interestingly, during the two weeks prior to acrobatic training (basal condition), 10% of the parallel fiber terminals continuously appeared and disappeared. However, during acrobatic training this effect was reduced, and there was a net decrease in the number of new parallel fiber varicosities (Carrillo et al., 2013). Carrillo et al. (2013) state that it is unclear how these findings relate to the increase in parallel fiber-Purkinje cell synapses detected after acrobatic training in the PML postmortem. However, they infer that parallel fiber structural plasticity is reduced because intracellular resources are directed towards converting a population of existing parallel fiber varicosities into

multi-synaptic terminals, instead of continuing to generate new varicosities (Carrillo et al., 2013).

Because astrocytes are a fundamental component of the synapse, in addition to quantifications of spinal and synaptic plasticity, structural changes in cerebellar astrocytes were assessed following acrobatic motor learning in the PML. After 28 days of acrobatic training using female rats, there was an increase in the volume of astrocytes per Purkinje cell, compared to rats that engaged in wheel running or remained inactive for the duration of acrobatic training. This increase in astrocytic volume was proportional to the increase in synaptogenesis (Anderson et al., 1994). As determined previously, the increase in synapse number following acrobatic training is maintained, even after training is terminated. Therefore, the persistence of this increase in astrocyte volume was also analyzed, to determine whether or not it mirrors synaptic plasticity (Kleim et al., 1997; Kleim et al., 2007). Female rats were either in an "early" condition, where they were trained on the acrobatic course for 10 days, a "delay" condition where they trained for 10 days and then were inactive for 18 days, or a "continuous" condition where they trained on the acrobatic course for the full 28 days. Rats in the "early" and "continuous" groups had increased astrocyte volumes, relative to the motor control group. In contrast, the astrocyte volume in the "delay" condition was reduced to levels matching those of the motor control group. Findings indicate changes in astrocyte volume induced by motor-skill training do not persist without continued training, unlike increases in synapse number per Purkinje cell (Kleim et al., 2007). The increased synaptogenesis was stable for at least four weeks following the cessation of acrobatic training (Kleim et al., 1997). Although the functional consequence of this learning-induced increase in astrocyte volume per Purkinje cell is unclear, Kleim et al. (2007) propose one plausible explanation is that it directly relates to increased synaptogenesis and may

be driven by the activity of the newly formed parallel fiber-Purkinje cell synapses. Because astrocyte volume was not correlated with task performance or synaptogenesis after acrobatic training was terminated, astrocytic hypertrophy is likely not necessary for maintaining synapse formation or behavioral performance in this paradigm (Kleim et al., 2007).

Evidence suggests synaptogenesis in the PML underlies motor-skill learning, but no experiments were found that disrupt activity in the PML during or following acrobatic learning to determine whether or not this structural plasticity is essential for task performance. Furthermore, the earliest that structural plasticity has been assessed in the cerebellum following acrobatic motor-skill learning is 10 days, which is when animals have already mastered the task and synaptogenesis has reached its peak. Characterizing synaptogenesis and astrocytic plasticity earlier in training could provide useful information regarding whether depression and strengthening of synapses occurs in parallel or successively. The rapidity of astrocytic hypertrophy is also of interest, to determine whether it is present during the early phases of training where there is active synaptogenesis. Also, whether or not astrocytic activity contributes to parallel fiber-Purkinje cell synapse formation or behavioral acquisition of motor-skills is not known. This dissertation aimed to address some of these questions, with the goal of furthering our understanding of how PML structural plasticity and astrocytic activity contributes to motor-skill learning.

Cerebellar Astrocytes and Astrocytic Modulation of Behavior

The cerebellum has two subtypes of astrocytes: Bergmann glia in the molecular/Purkinje cell layers and velate protoplasmic astrocytes in the granular cell layer (Hoogland & Kuhn, 2010; Palay & Chan-Palay, 1974). These acrobatic motor-skill learning experiments have focused on the cerebellar molecular layer and have thus quantified astrocyte volumetric changes in

Bergmann glia (Kleim et al., 2007). Bergmann glia are a specialized form of radial astrocyte specific to the cerebellum and outnumber Purkinje cells eight to one (Korbo et al., 1993). They are organized into longitudinal cerebellar zones, in a pattern that overlaps with the boundaries of the cerebellar zone patterns established for neurons (Reeber, Arancillo, & Sillitoe, 2018). Bergmann glial cell bodies are located in the Purkinje cell layer, and their five major processes extend up through the molecular layer, with their minor processes closely intertwined with parallel fiber terminations onto Purkinje cell dendrites (Palay & Chan-Palay, 1974). Bergmann glia ensheath Purkinje cell dendritic spines forming functional microdomains that encompass only a few synapses, and this close anatomical relationship suggests they have an important role in modulating synaptic function (De Zeeuw & Hoogland, 2015; Lippman et al., 2008). In the mature brain, most Purkinje cell spines are entirely surrounded by Bergmann glial processes. This differs from areas of the forebrain, such as in the hippocampus, where the degree of astrocytic coverage of synapses greatly varies and only about half of hippocampal synapses are fully enclosed by astrocytic processes (Spacek, 1985). In addition to their close structural relationship with Purkinje cell synapses, Bergmann glia can directly communicate with Purkinje cell neurons via gap junctions, but coupling is weak (Pakhotin & Verkhratsky, 2005). Bergmann glia are also known to express several transporters and receptors, including glutamate aspartate transporter (GLAST) that is highly expressed in Bergmann glia processes (Miyazaki et al., 2017), and α-amino-3-hydroxy-5-methyl-4-isoxazolepropionic acid (AMPA) receptors that lack GluR-2 subunits, making them highly permeable to calcium (Iino et al., 2001). Little is known about the velate protoplasmic astrocytes in the granule cell layer, other than that these cells are stellate in shape and exhibit calcium signals that are similar to those of the Bergmann glia in the molecular layer (Hoogland & Kuhn, 2010). Hoogland & Kuhn (2010) propose that these

astrocytes are likely important for regulating the information that reaches the molecular layer by influencing local neuronal synapses in the granular layer, but this has not been demonstrated experimentally.

Bergmann glia, and arguably all cerebellar astrocytes, are the most ignored population of cells in the cerebellum (Chrobak & Soltys, 2017). How cerebellar astrocytes contribute to circuit function is rudimentarily understood, but how cerebellar astrocytic activity influences the generation of behavior is relatively unknown. Due to their radial morphology, Bergmann glia research has emphasized their role in guiding granule cell migration and Purkinje cell dendrite growth during development (Araujo et al. 2019; Cheng et al., 2018; Leung & Li, 2018). During development, Bergmann glial GLAST expression positively correlates with Purkinje cell dendrite growth and synaptogenesis (Yamada et al., 2000). Bergmann glial GLAST expression was later found to be required for the proper organization and function of parallel and climbing fiber-Purkinje cell synapses and for maintaining the ensheathment of Bergmann glial processes around respective synapses (Miyazaki et al., 2017). In adulthood, conditional genetic modifications to Bergmann glial AMPA receptors that cause them to instead express GluR-2 subunits, making receptors formerly highly permeable to calcium now calcium impermeable, causes a retraction of glial ensheathment around synapses (Lippman et al., 2010). Bergmann glia wrapping of Purkinje cell synapses begins at the onset of developmental synaptogenesis and, functionally, may have a role in "capping" or stabilizing synapse number. Without Bergmann glial ensheathment at the late stages of developmental synaptogenesis, spine density and synapse number was increased (Lippman Bell et al., 2010). These results indicate that Bergmann glial synaptic enwrapping may be critical for regulating synapse number during development, with full ensheathment possibly inhibiting continued synaptogenesis or inducing synaptic pruning

(Lippman Bell et al., 2010). In adulthood, Bergmann glia can regulate the number and length of minor processes by AMPA receptor calcium mediated activation of RhoA signaling and, in turn, the reorganization of the actin cytoskeleton of Bergmann glia fibers (Rosas-Hernández et al., 2019).

Bergmann glia processes are sensitive to nearby neuronal activity and have receptors that allow the detection of both excitatory and inhibitory neurotransmitters at the synapse (De Zeeuw & Hoogland, 2015). Bergmann glia also tend to be more responsive to parallel fiber activity as opposed to climbing fiber activity (De Zeeuw & Hoogland, 2015). This is likely due to the close proximity between the Bergmann glia and the parallel fibers that they enwrap. Within a few milliseconds, Bergmann glial AMPA receptors can be activated by presynaptic glutamate release (Matsui, Jahr, & Rubio, 2005). In cerebellar slices, repeated simulation of parallel fibers increases calcium in Bergmann glial microdomains (Grosche et al., 1999). Repeated parallel fiber stimulation caused mostly inward currents in Bergmann glia that were complex in nature. These events were in part mediated by Bergmann glial AMPA receptor activation and the uptake of synaptic glutamate (Clark & Barbour, 1997). Nitric oxide released by parallel fibers upon stimulation can also trigger calcium increases in Bergmann glia, and this calcium increase was due to calcium influx alone rather than calcium release from internal stores (Matyash et al., 2001). The precise mechanism by which nitric oxide causes Bergmann glial calcium influx from the extracellular space is not known, as the blockade of all known neurotransmitter receptors did not prevent this effect (Bellamy, 2006). Calcium transients in Bergmann glia mediated by AMPA receptors tend to be small in amplitude and of short duration. Furthermore, these transients remain spatially restricted to the Bergmann glial microdomains nearest the location of neuronal stimulation (De Zeeuw & Hoogland, 2015).

Brief bursts of parallel fiber stimulation can also elicit slower calcium transients that last for tens of seconds and result from the release of calcium from intracellular stores. In contrast to the fast, spatially restricted transients mediated by AMPA receptors, these calcium transients begin near the dendritic microdomains but can quickly expand within the glial process, demonstrating these transients slowly propagate from the site of origination (De Zeeuw & Hoogland, 2015). Slow calcium transients in Bergmann glia can be prevented by a blockade of metabotropic purinergic (P2Y) or mGluR1 receptors, but not by blocking AMPA receptors (Piet & Jahr, 2007). At least in part, information about parallel fiber activity is relayed to the Bergmann glia by molecular layer interneurons. In response to strong parallel fiber burst stimulation, molecular layer interneurons produce the ATP that is required to activate Bergmann glial purinergic receptors (Piet & Jahr, 2007). Similar to what has been established in neurons, Gq-coupled, metabotropic receptor activation in these Bergmann glia leads to downstream phospholipase C (PLC) activation and, in turn, inositol trisphosphate (IP_3) production, causing calcium release from internal stores. Bath application of an IP_3 antagonist eliminated calcium transients in all Bergmann glia analyzed (Beierlein & Regehr, 2006). In addition to these fast and slow calcium transients that occur locally, Bergmann glia also display calcium waves that can propagate between few to numerous other Bergmann glia cells and processes. Some of these waves are spontaneous and detectable during basal conditions (Hoogland et al., 2009a), and waves are more numerous in awake compared to anesthetized mice (Nimmerjahn et al., 2009). Locomotion can also cause the propagation of a unique calcium wave pattern in the Bergmann glia of the cerebellar vermis *in vivo* (Nimmerjahn et al., 2009), and the application of ATP also elicits calcium waves suggesting calcium waves can be initiated by purinergic signaling (Hoogland et al., 2009). Unlike other brain regions where calcium waves can propagate via gap

junctions, in Bergmann glia, calcium influx that results from the activation of AMPA receptors closes gap junctions, making this mechanism less likely (Müller et al., 1996). *In vivo* these waves have been found to span hundreds of micrometers (Nimmerjahn et al., 2009). The significance of these calcium waves in the cerebellum is not known, but it is likely that these waves influence neuronal excitability and blood flow (Hoogland & Kuhn, 2010).

Not only do Bergmann glia respond to neuronal activity, but a bidirectional relationship exists where Bergmann glia can also modulate synaptic activity. One way Bergmann glia can modulate synaptic activity is through regulating the amount of glutamate available at the synaptic cleft. This is primarily mediated by Bergmann glia GLAST activity, the only glutamate transporter expressed on these cells, that quickly removes glutamate from the synaptic cleft after neurotransmitter release (Takayasu et al., 2005). One primary outcome of glutamate entry into Bergmann glia is the conversion of glutamate to glutamine, a central component of the glutamate/glutamine shuttle. Glutamine is then released back into the synaptic cleft to be taken up and used by the presynaptic granule cells for glutamate synthesis. Inhibition of the glutamate/glutamine shuttle at various stages impairs excitatory synaptic transmission (Bröer & Brookes, 2001). Entry of glutamate through GLAST triggers cell signaling cascades that are similar to those induced by receptor activation in neurons, influencing gene expression (Tiburcio-Félix et al., 2018). Glutamate availability is regulated with close precision by GLAST uptake activity, with one 30 min exposure to glutamate in culture causing the downregulation of GLAST uptake for up to three hours in Bergmann glia (Martínez et al., 2014). In the short-term, GLAST activity triggers calcium influx in cultured Bergmann glia, and, interestingly, this calcium influx inhibits GLAST translation (mammalian target of rapamycin, mTOR, mediated pathway) and expression (Martínez et al., 2014). This activation of mTOR in Bergmann glia was

found to be activity dependent (Zepeda et al., 2009). In the long-term, glutamate binding to AMPA receptors can also downregulate GLAST transcription (protein kinase C, PKC, mediated pathway; López-Bayghen et al., 2003; Martínez et al., 2014). Downregulation of GLAST activity likely strengthens glutamate transmission in these instances, and this suggests Bergmann glial translational regulation may be pertinent to neuronal function (Zepeda et al., 2009). Additionally, this effect, whereby increased GLAST activity leads to the downregulation of its own transporters, is unique to Bergmann glia. In other cortical astrocytes, glutamate increases GLAST activity (Duan et al., 1999).

Beyond regulating glutamate levels within and between synapses by their extensive synaptic ensheathment and rapid uptake of neuronal glutamate, Bergmann glia can also modulate synaptic transmission through the release of their own gliotransmitters. Thus, a second way Bergmann glia can influence activity at the synapse is through gliotransmitter release, which is induced by calcium transients (Cervetto et al., 2015). Activation of Bergmann glial AMPA receptors is coupled with the local release of glutamate from Bergmann glial processes at parallel fiber-Purkinje cell synapses. Some Bergmann glial processes contain glutamatergic vesicles, and vesicular release of glutamate from these processes was coupled with the influx of calcium through local Bergmann glial AMPA receptors (Cervetto et al., 2015). However, after repeated stimulation of parallel fibers, Bergmann glial release of glutamate decreases as vesicular stores are exhausted, and this leads to LTD of neuronal-glial transmission (Balakrishnan et al., 2011). Bergmann glial vesicular stores can be depleted quickly, even during instances of normal synaptic transmission, because these astrocytes are deficient in the fast neurotransmitter recycling mechanisms present in the active zones of neurons (Balakrishnan et al., 2011). Particular parallel fiber inputs can be depressed independently of each other, and climbing fiber

stimulation can also produce this same neuronal-glial LTD. This demonstrates neuronal-glial LTD is both activity dependent and input specific (Balakrishnan et al., 2011). Importantly, Bergmann glia can also cause LTD of parallel fiber-Purkinje cell signaling. In cerebellar slices that contained Bergmann glia expressing channelrhodopsin-2, optical stimulation caused the release of glutamate. The magnitude of glutamate released from Bergmann glia was sufficient to activate mGluR1 receptors on Purkinje cells and induce LTD of parallel fiber-Purkinje cell synapses. Application of an mGluR1 antagonist prevented the LTD (Sasaki et al., 2012). This indicates that Bergmann glia glutamate can have direct effects on the strength of parallel fiber-Purkinje cell synapses.

A third way Bergmann glia can regulate neuronal excitability, and as a result neuronal activity, is by influencing Purkinje cell membrane potential. Bergmann glia can serve as "sinks" for ions, particularly potassium, and this redistribution of ions can dramatically influence neuronal membrane potential (De Zeeuw & Hoogland, 2015). When activity is strong at parallel fiber-Purkinje cell synapses, potassium can quickly increase in the extracellular space, and, for activity to be maintained, potassium must be removed. Bergmann glia have a negative resting membrane potential (approximately -80 to -85 mV) and numerous inwardly rectifying potassium channels. These features give Bergmann glia the ability to fine-tune the concentration of extracellular potassium (Butt & Kalsi, 2006; Hounsgaard & Nicholson, 1983). Increases in Bergmann glial intracellular calcium produced a reduction in extracellular potassium concentrations in cerebellar slices and in the cerebella of live mice. This potassium buffering occurred at the same time as increased Purkinje cell spike activity. Furthermore, either depolarization of the Bergmann glia or reducing the potassium concentration of the bath produced an increase in Purkinje cell firing, and a blockade of Bergmann glial calcium release

from internal stores prevented these effects (Wang et al., 2012). This indicates Bergmann glial intracellular calcium signaling is necessary for modulating extracellular potassium concentrations and, as a result, the membrane potential and activity of nearby Purkinje cells (Wang et al., 2012).

It is that clear a bidirectional relationship between the Bergmann glia and the parallel fiber-Purkinje cell synapses they ensheath exists, but little is known about how this relationship contributes to behavior *in vivo*. However, a few studies were found that suggest Bergmann glia activity either correlates with and/or modulates motor behavior. Bergmann glia calcium waves in the cerebellar vermis correlated with mouse locomotion *in vivo* (Nimmerjahn et al., 2009). In mutant mice lacking vimentin, an intermediate filament protein present in Bergmann glia but not forebrain astrocytes throughout adulthood, Bergmann glia appeared morphologically atypical and motor coordination was impaired in these mice (Colucci-Guyon et al., 1999). In mutant mice lacking glial fibrillary acidic protein (GFAP), LTD at the parallel fiber-Purkinje cell synapses and eyeblink conditioning were impaired. There were no motor coordination deficits detected in these GFAP mutant mice (Shibuki et al., 1996). In mice that expressed channelrhodopsin-2 in all astrocytes, photostimulation to depolarize Bergmann glia near the cerebellar flocculus disrupted smooth eye pursuit during a task that involved repeatedly tracking visual stimuli (Sasaki et al., 2012). In a conditional genetic inactivation of Bergmann glial AMPA receptors, mice displayed an increased number of missteps on the Erasmus ladder task, which requires traversing a horizontal ladder, both during training and when some of the ladder rungs were adjusted to a sudden incline during challenge conditions. However, animals continued to improve on the task with repeated trials, albeit at a slower rate than controls. When the same animals were tested on the eyeblink task, the amplitude of the conditioned response was lower than controls. The

impairments in these AMPA receptor conditional knockout mice were associated with a retraction of Bergmann glial processes from the Purkinje cell synapses they typically enwrap (Saab et al., 2012). Although these experiments provide preliminary support for a role for cerebellar astrocytes in modulating behavior, additional experiments are necessary. Specifically, experiments are needed that target specific lobules and zones of the cerebellum, rather than the cerebellum as a whole, as it is not functionally homogeneous. New optogenetic and chemogenetic techniques that allow for close temporal control of cerebellar astrocytic activity during behavioral tasks should also continue to be applied to astrocytes. This dissertation employed chemogenetic techniques to investigate the role of cerebellar astrocytes in motor-skill learning.

Astrocytic contributions to learning and memory throughout the brain have only been investigated preliminarily *in vivo*, but by manipulating activity in these cells, it is becoming clear that astrocytes can have profound effects on neuronal function and behavioral outcomes. To investigate the role of astrocytes in motor learning, fluorocitrate was infused into the mouse primary motor cortex four hours before training on a forelimb-reaching task. Fluorocitrate is a metabolic inhibitor specific to astrocytes, and it was shown to reduce astrocytic calcium transients in primary motor cortex brain slices (Padmashri et al., 2015). Mice were trained on a forelimb reaching task for food pellets and, on all five days of training, the success rate (pellets retrieved/total attempts) was reduced in the fluorocitrate treated animals (Padmashri et al., 2015). Chemogenetic techniques, namely designer receptors exclusively activated by designer drugs (DREADD), which were used in this dissertation, have revealed astrocytic calcium signaling is involved in contextual learning and memory. By expressing the hM3Dq DREADD in GFAP positive hippocampal CA1 astrocytes, activation of the DREADD and, in turn, Gq-signaling in

these astrocytes, 30 min prior to fear conditioning training enhanced performance on the task. However, activation of the DREADD after training had no effect on performance, which suggests hippocampal astrocytes were involved in memory acquisition or consolidation, but not retrieval. For better temporal resolution, optogenetic techniques were then applied to this task, and it was determined that activation of the hM3Dq DREADD in astrocytes specifically enhanced the acquisition of the fear memory (Adamsky et al., 2018). In a similar experiment, hM4Di DREADD, to activate Gi-signaling, were instead expressed in hippocampal CA1 astrocytes and activated 30 min prior to fear conditioning. When mice were returned to the context where fear conditioning occurred the following day, there were no differences in freezing fear behavior suggesting this manipulation did not affect the retrieval of a recent memory. Interestingly, when mice were placed in this context 20 or 45 days later, those that experienced astrocytic hM4Di DREADD activation showed impaired retrieval of the remote fear memory demonstrated by a lack of freezing behavior in the fear-eliciting context. Researchers found that hM4Di DREADD activation in these astrocytes interfered with the recruitment of the hippocampal CA1 to anterior cingulate cortex neuronal projections during acquisition, and this disrupted remote recall (Kol et al., 2020). Manipulating astrocytic activity with hM3Dq and hM4Di DREADDs has impacts on other behaviors beyond contextual learning and memory. Expression of astrocyte specific hM3Dq DREADD in the prefrontal cortex enhanced cognitive flexibility on an attentional set-shifting task (Brockett et al., 2018). Expression of the astrocytic hM3Dq DREADD in the mouse medial basal hypothalamus inhibited feeding behavior, and hM4Di DREADD activation in the same structure enhanced feeding behavior (Yang et al., 2015). Findings are somewhat contradicting in regards to feeding behavior, and it was also found that hM3Dq DREADD activation in hypothalamic astrocytes increased feeding behavior but

hM4Di DREADD activation had no effect on feeding behavior (Chen et al., 2016). Discrepancies were attributed to clozapine-N-oxide (CNO; ligand that activates the DREADD) dose differences (Chen et al., 2016). The activation of the hM4Di DREADD in striatal astrocytes produced hyperactivity and attentional impairments in mice (Nagai et al., 2019). In summary, it is clear that activation of hM3Dq and hM4Di DREADDs in astrocytes can influence behavior and serve as a useful technique to disentangle the contributions of astrocytes to complex behaviors. The hM4Di DREADD technique was used in this dissertation to manipulate PML astrocytic Gi-signaling during motor-skill training on the acrobatic task.

Aims and Hypotheses

Aim 1

Characterize early structural plasticity, including synaptogenesis and astrocytic hypertrophy, in the acquisition phase of motor-skill learning.

Hypothesis: It was hypothesized that there would be an increase in parallel fiber-Purkinje cell synapses and astrocytic hypertrophy after only four days of training on the acrobatic course. This prediction was based on the rapid increase in thin spines in the PML early in acrobatic training (González-Tapia et al., 2017) and increased synaptogenesis in the motor cortex after only five days of acrobatic training (Kleim et al., 1996).

Aim 2

Determine whether cerebellar astrocytic activity, via hM4Di DREADD activation, impairs or enhances motor-skill learning on the acrobatic course.

Hypothesis: It was hypothesized that activation of astrocytic Gi-signaling through the hM4Di DREADD would impair motor-skill learning on the acrobatic course. This prediction was based on the effects of the astrocytic hM4Di DREADD in the hippocampus (Kol et al., 2020) and the motor learning impairment detected in AMPA receptor conditional knockout mice (Saab et al., 2012).

Aim 3

Identify how the activation of the hM4Di DREADD in astrocytes in the PML impacts the increased synaptogenesis and astrocytic hypertrophy typically associated with motor-skill learning.

Hypotheses: It was hypothesized that synaptogenesis and astrocytic hypertrophy would be decreased by activating Gi-signaling in cerebellar astrocytes. It was also hypothesized that c-Fos (activity marker) expression would be increased in neurons following acrobatic training, relative to motor controls, in all rats except those expressing the hM4Di DREADD. These predictions were based on evidence suggesting astrocytic processes can retreat when calcium levels are decreased via AMPA receptor manipulations (Lippman et al., 2008; Miyazaki et al., 2017) and that c-Fos levels were elevated in the primary motor cortex after 1-5 days of acrobatic training (Kleim et al., 1996).

Chapter Two: Materials and Methods

Subjects

Male and female, 175 g, Long Evans rats (n = 26/sex) were purchased from Envigo (Madison, WI, USA). Sample size was selected based on other acrobatic task experiments investigating cerebellar plasticity conducted using male or female rats (Black et al., 1990; Federmeier et al., 2002; González-Tapia et al., 2015; Kleim et al., 2007). Rats were housed individually in standard shoebox cages with unlimited food and water access. The animal colony was on a 12 hr light/dark cycle, and experimental procedures occurred during the light cycle. Rats were weighed daily and allowed to acclimate for at least one week prior to beginning experimental procedures. All procedures were approved by the University of Wisconsin-Milwaukee Animal Care and Use Committee and adhered to the National Institute of Health's ethical guidelines.

Behavioral Apparatuses

Acrobatic training occurred on a nine-obstacle elevated course built in-house. The course platforms were elevated 40 cm off the table, and the entire course was approximately 6 m in length. Between each platform was an obstacle. Obstacles included a steep ladder, suspended metal linked chain, a rotating rope made of cylindrical blocks, a narrow beam with block barriers, a suspended wire with large hoops, a suspended wire with small hoops, a wobbly plastic block bridge, a suspended doweled string, and a suspended metal spring. The motor control alleyway was an enclosed Plexiglas runway that is 3 m in length x 14 cm in width and is flat and free of obstacles. This runway was built in-house. Traversing the runway twice equated to traveling the acrobatic course once.

The three apparatuses used only for motor performance testing are listed next. The first apparatus was an accelerating rotarod (Omnitech Electronic Inc., Columbus, OH, USA) with a 70 mm diameter rotating cylinder and 40 cm fall height. The second apparatus was an open field box that is 91.5 x 95.5 cm square with walls extending 57.5 cm in height. The bottom of the open field box was gridded into 36 equal squares and covered with Plexiglas built in-house. The third apparatus was a gait analysis runway that is enclosed, and 80 cm in length x 14 cm in width built in-house. For each rat, the runway was lined with white paper and red nontoxic paint (Artisa II Washable Tempera-Paint, Crayola) was used to capture rat paw prints for stride length and width measurements.

DREADD Surgery Procedure

Viral vectors were manufactured by the Duke University Viral Vector Core (Durham, NC, USA) and included an hM4Di DREADD virus with an astrocyte specific promoter (AAV8-GFAP-hM4D(Gi)-mCherry, $6x10^{12}$ vg/ml) and an mCherry control virus with an astrocyte specific promoter that was identical to the previous with the exception of the hM4Di DREADD component (AAV8-GFAP-mCherry, $2x10^{13}$ vg/ml). A subset of animals were infused with the hM4Di DREADD virus (n = 9 males, n = 9 females) or the mCherry control virus (n = 9 males, n = 9 females) for Experiment 2. Prior to beginning surgery, the appropriate virus was loaded into a 10 µl, 34-gauge needle Hamilton syringe (Hamilton Co, Reno, NV, USA.) and placed into a stereotaxic microsyringe pump (KD Scientific, Holliston, MA, USA). In preparation for surgery, rats were anesthetized with 4% isoflurane in oxygen. After placement in the stereotaxic apparatus (Stoelting Co., Wood Dale, IL, USA), isoflurane levels were maintained between 1.5-2.5% for the duration of the surgery. Following surgical preparations, a Dremel tool was used to drill bilateral holes above the PML (from bregma: AP: -13.4 mm; L: ± 3.2 mm; DV 6.7; Paxinos

& Watson, 2007) for bilateral virus infusions. In each hemisphere, injections were made at two depths in the PML (6.7 mm and 6.2 mm) at a speed of 0.2 µl/min until a total of 0.8 µl of virus was injected per location. Prior to beginning the first injection in each hemisphere, the syringe was lowered to 6.8 mm for 2 min to create a pocket to inject virus into. Following each injection, the syringe remained in place for 5 min to allow time for the virus to diffuse away from the needle tract, and then the syringe was slowly withdrawn. Lastly, skull holes were covered with bone wax, incisions were sutured and closed with Vetbond tissue adhesive, and rats received 4 ml of 0.9% sterile saline subcutaneously. For pre- and postoperative analgesia, rats received Rimadyl (5 mg/kg; Bio-serv, Flemington, NJ, USA). To allow time for recovery and DREADD expression, acrobatic training began at least two weeks post-surgery. One female rat infused with the mCherry control virus did not wake from anesthesia leaving a total of 17 rats that expressed the mCherry control virus and 18 rats that expressed the hM4Di DREADD virus.

Clozapine-N-Oxide (CNO) Preparation

Prior to behavioral training, all rats infused with viral vectors in Experiment 2 received daily intraperitoneal injections of the DREADD activating pharmacological ligand clozapine-N-oxide (CNO; 4 mg/kg; Cayman Chemical, Ann Arbor, MI, USA). These injections occurred 20 min prior to acrobatic or motor control training, and all rats in Experiment 2 received the injections. These injections were necessary to activate the DREADDs, and this dose has not been found to produce large off-target behavioral effects in Long Evans rats (MacLaren et al., 2016). Stock solutions of CNO were prepared by dissolving the CNO into 100% dimethyl sulfoxide (DMSO; 100 mg/ml). The stock solution was placed in 10 µl aliquots and stored at -20°C until use. Prior to injections, CNO was prepared by diluting the stock to a concentration of 1 mg/ml in 0.9% saline containing 2% DMSO (Tuscher et al., 2019).

Acrobatic Training Procedure

Experiment 1

This experiment addressed Aim 1, which involved characterizing early structural plasticity, including synaptogenesis and astrocytic hypertrophy, in the acquisition phase of motor-skill learning. Male and female rats (n = 8/sex) were equally assigned to either an acrobatic training (AT; n = 4/sex) or motor control (MC; n = 4/sex) group. These rats did not undergo surgery for virus infusion. All rats were transported and handled for two days before beginning acrobatic or motor control training. For acrobatic motor-skill training, rats completed four trials/day, for four days, on the acrobatic course. On each trial, a researcher cradled the tails of the rats, catching rats after foot-faults and gently prodding if the rats stop midway through an obstacle. The number of prods, errors (foot-faults) and time spent per obstacle/trial were recorded. On the first trial, heavy guidance from the researcher was required for the rat to complete the course, but the rats traversed the course more independently after just a few trials. As each AT rat was trained, an MC rat walked the motor control alleyway. Each time the AT rat was prodded by a researcher, the MC rat was also prodded. This controlled for handling and locomotor exercise. After each trial was complete, rats received a food reward (Lucky Charms Original Breakfast Cereal). After completing training on Day 4, all rats were euthanized.

Experiment 2

This experiment addressed Aims 2 and 3, which assessed how the manipulation of cerebellar Gi-signaling impacts motor-skill learning and structural plasticity at the parallel fiber-Purkinje cell synapse. Rats expressing the hM4Di DREADD and mCherry control virus (n = 35) were assigned to either an acrobatic training (AT; n = 18) and or a motor control (MC; n = 17) group. Twenty minutes before behavioral training, all rats were injected with CNO (4 mg/kg). As

in Experiment 1, AT rats completed four trials/day, for four days, on the acrobatic course. The number of prods, errors (foot-faults), and time spent per obstacle/trial were recorded (Aim 2). As each AT rat was training, a MC rat traversed the motor control alleyway following the procedure described in Experiment 1. After each trial was completed, rats again received a food reward (Lucky Charms Original Breakfast Cereal). During behavioral training, researchers were blind to the virus condition. After rats completed training on Day 4, all rats were euthanized for an assessment of structural plasticity (Aim 3).

Motor Performance Testing. Although robust off-target CNO effects were not expected at this dose (MacLaren et al., 2016) it was important to verify that CNO treatment itself did not contribute to any behavioral effects identified on the acrobatic course. Training on the acrobatic task also restores motor abilities to control levels in rodent models of neonatal alcohol exposure, which is a model that causes a loss of 40% of Purkinje cells and decreased neuronal density in the PML (Klintsova et al., 1998, 2002). It is thus possible that acrobatic training could reverse any motor performance deficits caused by the hM4Di DREADD activations, and that the behavioral impairments identified on the acrobatic course are due to motor performance deficits rather than motor learning deficits. Therefore, rats in Experiment 2 underwent motor performance testing prior to acrobatic training. Rats were habituated to handling, transport, and all apparatuses prior to testing. For the two habitation days, rats had a 10-min open field exposure, a 5-min exposure to the sound of the rotarod, and two exposures to the gait analysis alleyway. Rats also underwent rotarod training to ensure they had learned the task prior to the motor performance assessment on the acceleration test days. Rats completed four days of rotarod training (2 trials/day, 60-sec each, speed of 10 rpm). On the first day of motor performance testing, half of the rats were injected with saline vehicle and half with CNO (4 mg/kg). This was

reversed on the second day of testing, and groups were counterbalanced across days. Twenty minutes after these injections, rats were tested on the motor performance apparatuses. This first test was a 10-min session in the open field to assess baseline locomotor activity (n = 35). The total number of grid squares crossed, and the number of rears were counted during the recorded 10-min session. Second, rats completed a 60-sec trial on the rotarod, which was accelerated to 30 rpm after rats acquired 10-sec at the training speed of 10 rpm (n = 24). The latency to fall during the 60-sec trial was recorded. If rats could not acquire 10-sec at the training speed on the test days, they were excluded from the acceleration test. Third, the paws of the rats were dipped in non-toxic paint, and rats were guided down the gait analysis alleyway lined with white paper to capture pawprints for stride length and width measurements (n =35). Front and back paw width and length were manually measured (mm).

Electron Microscopy and Immunofluorescence Procedures

Experiment 1

Electron Microscopy. After euthanasia, all rats were perfused with 4% paraformaldehyde/2% glutaraldehyde (Electron Microscopy Sciences, Hatfield, PA, USA). Cerebella were dissected from the forebrains and stored in the same fixative at 4°C until sectioning. For sectioning, cerebella were hemisected and sagittal 300 µm sections were collected through the PML using a vibratome (Ted Pella Inc., Redding, CA, USA). Sections were stored in welled plates containing fixative (2% glutaraldehyde in 0.2 M sodium cacodylate buffer, pH 7.4) until additional post-fixation, heavy metal staining, dehydration and embedding procedures.

For each rat, two punches of the PML were collected from each 300 µm section using a Miltex biopsy punch (Fisher Scientific). PML punches were placed in shell vials filled with 0.1

M cacodylate buffer to wash out remaining fixative. Tissue were washed 3x, for 5 min each, in cacodylate buffer. Tissue then underwent post-fixation in 1% osmium tetroxide (Ted Pella Inc., Redding, CA, USA)/ 1.5% potassium ferrocyanide (Allied Chemical, Pottsville, PA, USA) in 0.1 M cacodylate buffer for 40 min. Heavy metal staining involved staining tissue in 1% osmium tetroxide in cacodylate buffer for 40 min, followed by a rinse in double-distilled water for 3 min, and then staining with 1% uranyl acetate (Electron Microscopy Sciences, Hatfield, PA, USA) for 40 min (Kleim et al., 2007). After heavy metal staining was complete, tissue was rinsed in double-distilled water and dehydrated in a graded series of ethanol (Fisher Scientific) rinses: 1x in 50%, 1x 70%, 1x in 90%, 1x in 95%, and 3x in 100% all for 10 min each. After the final dehydration, tissue was embedded in LR White resin, medium grade (benzoyl peroxide catalyst, Ted Pella, Inc., Redding, CA, USA), prepared per the kit directions. Tissue was first moved to a 1:1 LR White/100% ethanol mixture and agitated overnight. Tissue was then moved through two changes of 100% LR White resin for 3 hr each, and then embedded into individual gelatin capsules filled with LR White resin. Gelatin capsules were polymerized at 60°C for 24 hr.

After removal of the gelatin capsule, two randomly selected blocks were faced into ~1.0 mm trapezoids for ultramicrotomy using an RMC MT-700 Ultramicrotome (Boeckeler Instruments, Inc., Tucson, AZ, USA) equipped with a Histo Jumbo diamond knife (DiATOME, Hatfield, PA, USA). Eighty, 1 μm, semithin sections were collected through the PML. These sections were mounted onto glass slides and stained with Toluidine blue. Semithin sections served as a guide for shaping the block for ultrathin sectioning and were used for later Purkinje density quantifications using a light microscope (Olympus Co.) with attached digital camera (Diagnostic Instruments, Inc., Sterling Heights, MI, USA). After semithin sectioning, the block was reexamined under a stereomicroscope and a smaller, ~0.5 mm, trapezoid was trimmed into

the molecular layer of the PML. Ribbons of approximately thirty 100 nm gold, ultrathin sections were cut per block and placed onto glass slides. Ultrathin sections were stained with aqueous 1% uranyl acetate followed by Reynold's lead citrate prior to carbon coating using a vacuum thermal evaporation system (Edwards 306 A, Edwards Vacuum Co., Burgess Hill, UK) the following day for scanning electron microscopy. The slides containing the ultrathin sections (1 slide per rat, ~30 sections per slide) were imaged using a Hitachi S-4800 Field Emission- Scanning Electron Microscope (FE-SEM). Use of the upper secondary electron detector in energy filtering mode was used to collect backscattered electron images, using a 5.0 kV accelerating voltage, and a 3.4 mm working distance and setting of LA 20. A magnification of 20,000x allowed for the collection of electron micrographs of sufficient quality to view necessary ultrastructure (Micheva & Smith, 2007). For each slide, one micrograph was captured from the same region of each tissue section.

Experiment 2

After euthanasia, all rats were perfused with 4% paraformaldehyde. Cerebella were dissected from the forebrains and hemisected. One hemisphere was stored in the 4% paraformaldehyde fixative overnight at 4°C in preparation for immunofluorescence labeling, and the other hemisphere was stored in 4% paraformaldehyde/2% glutaraldehyde overnight at 4°C in preparation for electron microscopy.

Electron Microscopy. As in Experiment 1, the cerebellar hemispheres used for electron microcopy were sectioned at 300 μm with a vibratome 24 hr after perfusions (n = 24). PML samples were punched from these sections as described in Experiment 1 and all embedding, ultramicrotomy, and SEM procedures were also identical to Experiment 1.

Immunofluorescence. The cerebellar hemispheres used for immunolabeling were moved to 3.5% sucrose in phosphate buffer at 4°C for cryoprotection 24 hr after perfusions (n = 24). These cerebellar hemispheres were then frozen and 20 μm thick sections were collected through the PML using a cryostat (Leica CM3050S, Leica Biosystems, Wetzlar, Germany). Each slide contained sections representative of the entire PML. One slide per rat was used for immunofluorescence labeling of GFAP (to verify the viruses were expressed in astrocytes) and one slide for immunofluorescence labeling of c-Fos (an immediate early gene/activity marker that was used to assess activation of the hM4Di DREADD in astrocytes and its effects on non-glial cell activity). For immunofluorescence, sections were rehydrated and washed 3x in 0.05% Tween 20 in phosphate buffered saline for 5 min each. Sections were then permeabilized for 15 min in 0.3% Triton X-100 in phosphate buffered saline and blocked in 10% goat serum/0.5% Triton X-100 in phosphate buffered saline for 1 hr. GFAP (1:200; mouse anti-GFAP, Santa Cruz Biotechnology, sc-3373) or c-Fos (1:1,000; rabbit anti-c-Fos, Synaptic Systems, 226 003) primary antibodies were then applied and slides incubated overnight at 4°C (GFAP) or room temperature (c-Fos). The following day, slides were washed in 0.05% Tween-20/phosphate buffered saline 3x for 10 min each and then treated with the appropriate secondary antibodies (GFAP: 1:200 Goat anti-mouse Alexa Fluor 594; c-Fos: 1:200 Goat anti-rabbit Alexa Fluor 594, Thermo Fisher) for 2 hr at room temperature in the dark. Lastly, slides were washed 2x with phosphate buffered saline for 10 min each before being coverslipped with Prolong Diamond medium containing DAPI (Thermo Fisher). Images of immunofluorescence labeling were collected using an epifluorescence microscope (Nikon Eclipse, Nikon Instruments Inc.). Images of virus expression, GFAP, and c-Fos were collected at 200x magnification from five sections, per rat. Two non-overlapping images were captured per slice and exposure times were held

constant for each channel across all groups.

Ultrastructural and Immunolabeling Quantification Procedures

Experiment 1

Purkinje Cell Density. For the slides containing semithin sections stained with Toluidine blue (two slides per rat, ~80 sections per slide), sequential images were captured of the Purkinje cell layer using a 60x objective on a light microscope (Olympus Co.) with attached digital camera (SPOT, Diagnostic Instruments Inc., Sterling Heights, MI, USA). These serial images were stacked and aligned in Adobe Photoshop 2020 (Adobe Inc., San Jose, CA, USA). After the stack of images was aligned, a 200 μm x 200 μm unbiased counting frame was centered on the Purkinje cell layer of the tissue section, and the physical disector method was employed to quantify Purkinje cell density (Black et al., 1990; Kleim et al., 1997, 1998; Sterio, 1984). Comparisons were made between two serial sections at a time. The first section served as the reference section and the second section served as the lookup section. If a Purkinje cell nucleolus (each Purkinje cell has only one) was present in the counting frame on the reference section, but not the lookup section, the cell was counted. Next, section two became the reference section and section three became the lookup section. This process continued until all tissue sections in the image stack were sampled (Black et al., 1990; Kleim et al., 1997, 1998). All slides were analyzed in this manner. The area of the counting frame was then multiplied by the total number of 1 μm thick semithin sections analyzed to get the total tissue volume. To obtain a measurement of Purkinje cell density, the total number of Purkinje cell nucleoli counted per rat was divided by the total tissue volume sampled per rat. This Purkinje cell density measurement was used later to determine the density of synapses per Purkinje cell (Black et al., 1990; Kleim et al., 1997, 1998).

Synapse Density. The physical disector method, as described previously, was used to quantify the density of parallel fiber-Purkinje cell synapses in the electron micrographs from each rat. After the micrographs were stacked and aligned for each rat using Adobe Photoshop 2020 (Adobe Inc., Sterling Heights, MI, USA) a 2 μm x 2 μm unbiased counting frame was then superimposed onto the stack of aligned images. This time, the number of synapses present in the reference, but not the lookup section, were counted. Parallel fiber-Purkinje cell synapses were identified by their unique morphological features, including terminals with small rounded vesicles clustered adjacent to spines with a fine extracellular matrix (Kleim et al., 1998; Klintsova et al., 1998). Synapse density was calculated by dividing the number of parallel fiber-Purkinje cell synapses counted by the total volume of tissue analyze. The synapse density when divided by Purkinje cell density provided an estimate of the number of parallel fiber-Purkinje cell synapses per Purkinje cell. Synapse estimates were quantified for each rat in this manner (Kleim et al., 1996; 1997).

Synapse and Spine Measurements. In addition to quantifying synapse density per Purkinje cell, the length of the synapses, circumference of the Purkinje cell spines, and fraction of the Purkinje cell spine ensheathed by astrocytes was measured using methods similar to those described by Lippman Bell et al. (2010). These measurements were collected from the same synapses counted above. For consistency, measurements were taken only when the synapse was fully visible, not when it was appearing or disappearing from the aligned image stack. To do these measurements, images containing the quantified synapses were opened in Fiji (NIH, Bethesda, MD, USA) and, using the calibrated drawing tool, the length of the synapse was measured, as was the circumference of the Purkinje cell spine (excluding the area in contact with the presynaptic terminal). The length of the Purkinje cell spine in contact with astrocytic

processes was also measured. To get an estimate of the fraction of the spine covered by astrocytic processes, the length of the spine in contact with astrocytic processes was divided by the total spine circumference (Lippman Bell et al., 2010). The average synapse length, spine circumference, and astrocytic spine coverage fraction was calculated for each rat.

Astrocyte Volume. To get an estimate of the total astrocyte volume fraction for each rat, every fifth electron micrograph was opened in Fiji (NIH, Bethesda, MD, USA) and a point grid, with equally spaced points, in 1.5 cm intervals, was overlaid onto the entire micrograph. This unbiased stereological technique was used to estimate volume fraction. Astrocyte volume fraction was calculated by dividing the total number of points falling on astrocytic processes by the total number of points on each micrograph (Kleim et al., 2007). Astrocytic processes were identified by their unique features, including a cytoplasm with few fibrils and sparse organelles, and their tendency to trace the path of other cellular processes (Kleim et al., 2007). For each rat, an average astrocyte volume fraction was calculated.

Experiment 2

Quantification methods to assess parallel fiber-Purkinje cell synapse density and astrocyte volume fraction were identical to Experiment 1. In addition, analyses of c-Fos and GFAP immunofluorescence labeling were completed.

Immunofluorescence Analyses of GFAP and c-Fos Expression. For each rat, two images were captured from five PML sections expressing virus at 200x magnification. Images were saved as composite, 12-bit TIFF files and Fiji (NIH, Bethesda, MD, USA) was used for cell counts and particle quantifications. To assess the specificity of the viruses to targeting astrocytes, one image per rat was selected to analyze GFAP and virus colocalization manually with the "Cell Counter" tool in Fiji. The number of virally labeled somas that colocalized and did not

colocalize with GFAP were counted. The percentage of virally positive cells expressing GFAP was then calculated for the hM4Di DREADD virus and mCherry control virus groups. Automated thresholding and particle analyses were used to quantify c-Fos expression. The multiple methods of thresholding available in Fiji were tested, and the method that most accurately captured cell somas for each label was selected. The Li thresholding method was used for the DAPI labeling, the triangle thresholding method was used for c-Fos labeling, and the max entropy thresholding method was used for the viral labeling. After generating these binary images, particles greater than 4 pixels in diameter were analyzed using the "Analyze Particle" function. To assess colocalized particles, binary images of virus and c-Fos expression were overlayed and the overlapping particles were quantified using the "Analyze Particle" function. Colocalized c-Fos expression was calculated for each rat by dividing the area of c-Fos particles that colocalized with virus particles by the area of virus particles in the ROI. c-Fos expression that did not colocalize with virus was calculated by subtracting the area of c-Fos particles colocalized with virus from the total area of c-Fos particles in the ROI. This estimate of non-colocalized c-Fos was then normalized to the total area occupied by DAPI in the ROI to ensure any effects detected were not due to differences in the total number of cells sampled across groups. Particle area, instead of particle number, was selected as the term of measurement because it was challenging to get accurate estimates of DAPI particle number in the densely packed granule cell layer. The average area of c-Fos particles that colocalized and did not colocalized with virus expression was calculated for each rat.

Statistics

Experiment 1

All statistics were computed in GraphPad Prism 8 (La Jolla, CA, USA). To assess behavioral performance for the AT group, a mixed-model analysis of variance (ANOVA) compared the mean latency/trial/day, the mean errors/trial/day, or the mean prods/trial/day between sexes (male or female; between subject factor) across the four days of training (within subject factor). Two-factor ANOVAs compared synapse density, synapse length, spine circumference, astrocyte volume fraction, or astrocytic spine coverage fraction, between sexes (male or female) and training conditions (AT or MC). All data are reported as mean (M) ± standard error of the mean (SEM) and statistical significance for all analyses was $p < 0.05$.

Experiment 2

All statistics were computed using IBM SPSS Software (IBM Co., Chicago, IL, USA). A mixed model analysis of variance (ANOVA) compared the effects of virus type (mCherry control or hM4Di DREADD; between subject factor), sex (male or female; between subject factor), and training day (4 days; within subject factor) on performance on the acrobatic course (mean latency/trial/day, mean errors/trial/day or mean prods/trial/day). Three-factor ANOVAs compared colocalized and non-colocalized c-Fos, synapse density, and astrocyte volume fraction between sexes, virus types, and training conditions. For motor performance testing, a mixed model ANOVA compared the effects of virus condition, sex, and drug treatment (CNO or saline vehicle; within subject factor) for each of the respective measures. When appropriate, ANOVAs were followed up with pairwise comparisons, and the Bonferroni adjusted significance test was applied to correct for multiple comparisons. All data are reported as mean (M) ± standard error of the mean (SEM) and statistical significance for all analyses was $p < 0.05$.

Chapter Three: Results

Experiment 1

Behavioral Performance on the Acrobatic Course Improved as Training Progressed

AT rats showed an overall improvement in performance on the acrobatic course across the four days of training (**Fig. 1**). The latency/trial/day ($F_{(3,18)} = 115.20$; $p < 0.0001$; **Fig. 1A**), errors/trial/day ($F_{(3,18)} = 81.71$, $p < 0.0001$; **Fig. 1B**), and prods/trial/day ($F_{(3,18)} = 123.00$; $p < 0.0001$; **Fig. 1C**) significantly decreased as acrobatic training progressed. The interaction between sex and training day was significant for both latency ($F_{(3,18)} = 14.19$, $p < 0.001$) and errors ($F_{(3,18)} = 3.332$, $p = 0.043$), indicating females performed better than males, particularly on the initial days of training (**Fig. 1A,B**). Female rats had shorter latencies ($F_{(1,6)} = 6.562$, $p = 0.043$; **Fig. 1A**) and made fewer errors ($F_{(1,6)} = 6.326$, $p = 0.046$) than male rats, with no sex difference found in the number of prods ($F_{(1,6)} = 4.270$, $p = 0.084$). Navigating the course faster, making fewer foot-faults, and pausing less during training all demonstrate the rats were acquiring the necessary motor-skills to complete the acrobatic task.

Figure 1

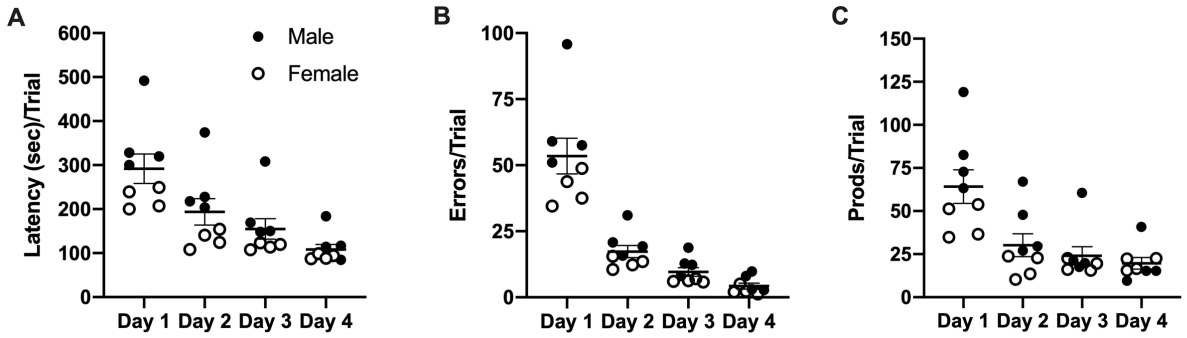

Figure 1: **Behavioral performance for rats that completed acrobatic training. (A)** Rats showed decreased latencies per trial as training progressed across the four days $p < 0.0001$. Overall, female rats (open circles) had shorter latencies that male rats (black circles) $p = 0.043$. **(B)** All rats also made fewer errors per trial as training continued $p < 0.0001$, with females making fewer errors than male rats $p = 0.046$. (**C)** Prods per trial also decreased across the four training days $p < 0.0001$. There was no sex difference in the number of prods per trial, $p = 0.084$. Data are reported as mean ± standard error of the mean. Each data point represents an individual rat.

Acrobatic Training Increased Synaptogenesis and Decreased Synapse Length

Per Purkinje cell, the MC group had a reduced density of parallel fiber-Purkinje cell synapses ($M = 165{,}156$, $SEM = 13{,}405$) compared to the AT group ($M = 271{,}140$, $SEM = 31{,}341$; $F_{(1,12)} = 9.174$, $p = 0.011$; **Fig. 2A-C**). There was no sex difference in the density of parallel fiber-Purkinje cell synapses between males and females ($F_{(1,12)} = 0.530$, $p = 0.481$). The length of the parallel fiber-Purkinje cell synapses were longer in the MC group ($M = 0.310$, $SEM = 0.0131$) relative to the AT group ($M = 0.260$, $SEM = 0.0097$; $F_{(1,12)} = 8.682$, $p = 0.012$; **Fig. 2D**). There was no difference in the circumference of the Purkinje cell spines between the MC and AT groups ($F_{(1,12)} = 1.919$, $p = 0.191$; **Fig. 2E**). Synapse length ($F_{(1,12)} = 0.025$, $p = 0.876$; **Fig. 2D**) and spine circumference ($F_{(1,12)} = 0.766$, $p = 0.399$; **Fig. 2E**) did not differ between sexes.

Figure 2

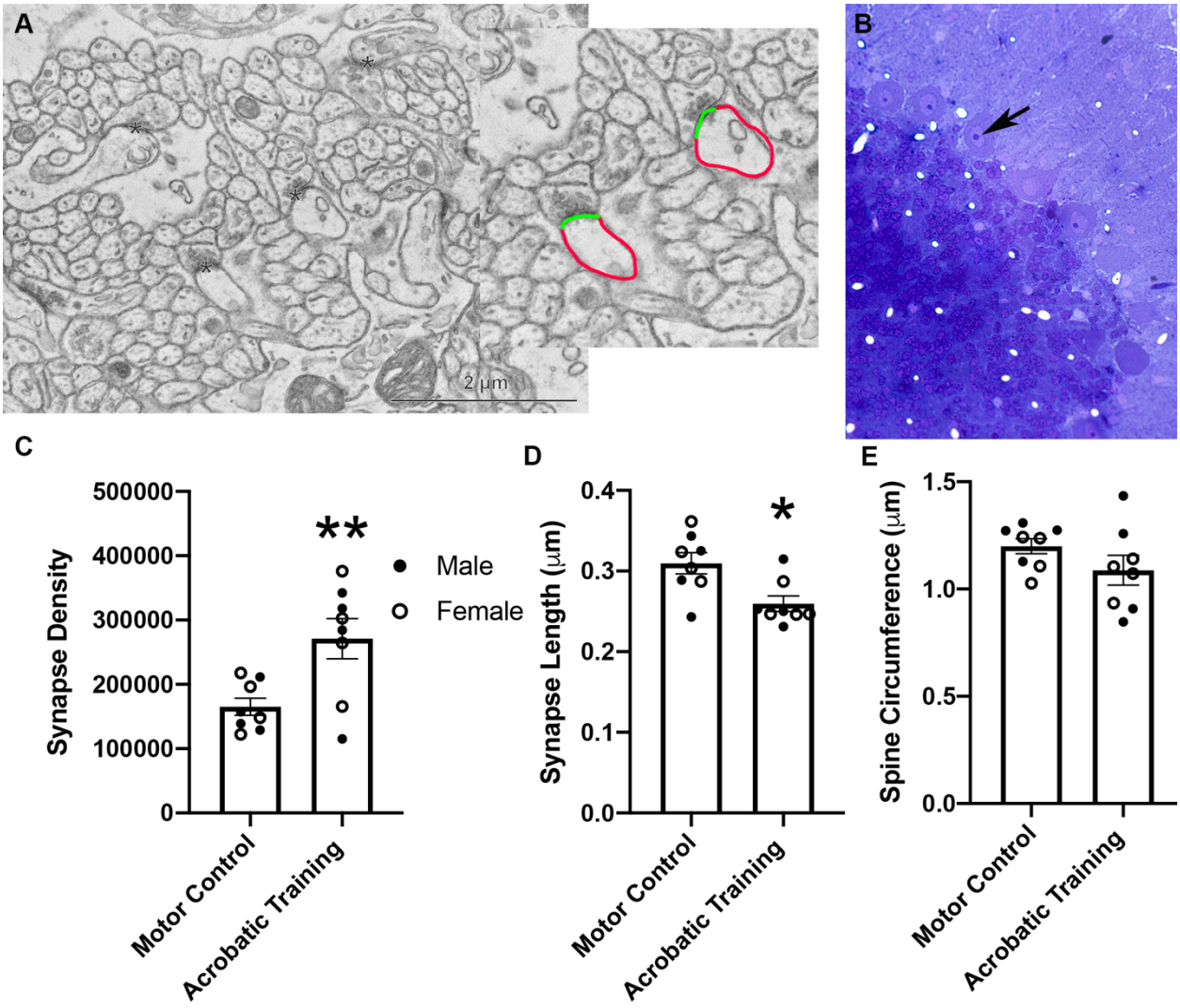

Figure 2: Synaptic plasticity following acrobatic training. (A) Representative electron micrograph with parallel fiber-Purkinje cell synapses labeled (*). These were the synapses quantified using the physical disector method. The length of these quantified synapses was also measured (green), as was the circumference of the Purkinje cell spine (red). **(B)** To obtain the density of parallel fiber-Purkinje cell synapses per Purkinje cell, the density of Purkinje cells was also quantified using the physical disector method. The dark purple Purkinje cell nucleolus (arrow) was the feature used to count Purkinje cells. **(C)** Acrobatic training increased the density of synapses per Purkinje cell compared to the motor control group $^{**}p = 0.011$. **(D)** Acrobatic training also decreased the length of the parallel fiber-Purkinje cell synapses, relative to the motor control group $^{*}p = 0.012$. **(E)** Acrobatic training did not affect spine circumference, $p > 0.05$. There were no sex differences in any of these measures, $p > 0.05$. Data are reported as mean ± standard error of the mean. Each data point represents an individual rat.

Acrobatic Training Increased Astrocytic Volume and Ensheathment of Synapses

The MC group had a reduced astrocyte volume fraction ($M = 0.130$, $SEM = 0.005$) compared the AT group ($M = 0.162$, $SEM = 0.008$; $F_{(1,12)} = 12.47$, $p = 0.004$; **Fig. 3A,C**). In addition to showing an overall increase in astrocyte volume fraction, there was also an increase in the fraction of astrocytic coverage of the Purkinje cell spines that formed synapses with parallel fibers in the AT group ($M = 0.887$ $SEM = 0.0204$) compared to the MC group ($M = 0.764$, $SEM = 0.045$; $F_{(1,12)} = 7.313$, $p = 0.019$; **Fig. 3B,D**). No sex differences were found in overall astrocyte volume fraction ($F_{(1,12)} = 1.407$, $p = 0.259$; **Fig. 3C**) or the fraction of astrocytic Purkinje cell spine coverage ($F_{(1,12)} = 1.206$, $p = 0.\ 294$; **Fig. 3D**).

Figure 3

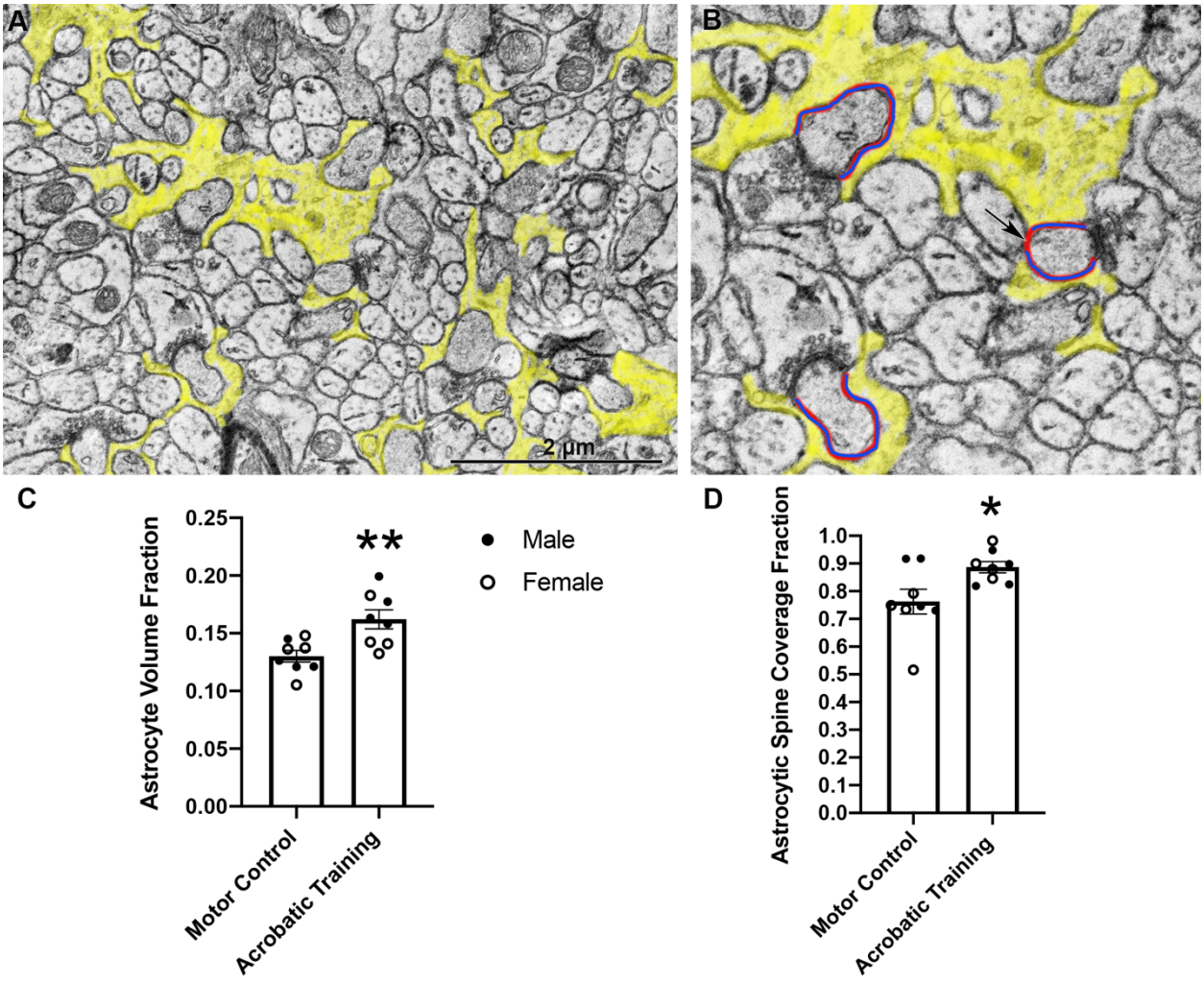

Figure 3: Astrocytic plasticity following acrobatic training. **(A)** Representative electron micrograph of the molecular layer of the cerebellar paramedian lobule. Astrocytic processes are shaded in yellow. To quantify astrocyte volume fraction, a point grid was overlaid on these images, and the points that fell on astrocytic processes were counted and then divided by the total number of points on the grid. **(B)** To quantify the degree of astrocytic Purkinje cell spine coverage, the circumference of the Purkinje cell spine covered by astrocytic processes (blue) was divided by the total circumference of the spine (red). An area of a spine not covered by astrocytic processes is labeled (black arrow). **(C)** Acrobatic training increased astrocyte volume fraction $^{**}p = 0.004$ and **(D)** astrocytic spine coverage fraction of Purkinje cell spines that formed synapses with parallel fibers $^{*}p = 0.019$, relative to the motor control group. There were no sex differences detected in either measure, $p > 0.05$. Data are reported as mean ± standard error of the mean. Each data point represents an individual rat.

Experiment 2

Motor Performance Testing

CNO Treatment did not Affect Open Field Locomotor Behavior. There was no difference in the number of grids crossed in the open field based on saline vehicle or CNO treatment ($F_{(1,31)} = 0.850$, $p = 0.773$; **Fig. 4A**). There were no differences in the number of grids crossed between sexes (male or female; $F_{(1,31)} = 0.481$, $p = 0.493$) or between virus types (mCherry control or hM4Di DREADD; $F_{(1,31)} = 1.139$, $p = 0.294$). Similarly, there were no differences in the number of rears in the open field based on saline or CNO treatment ($F_{(1,31)} = 0.018$, $p = 0.895$; **Fig. 4B**), and there were no differences between sexes ($F_{(1,31)} = 0.077$, $p = 0.783$) or virus types ($F_{(1,31)} = 2.884$, $p = 0.099$).

hM4Di DREADD Rats Treated with CNO had Shorter Rotarod Fall Latencies. The mCherry control virus group ($M = 35.214$, $SEM = 3.819$) had longer latencies to fall from the rotating beam compared to the hM4Di DREADD group ($M = 27.069$, $SEM = 3.132$; $F_{(1,18)} = 4.674$, $p = 0.044$; **Fig. 4C**). When both of the virus groups were treated with CNO, the hM4Di DREADD virus group ($M = 18.684$, $SEM = 4.175$) had a shorter fall latency compared with the mCherry control group ($M = 35.453$, $SEM = 4.667$; $p = 0.015$; **Fig. 4C**), but there were no differences between the mCherry control and hM4Di DREADD virus groups in fall latency when both were treated with saline vehicle ($p = 0.376$). Shorter fall latencies are indicative of motor coordination deficits. There were no sex differences in rotarod performance ($F_{(1,18)} = 0.038$, $p = 0.847$).

CNO Treatment did not Affect Rodent Gait. There was no difference in stride width between the front paws ($F_{(1,31)} = 0.588$, $p = 0.449$) or back paws ($F_{(1,31)} = 0.017$, $p = 0.898$) within groups based on saline or CNO treatment (**Fig. 4D**). There was also no difference in left

stride length ($F_{(1,31)} = 0.277$, $p = 0.637$) or right stride length ($F_{(1,31)} = 0.501$, $p = 0.484$) based on saline vehicle or CNO treatment (**Fig. 4E**). Females had shorter stride widths between the front ($M = 3.227$, $SEM = 0.120$) and back ($M = 2.936$, $SEM = 0.123$) paws relative to males ($M = 3.726$, $SEM = 0.117$; $F_{(1,31)} = 8.829$, $p = 0.006$; $M = 3.455$, $SEM = 0.119$; $F_{(1,31)} = 9.193$, $p = 0.005$), regardless of CNO or saline treatment, or virus type.

Figure 4

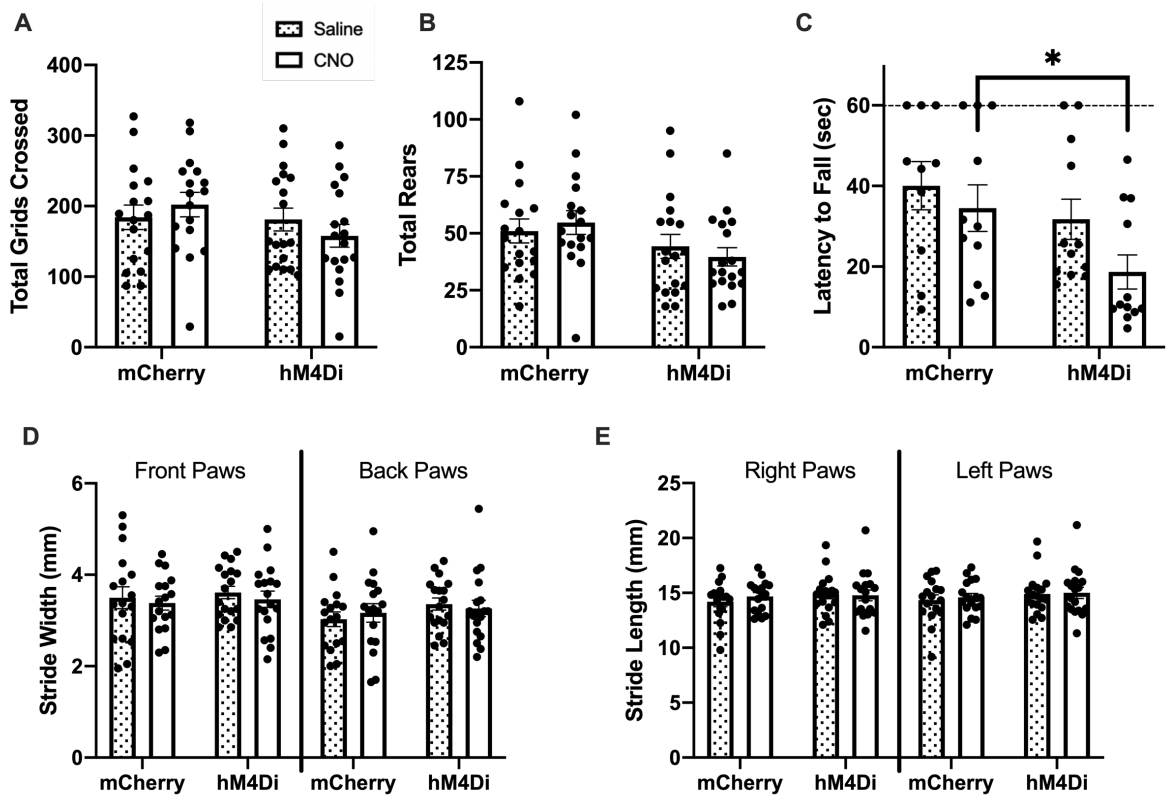

Figure 4: Motor performance testing comparing saline vehicle and CNO treatment between astrocytic mCherry control and hM4Di DREADD virus groups. **(A)** There were no differences in the number of grids crossed or **(B)** the number of rears between the mCherry control and hM4Di DREADD rats when they were treated with CNO or saline vehicle in the 10-min open field session, $p > 0.05$. **(C)** hM4Di DREADD rats treated with CNO had shorter latencies to fall from the rotarod, compared to mCherry control rats treated with CNO, $*p = 0.015$. **(D)** There were no differences in stride width or **(E)** length between mCherry control rats and hM4Di DREADD rats treated with CNO or saline vehicle, $p > 0.05$. Data are reported as mean ± standard error of the mean. Each data point represents an individual rat.

Acrobatic Training

Behavioral Performance on the Acrobatic Course Improved Across Days. The AT rats had an overall improvement in performance on the acrobatic course across the four days of training (**Fig. 5A-C**). The latency/trial/day ($F_{(3,42)} = 66.082$; $p < 0.0001$; **Fig. 5A**), errors/trial/day ($F_{(3,42)} = 41.230$, $p < 0.0001$; **Fig. 5B**), and prods/trial/day ($F_{(3,42)} = 74.723$; $p < 0.0001$; **Fig. 5C**) significantly decreased as acrobatic training progressed. This demonstrates all rats were acquiring the motor-skills necessary to complete the acrobatic course, regardless of sex or virus type.

hM4Di DREADD Rats had Longer Acrobatic Trial Completion Latencies. For latency, there was a significant difference between virus types, with the mCherry control group ($M = 117.631$, $SEM = 6.616$) traversing the course faster than the hM4Di DREADD group ($M = 161.976$, $SEM = 5.917$, $F_{(1,14)} = 24.962$, $p = 0.0002$; **Fig. 5D**), regardless of training day or sex. The interaction between training day and virus condition was also significant ($F_{(3,42)} = 3.239$, $p = 0.031$). The mCherry control virus group had significantly shorter latencies/trial, relative to the hM4Di DREADD groups on Day 1 ($p = 0.007$), Day 2 ($p = 0.001$), Day 3 ($p = 0.0001$) and Day 4 ($p = 0.001$; **Fig. 5A**). Similar to Experiment 1, there was also a sex difference for latency where male rats were slower to complete the acrobatic course ($M = 150.965$, $SEM = 6.376$) compared to female rats ($M = 128.642$, $SEM = 6.276$, $F_{(1,14)} = 6.325$, $p = 0.025$; **Fig. 5G**), regardless of virus type or training day.

hM4Di DREADD Rats Made More Errors on the Acrobatic Course. For errors, there was a significant difference between virus types with the mCherry control group ($M = 11.073$, $SEM = 2.100$) making fewer errors than the hM4Di DREADD group ($M = 18.510$, $SEM = 1.878$, $F_{(1,14)} = 6.970$, $p = 0.019$; **Fig. 5E**), regardless of training day or sex. The interaction between

training day and virus type was also significant ($F_{(3,42)} = 3.513$, $p = 0.023$). The mCherry control virus group made significantly fewer errors on Day 1 ($p = 0.033$), Day 3 ($p = 0.018$), and Day 4 ($p = 0.025$) compared to the hM4Di DREADD group (**Fig. 5B**). No sex differences were identified for the number of errors made between males and females ($F_{(1,14)} = 1.570$, $p = 0.231$), regardless of training day or virus type (**Fig. 5H**).

Prods between hM4Di DREADD and mCherry Control Rats did not Differ on the Acrobatic Course. For prods, there were no differences between virus types although the decreased number of prods for the mCherry control group ($M = 29.516$, $SEM = 2.401$) relative to the hM4Di DREADD group ($M = 36.156$, $SEM = 2.147$, $F_{(1,14)} = 6.970$, $p = 0.058$; **Fig. 5F**) approached statistical significance. The interaction between training day and virus type was significant ($F_{(3,42)} = 3.718$, $p = 0.019$), and the mCherry control group had fewer prods on Day 1 ($p = 0.015$) relative to the hM4Di DREADD group (**Fig. 5C**). No sex differences were identified for the number of prods between males and females ($F_{(1,14)} = 3.857$, $p = 0.070$), regardless of training day or virus type (**Fig. 5I**).

hM4Di DREADD Rats Were Slower on Trial 1; Speed Improved at the Same Rate Between Virus Types. To assess whether the hM4Di DREADD group exhibited a motor impairment prior to beginning acrobatic training, performance on the first trial (Day 1, Trial 1) was assessed. If a learning deficit was solely driving performance differences, performance between the mCherry control and hM4Di DREADD group should be similar on the first trial, when both groups have had no experience on the course. On Day 1, Trial 1, the mCherry control group ($M = 220.179$, $SEM = 23.178$) had shorter latencies than the hM4Di DREADD group ($M = 287.004$, $SEM = 20.731$, $F_{(1,14)} = 4.618$, $p = 0.0496$; **Fig. 6A**). The difference in the number of errors ($F_{(1,14} = 3.107$, $p = 0.0997$; **Fig. 6B**) and the number of prods ($F_{(1,14)} = 0.149$, $p = 0.706$;

Fig. 6C) between virus conditions on Day 1, Trial 1 did not differ. Longer latencies on the first trial of training in the hM4Di DREADD group suggests a motor impairment contributed to performance deficits.

Additionally, the percent change in latency was compared between training days (percent change from Day 1 to Day 2, Day 2 to Day 3, and Day 3 to Day 4), to determine if the rats expressing the hM4Di DREADD and mCherry control virus were learning, or getting faster at the acrobatic course, at the same rate. The percent change in latency for the mCherry control virus and the hM4Di DREADD group decreased as training progressed ($F_{(2,28)} = 9.966$, $p = 0.001$), and there was no interaction between virus type and day ($F_{(2,28)} = 0.055$, $p = 0.947$). Importantly, there was no between group difference for virus type ($F_{(1,14)} = 0.067$, $p = 0.799$), meaning the percent change in latency between days was the same for rats expressing the mCherry control or hM4Di DREADD virus (**Fig. 6D**). This suggests that although the hM4Di DREADD rats were slower at completing the course, both virus types got faster at the same rate across days. There was an interaction between sex and day ($F_{(2,28)} = 6.579$, $p = 0.005$), and an analysis of simple effects showed females had a smaller percent change from Day 3 to Day 4 ($M = 0.043\%$, $SEM = 2.094$) compared to males ($M = 19.653\%$, $SEM = 2.094$; $p = 0.0001$; **Fig. 6D**).

Figure 5

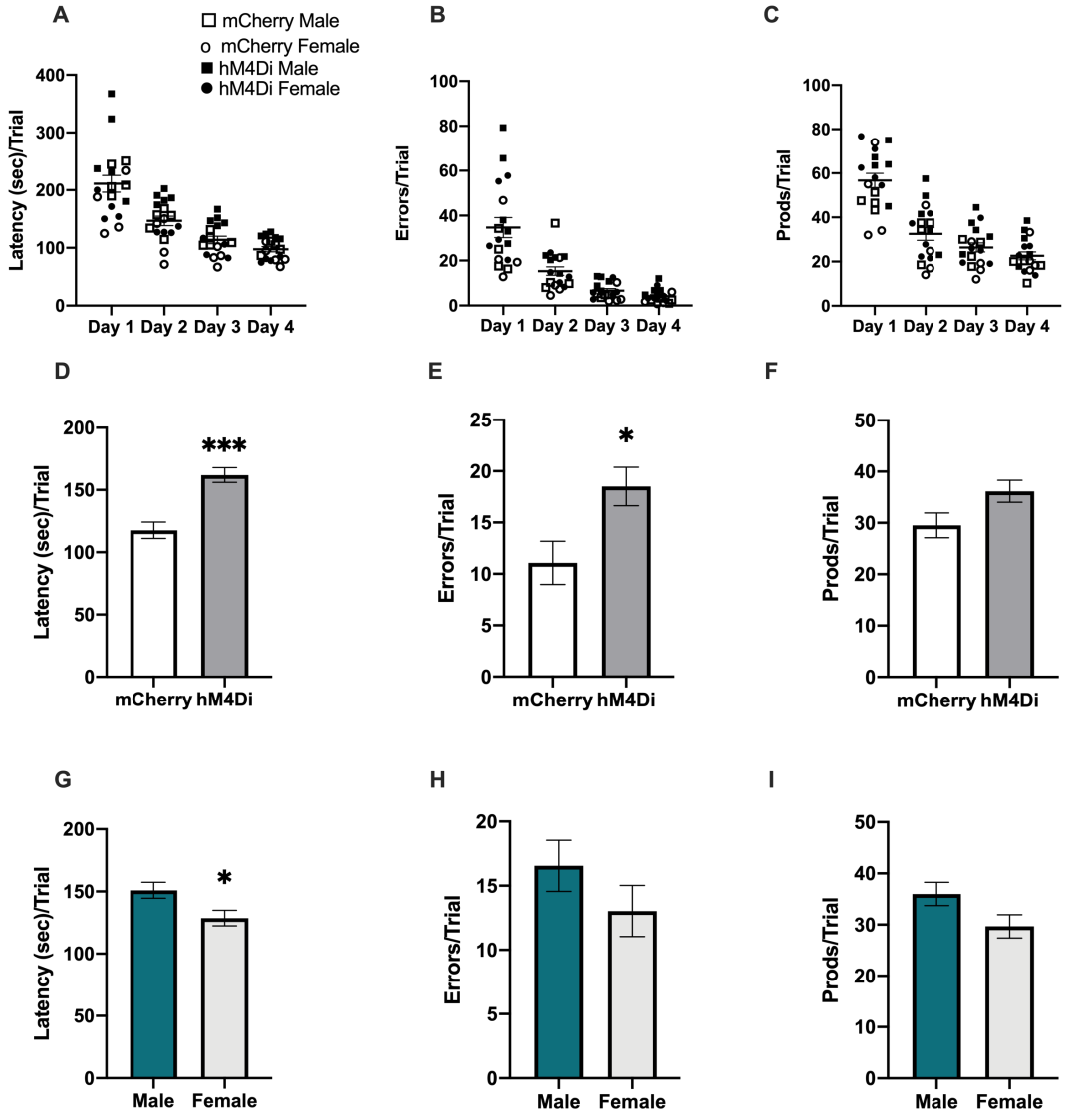

Figure 5: Acrobatic training performance for rats expressing the astrocytic mCherry control and hM4Di DREADD viruses. All rats, regardless of sex and virus type showed **(A)** decreased latencies, $p < 0.0001$ **(B)** decreased errors, $p < 0.0001$ and **(C)** decreased prods, $p < 0.0001$, across the four training days. **(D)** The mCherry control group took fewer sec to complete trials of the acrobatic course compared to the astrocytic hM4Di DREADD group ***$p = 0.0002$. **(E)** The mCherry control group also made fewer errors/trial on the acrobatic course than the hM4Di DREADD group *$p = 0.019$. **(F)** The mCherry control group and hM4Di DREADD group did not differ in the number of prods/trial on the acrobatic course, $p > 0.05$. **(G)** Males exhibited longer latencies than females/trial on the acrobatic course *$p = 0.025$. **(H)** Males and females did not differ in the number of errors or **(I)** prods per trial on the acrobatic course, $p > 0.05$. Data are reported as mean ± standard error of the mean. Each data point represents an individual rat.

Figure 6

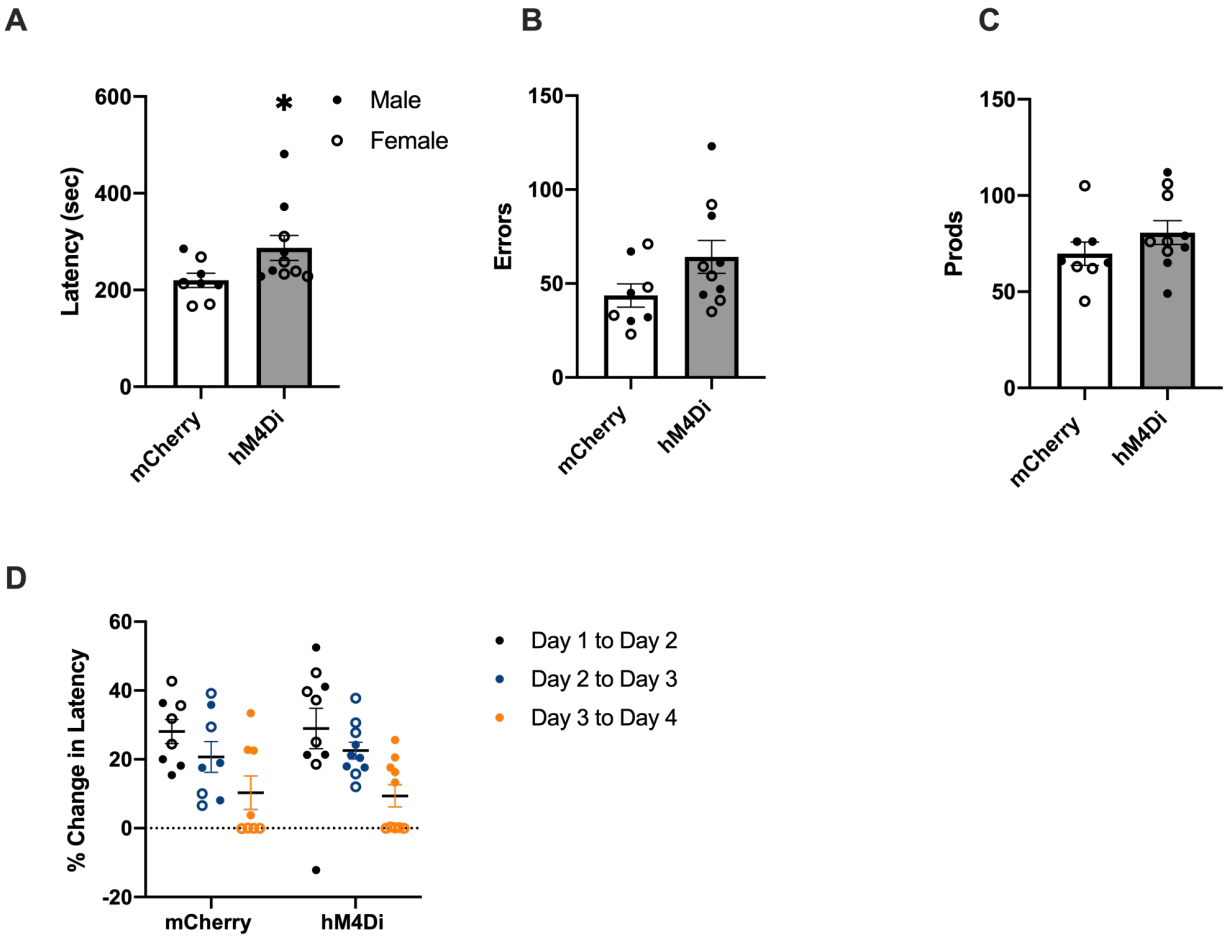

Figure 6: Acrobatic task performance on the first trial and percent change in latency between days for astrocytic mCherry control and hM4Di DREADD rats. **(A)** mCherry control rats exhibited shorter latencies completing Trial 1 compared to the hM4Di DREADD rats *$p = 0.0496$. **(B)** mCherry control and hM4Di DREADD rats did not differ in the number of errors or **(C)** the number of prods on Trial 1, $p > 0.05$. **(D)** There was no difference in the percent change in latency between days for the mCherry control and hM4Di DREADD rats. Rats expressing the hM4Di DREADD and mCherry control virus were getting faster at the task at the same rate. From Day 3 to Day 4, female rats had a lower percent change in speed compared to males, $p = 0.0001$. Data are reported as mean ± standard error of the mean. Each data point represents an individual rat.

Immunofluorescence

All Rats Exhibited Astrocytic Virus Expression in the PML. Virus expression in the PML was verified (n = 12/virus type). Virus expression was primarily restricted to the PML (**Fig. 7A**) and morphology appeared astrocytic (**Fig. 7B-G**). In regard to specificity, 96.6% ± 1.20% of the cells that expressed the mCherry control virus colocalized with GFAP (**Fig. 7B-D**) and 91.3% ± 4.78% of cells that expressed the hM4Di DREADD virus colocalized with GFAP (**Fig. 7E-G**). Virus expressing cells that did not colocalize with GFAP were primarily interneurons in the molecular layer (**Fig. 7G**).

Figure 7

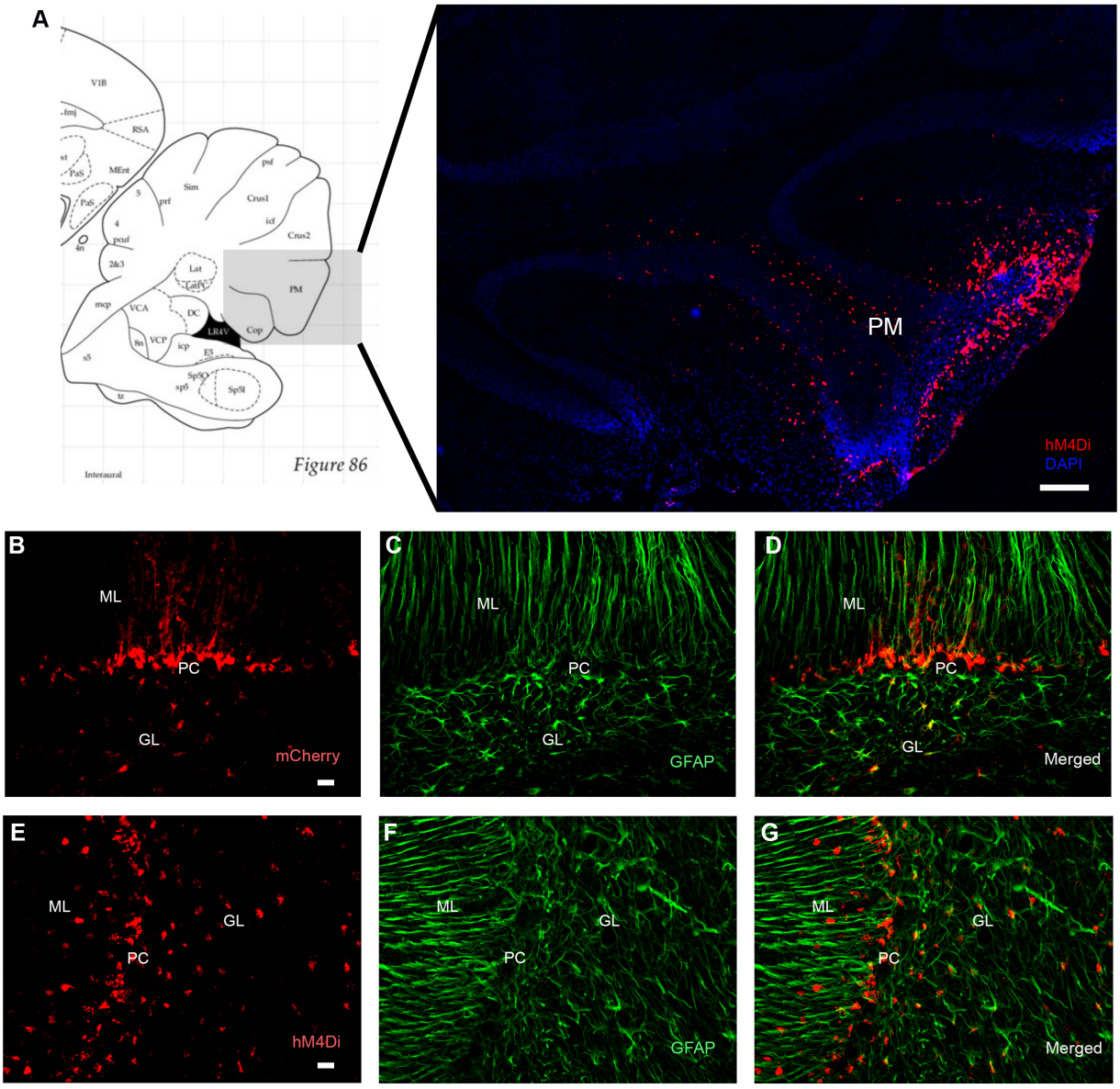

Figure 7: Astrocytic mCherry control and hM4Di virus expression in the rat paramedian lobule (PM). (A) The figure on the left (Paxinos and Watson, 2007) displays the PM (grey box) in the rat brain atlas, and a representative image of this region is on the right with DAPI (blue) and virus (red) expression. hM4Di-mCherry DREADD and mCherry control virus expression was largely localized to the PM, scale bar = 200 µm **(B-D)** mCherry control virus (red) and **(E-G)** hM4Di DREADD virus (red) primarily targeted astrocytes labeled with GFAP (green), scale bars = 20 µm. There was robust expression in Bergmann glia somas in the Purkinje cell layer (PC) and weaker expression in Bergmann glial processes in the molecular layer (ML). Expression was also detected in velate astrocytes in the granular layer (GL). Atlas image is from Figure 86 in Paxinos, G., & Watson, C. (2007). *The rat brain in stereotaxic coordinates.*

hM4Di Rats had Increased c-Fos; Acrobatic Training did not affect c-Fos Levels.

The mCherry control group had less c-Fos expression colocalized with the virus ($M = 0.081$, $SEM = 0.022$) compared to the astrocytic hM4Di DREADD group ($M = 0.187$, $SEM = 0.022$, $F_{(1,16)} = 12.226$, $p = 0.003$; **Fig. 8A-I**) regardless of sex and training condition. Additionally, the mCherry control group had less c-Fos expression that was not colocalized with the virus ($M = 0.142$, $SEM = 0.029$) relative to the hM4Di DREADD group ($M = 0.250$, $SEM = 0.029$, $F_{(1,16)} = 6.873$, $p = 0.019$; **Fig. 8J**). Together this suggests the astrocytic hM4Di DREADD was activated, and this activation impacted neighboring cells labeled with DAPI. Alternatively, it is possible that these non-colocalized cells were also weakly expressing the hM4Di DREADD virus, at a level not captured with the thresholding methods employed. Acrobatic training did not affect c-Fos expression itself ($F_{(1,16)} = 0.658$, $p = 0.429$). However, there was significant interaction between virus type and training condition for non-colocalized c-Fos, and the hM4Di DREADD virus group that completed acrobatic training had the highest c-Fos expression that was not colocalized with the virus, relative to all other groups ($F_{(1,16)} = 11.748$, $p = 0.003$; **Fig. 8J**). There were no sex differences in colocalized ($F_{(1,16)} = 0.296$, $p = 0.594$) or non-colocalized ($F_{(1,16)} = 0.715$, $p = 0.410$) c-Fos expression.

Figure 8

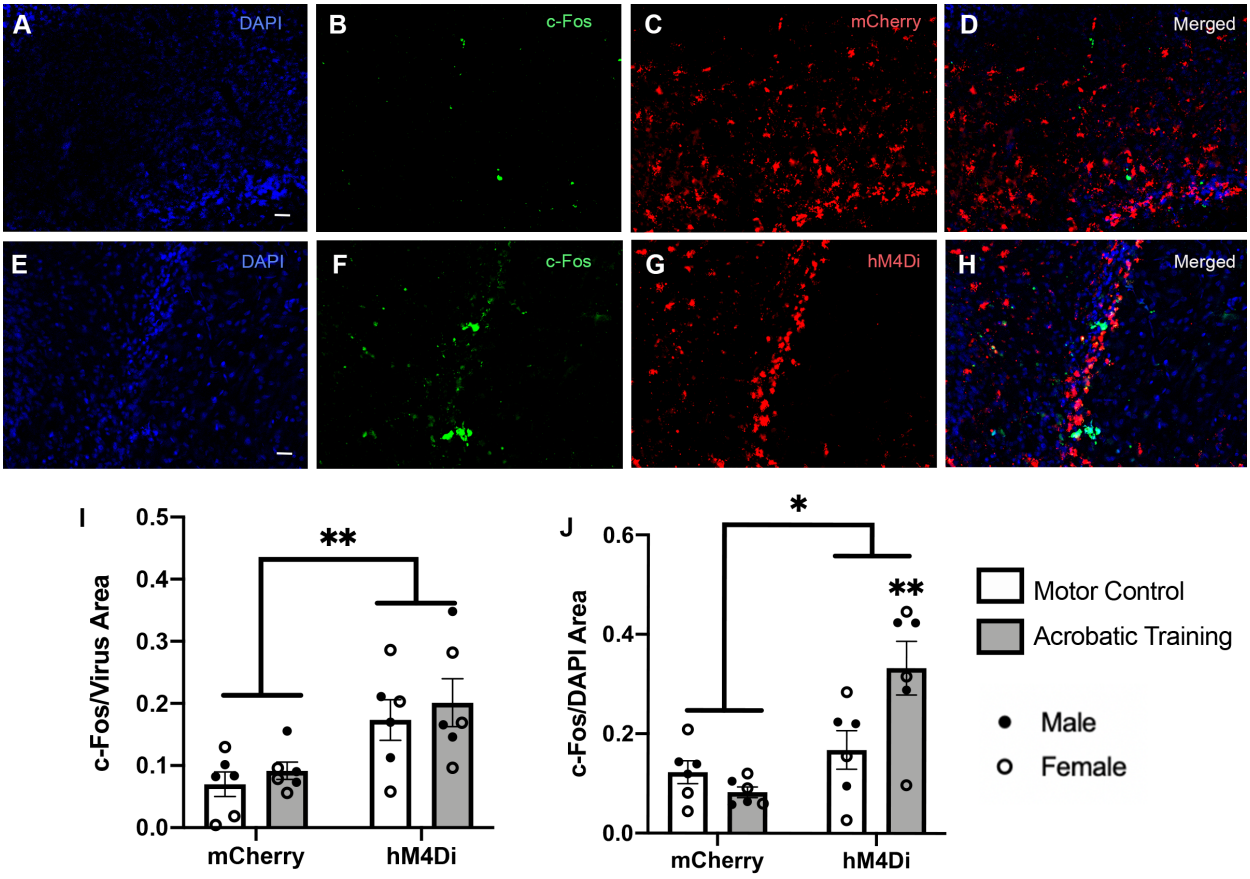

Figure 8: c-Fos expression in rats expressing astrocytic mCherry control and hM4Di DREADD viruses. (A-D) Representative images of DAPI (blue), c-Fos (green), and mCherry control virus (red) or **(E-H)** hM4Di DREADD (red) expression. **(I)** Rats in the hM4Di DREADD group had increased c-Fos expression that colocalized with virus, relative to the mCherry virus group $^{**}p = 0.003$. **(J)** The hM4Di DREADD group also had increased c-Fos expression that was not colocalized with virus, relative to the mCherry control group $^{*}p = 0.019$, and the hM4Di DREADD rats that completed acrobatic training had the highest c-Fos expression compared to all other groups $^{**}p = 0.003$.

Electron Microscopy

hM4Di Rats had Increased Synapse Density. The mCherry control virus group had fewer parallel fiber-Purkinje cell synapse densities per Purkinje cell ($M = 173{,}518$, $SEM = 16{,}717$) relative to the hM4Di DREADD virus group ($M = 247{,}361$, $SEM = 16{,}717$; $F_{(1,16)} = 9.756$, $p = 0.007$; **Fig. 9A**), regardless of sex and training condition. There was no difference in synapse density between sexes ($F_{(1,16)} = 0.009$, $p = 0.924$) or between training conditions ($F_{(1,16)} =$

0.726, $p = 0.407$). This lack of difference between the AT and MC groups was likely in part driven by the elevated parallel fiber-Purkinje cell synaptogenesis in the MC rats expressing the hM4Di DREADD virus (**Fig. 9A**).

hM4Di Expression and Acrobatic Training Increased Astrocyte Volume. The mCherry control virus group also had a reduced astrocytic volume fraction ($M = 0.139$, $SEM = 0.007$) compared to the hM4Di DREADD virus group ($M = 0.160$, $SEM = 0.007$; $F_{(1,16)} = 4.868$, $p = 0.042$; **Fig. 9B,C**), regardless of sex and training condition. There was also a training effect for astrocytic volume fraction, with the MC group having reduced astrocyte volume fractions ($M = 0.135$, $SEM = 0.007$) compared with the AT group ($M = 0.164$, $SEM = 0.007$; $F_{(1,16)} = 9.033$, $p = 0.008$; **Fig. 9B,D**), regardless of virus type or sex. There was no sex difference in overall astrocyte volume fraction ($F_{(1,16)} = 0.253$, $p = 0.621$).

Figure 9

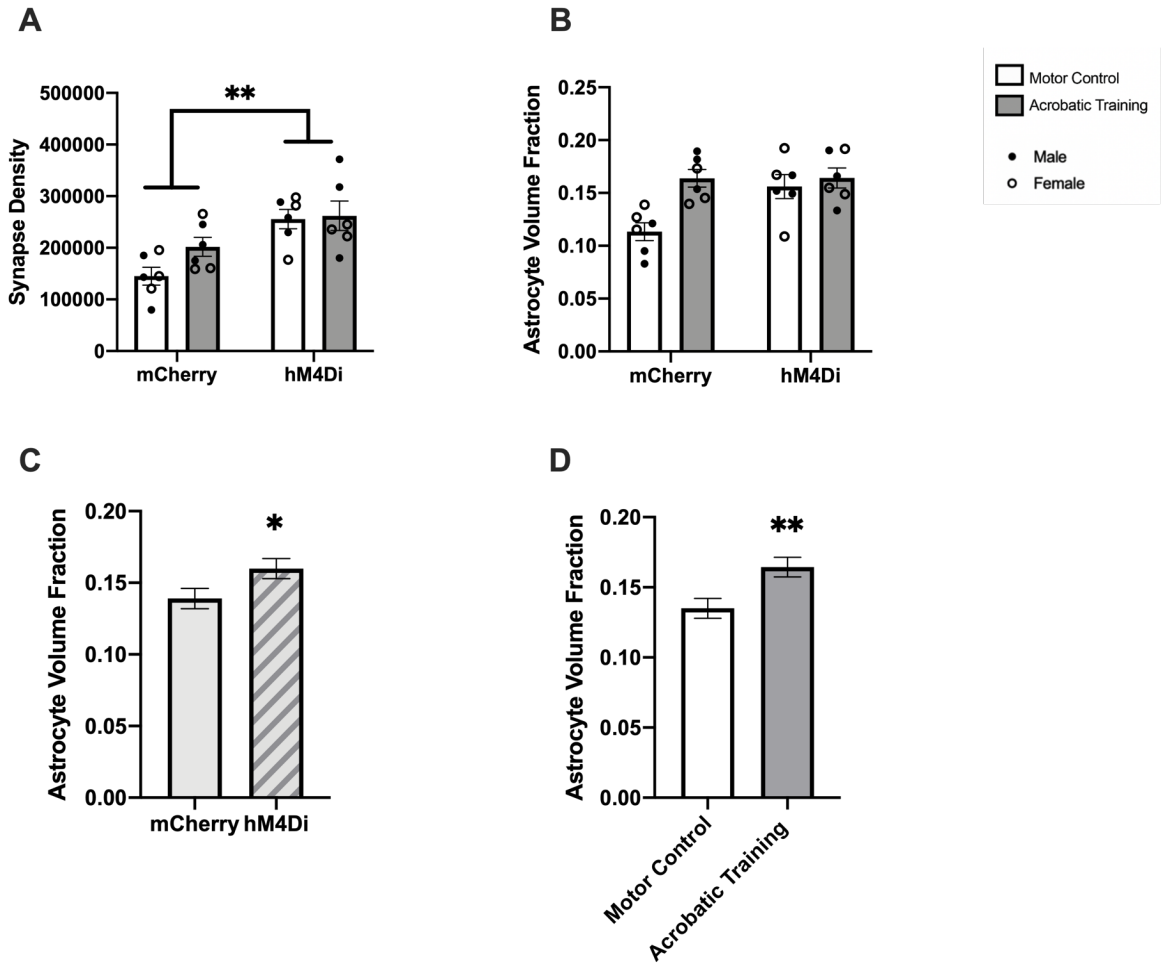

Figure 9: Synaptic and astrocytic plasticity for hM4Di DREADD and mCherry control rats that completed acrobatic or motor control training. (A) The hM4Di DREADD group had increased parallel fiber-Purkinje cell synaptogenesis, compared to the mCherry control virus group $^{**}p = 0.007$. **(B)** Astrocytic volume fraction for rats in the mCherry control virus and hM4Di virus groups. **(C)** The hM4Di DREADD group had an elevated astrocyte volume fraction compared to the mCherry control virus group $^{*}p = 0.042$. **(D)** The acrobatic training group also had an increased astrocytic volume fraction compared to the motor control group $^{**}p = 0.008$. Data are reported as mean ± standard error of the mean. Each data point represents an individual rat.

Chapter Four: Discussion

Summary of Aims, Hypotheses, and Key Findings

These experiments had three primary aims. Experiment 1 aimed to characterize early structural plasticity, including synaptogenesis and astrocytic hypertrophy, during the acquisition phase of motor-skill learning. It was hypothesized that increased parallel fiber-Purkinje cell synaptogenesis and astrocytic hypertrophy would be detectable after only four days of acrobatic training. This hypothesis was supported. The AT rats had elevated synaptogenesis and astrocyte volume fractions compared to the MC group after four days of training. In addition, the AT group also had reduced synapse lengths and increased astrocytic ensheathment of parallel fiber-Purkinje cell spines. A sex difference was also detected in behavioral training, with female rats completing the acrobatic course faster, with fewer errors, compared to male rats. No sex differences were identified in analyses of ultrastructure.

Experiment 2 first aimed to determine whether cerebellar astrocytic activity, via hM4Di DREADD activation, impairs or enhances motor-skill learning on the acrobatic course. It was hypothesized that the activation of Gi-signaling through the hM4Di DREADD would impair motor-skill learning on the acrobatic course. This hypothesis was partially supported. Performance significantly improved across acrobatic training days for groups expressing the mCherry control and hM4Di DREADD viruses, indicating that all rats were learning the task. However, hM4Di DREADD activation did impair performance on the acrobatic course, as indicated by longer latencies and more errors committed by the hM4Di DREADD virus group compared to the mCherry control virus group. Motor performance testing revealed that a motor coordination impairment may be driving this effect. The hM4Di DREADD group treated with

CNO had shorter fall latencies compared to the mCherry control virus group treated with CNO on the rotarod. Furthermore, on Day 1 Trial 1 of acrobatic training, a point at which significant motor learning has not yet taken place, the hM4Di DREADD group exhibited longer latencies on this trial compared to the mCherry control virus group. The number of errors and prods on Day 1, Trial 1 did not differ between groups. As in Experiment 1, a sex difference was also identified, with female rats, regardless of virus type, completing the acrobatic course faster than male rats.

The second aim of Experiment 2 was to determine if activation of the hM4Di DREADD in astrocytes in the PML impacts the increased synaptogenesis and astrocytic hypertrophy typically associated with motor-skill learning. It was hypothesized that synaptogenesis and astrocytic hypertrophy would be decreased by activating Gi-signaling in cerebellar astrocytes. This hypothesis was not supported. hM4Di-DREADD activation increased synaptogenesis and astrocytic hypertrophy in both the AT and MC groups. Although speculative, these findings indicate that this enhanced ultrastructural plasticity may be deleterious to motor performance. It was also hypothesized that c-Fos would be increased in neurons in all of the rats that completed acrobatic training, except for in the hM4Di DREADD group. This hypothesis was not supported. Compared to the MC group, c-Fos was not elevated in the AT group after four days of training, and hM4Di-DREADD activation increased c-Fos expression in cells both colocalized and non-colocalize with the virus. It was recently found that, in contrast to neuronal DREADD experiments, astrocytic hM4Di and hM3Dq activation both increase c-Fos in astrocytes (Kol et al., 2020). Our results are similar to these recent findings and indicate that hM4Di DREADD was activated by CNO, and that this activation may affect neighboring neuronal cells. No sex differences were identified in c-Fos expression or cerebellar ultrastructure between groups.

Behavioral Findings

Acrobatic Motor-Skill Learning and hM4Di DREADD Activation

Rats in the AT group for Experiment 1 and Experiment 2 all acquired the acrobatic course. AT rats completed the course faster, made fewer errors, and required fewer prods to continue traversing the course across the four training days. Improved performance on the acrobatic course with continued training is well established in both male and female rats (Black et al., 1990; Federmeier et al., 2002; González-Tapia et al., 2015; 2017; Kleim et al., 1996; 1997, 1998; 2007; Lee et al., 2013). Experiment 2 of this dissertation expands our understanding of the contributions of astrocytes to motor behavior on the acrobatic course finding rats expressing the hM4Di DREADD have increased latencies per trial and make more errors per trial, relative to the mCherry control group. These differences in latency and errors were detectable on nearly all days of acrobatic training. Importantly, our motor performance testing found that when rats were treated with CNO, those expressing hM4Di DREADD had shorter fall latencies on the rotarod test of motor coordination compared to the mCherry control group. On the initial trial of the acrobatic course, the hM4Di DREADD rats were also slower to complete the obstacles compared to the mCherry control group. Although being slower on the acrobatic course itself does not indicate a motor coordination deficit, there was also no difference in baseline locomotor behavior in the open field suggesting slower navigation on the acrobatic course may be related to the challenge of making skilled movements. Furthermore, the percent change in latency between training days was the same for the hM4Di DREADD and mCherry control rats. Together, this indicates that the activation of astrocytic Gi-signaling in the PML may be producing a motor coordination deficit, rather than a motor learning deficit. The hM4Di DREADD rats did get better at the acrobatic course across days, showing that they were acquiring the skills necessary

to complete the task. This motor-skill learning was just occurring more slowly because the hM4Di DREADD rats had to overcome a motor coordination impairment. Our findings were similar to those of Saab et al. (2012), where they found that when Bergmann glial processes are retracted in adulthood, mice exhibit deficits in fine motor coordination. Mice with retracted Bergmann glial processes were able to acquire the motor skills necessary to cross the Erasmus ladder with repeated training. However, during a challenge condition where the ladder rungs were elevated, the mice with retracted Bergmann glial processes made more missteps (Saab et al., 2012). The researchers attributed this effect to deficits in fine motor coordination, not learning. Accurate coordination of the forelimbs is critical for the completion of the complex obstacles that comprise the acrobatic paradigm, and deficits in motor coordination would certainly impair performance on this task. Conversely, the complexity of the acrobatic paradigm means that it also relies on other motor processes, including balance and proprioception, and non-motor processes, including motivation and non-motor learning (Lee et al., 2013). Although deficits in rotarod performance suggest a motor coordination deficit is present, characterizing this motor performance deficit on the acrobatic course after astrocytic hM4Di DREADD activation using simpler motor assessments, such as the skilled forelimb reaching task, the Erasmus ladder, or tests of grip strength, is also necessary.

Acrobatic Training and Sex Differences

Although other experiments assessing behavioral performance on the acrobatic paradigm have employed both sexes (Black et al., 1990; Federmeier et al., 2002; González-Tapia et al., 2015; 2017; Kleim et al., 1996; 1997, 1998; 2007; Lee et al., 2013), previous experiments have not included both sexes within the same experiment to directly compare behavioral performance between male and female rats. Experiment 1 and Experiment 2 of this dissertation included both

male and female rats in the AT group. Female rats had shorter latencies (Experiment 1 and Experiment 2) and made fewer errors (Experiment 1) than male rats on the acrobatic course. On other motor learning tasks, female rodents have done better than males (Buitrago et al., 2004; Dalla & Shors, 2009; Wagner et al., 2013). For example, in a forelimb reaching task, female rats acquired the task faster than males, although all rats reached similar performance plateaus (Buitrago et al., 2004). These results on this forelimb reaching task are similar to those of our experiment. Successfully navigating many of the obstacles on the acrobatic course require precise forelimb movements, and, in Experiment 1, we also found that male and female rats exhibited the greatest difference in behavioral performance on the first two days of acrobatic training. Additionally, in Experiment 2 when percent change in latency was analyzed between days, female rats had a smaller percent change in speed compared to males between Day 3 and Day 4, likely because female rats are reaching asymptotic performance faster. There were no differences in cerebellar ultrastructure between sexes, but it would be interesting to see if analysis of synapse density earlier in training where performance differences between males and females is most robust would yield different results.

Interestingly, sex differences in motor performance have also been attributed to sex differences in motivation. Male and female rats were trained on an accelerating rotarod, which requires rats to maintain balance and motor coordination as they run on a rotating cylinder, and, in one condition, cold water was added below the rotarod to motivate the rats to stay on the rotarod. In the condition where the cold water was added, learning was enhanced in female rats, and this was attributed to the motivating properties of the cold water (DiFeo et al., 2015). Although motor learning is a central component of the acrobatic task, the task is complex and has aspects that are non-motor, including motivational features (Lee et al., 2013). The acrobatic

course is elevated, and this could be considered a motivating feature because if rats attempt to escape the course, they risk falling. Rats also received a food reward after completing each trial, which could be another motivating feature. It would be interesting to modify the motivating aspects of the acrobatic course in the future, to determine whether or not these features account for the enhanced performance observed in female rats. It should also be noted that, in some experiments, female rodents were found to be more active, moving faster and for longer distances, than male rodents (Bartling et al., 2017; Blizard et al., 1975; Tucker et al., 2016; Van Swearingen et al., 2013; Võikar et al., 2001). Although this does not explain the decreased rate of errors in female rats observed in Experiment 1, and we did not detect a sex difference in open field locomotion in Experiment 2, it is possible that the tendency for female rodents to exhibit increased locomotor activity contributed to their decreased latencies on the acrobatic task.

Ultrastructural Plasticity Findings

Acrobatic Training Rapidly Induces Synaptogenesis

Acrobatic training increases parallel fiber-Purkinje cell synapse formation in the cerebellar PML (Black et al., 1990; Federmeier et al., 2002; Kim et al., 2002; Kleim et al., 1997, 1998; Lee et al., 2013), and the results in Experiment 1 replicate and expand upon this effect. Although we did not detect an acrobatic training-induced elevation in synaptogenesis in Experiment 2, this is likely due to the high levels of synaptogenesis in hM4Di DREADD rats, regardless of training condition. The majority of experiments that have analyzed synaptogenesis in the cerebellum have done so after nearly one month of acrobatic training (Black et al., 1990; Federmeier et al., 2002; Kim et al., 2002; Kleim et al., 1998; Lee et al., 2013), with the earliest assessment completed after 10 days of training (Kleim et al., 1997). The first four days of acrobatic training have been considered the acquisition phase, where behavioral performance on

the task is improving. After five days of training rats enter the maintenance phase where performance on the task is optimal and stable (Kleim et al., 1996). We quantified synaptogenesis near the end of the acquisition phase, on day four, where rats show drastic improvement on the course, but performance is not quite asymptotic. Our results demonstrate synaptogenesis is already elevated at this timepoint. Detecting synaptogenesis early in training indicates the addition of these parallel fiber-Purkinje cell synapses occurs when rats are actively acquiring the task. Similarly, significant increases in synapses per neuron have also been detected in the motor cortex after only five days of acrobatic training (Kleim et al., 1996). In the motor cortex, synaptogenesis was increased significantly after 5, 10, and 20 days of training, and the density of synapses per neuron did not differ across these three days (Kleim et al., 1996). These results suggest that, once the task is learned after five days of training, it is not necessary to add additional synapses in the motor cortex. Our results imply a similar phenomenon is also occurring in the cerebellum, possibly at a faster rate. In the AT rats, the degree of synaptogenesis measured in the PML is similar in magnitude to those reported after 10, 20, and 30 days of training (Black et al., 1990; Kleim et al., 1997; Federmeier et al., 2002), and we did not detect an elevation in c-Fos with acrobatic training. In the motor cortex, c-Fos expression was highest during the initial five days of training and decreased when measured on Days 10 and 20, when the number of synapses added also stabilized (Kleim et al., 1996). In our experiment, it is possible that c-Fos expression in the PML was elevated earlier, on Day 1 or 2 of acrobatic training, and already decreased by Day 4. It could be that the majority of cerebellar learning and associated synaptogenesis has already occurred and therefore c-Fos is no longer elevated.

In Experiment 1, measurements of parallel fiber-Purkinje cell synapse length and Purkinje cell spine circumference were also completed. Plasticity in Purkinje cell spines in the

cerebellar PML has been assessed during the first six days of acrobatic training. In male rats, thin spines were elevated on all six days of training, reaching statistical significance on Days 1, 3, and 6 (González-Tapia et al., 2017). Thin spines were also increased after 26 days of acrobatic training (González-Tapia et al., 2015; Lee et al., 2007), along with mushroom and stubby spines (González-Tapia et al., 2015). In Experiment 1, we did not find a significant difference in Purkinje cell spine circumference after four days of acrobatic training, although the circumference of the spines did tend to be reduced in the AC group. In the future, it will be important to assess spine dynamics with standard methods such as Golgi staining, because it is possible that this two-dimensional assessment of spines, cut at varying orientations, caused too much variability to detect differences. However, we did find that the length of the parallel fiber-Purkinje cell synapses was shorter after acrobatic training, and thin spines tend to contain smaller excitatory synapses. Thin spines have greater capacity for strengthening and have been coined learning spines (Berry & Nedivi, 2017). They are highly plastic, appearing and disappearing relative to synaptic activity (Bourne & Harris, 2007). It seems plausible that the decreased length of the parallel fiber-Purkinje cell synapse we observed in Experiment 1 is linked with the increased formation of thin spines also associated with acrobatic motor learning (González-Tapia et al., 2015; 2017; Lee et al., 2007).

Whether this overall decrease in length of the parallel fiber-Purkinje cell synapses observed in Experiment 1 is associated with the strengthening or weakening of synaptic transmission is difficult to discern. It is tempting to speculate that the decreased parallel fiber-Purkinje cell synapse length, taken together with the increased density of parallel fiber-Purkinje cell synapses, represents a strengthening of the system where these smaller synapses are new, immature synapses that have been added as a consequence of motor learning. In contrast, a

decrease in the size of the Purkinje cell postsynaptic densities after acrobatic learning has been attributed to a weakening of synaptic transmission in male rats (Lee et al., 2013). After acrobatic learning, there were increases in both single and multiple parallel fiber-Purkinje cell synapses (Federmeier et al., 2002; Kim et al., 2002; Lee et al., 2013b), and the synapses less than 2 μm from the multi-synapses (between one parallel fiber varicosity and two Purkinje cell spines) had smaller postsynaptic densities compared to those that were further away (Lee et al., 2013). Lee et al. (2013) suggest that, rather than an exclusive strengthening or weakening of synaptic strength, both occur in a coordinated manner to optimize motor learning and enhance the synaptic weight of particular parallel fiber-Purkinje cell synapses. Although we did not differentiate between single and multi-synapses in our synapse density quantification in our experiments, it appeared that the majority of synapses quantified were single parallel fiber-Purkinje cell synapses. It is possible that the decrease in synapse size observed in our experiment is related to the weakening of particular parallel fiber-Purkinje cell synapses, occurring to adjust for the later addition of stronger multi-synapses. Most likely, multiple forms of synaptic plasticity are occurring in this region following acrobatic motor learning, and future experiments should aim to better dissociate these mechanisms. As with c-Fos expression, it will be interesting for future studies to look even earlier in the acrobatic course acquisition phase to characterize synaptic ultrastructure in the cerebellum during the first day or two of training.

Acrobatic Training Rapidly Induces Astrocytic Plasticity

Regarding astrocytic plasticity, we found an increase in overall astrocyte volume fraction and an increase in the fraction of Purkinje cell spines covered by astrocytic processes after four days of acrobatic motor-skill learning in Experiments 1 and 2. Increased astrocyte volume fraction has also been identified after 10, 28, and 38 days of continuous acrobatic training in

female rats (Anderson et al., 1994; Kleim et al., 2007). Our results indicate this increase in astrocyte volume is also present earlier, during the acquisition phase of motor learning. Increased astrocyte volume does not seem to be important for the maintenance of synaptogenesis or behavioral performance on the acrobatic task; however, astrocytic plasticity may be important for regulating synapse formation (Kleim et al., 2007). When the degree of astrocytic ensheathment of Purkinje cell spines was decreased, synaptogenesis was increased in postnatal week three mice. At this developmental stage, astrocytic ensheathment of Purkinje cell synapses is typically almost complete (Lippman Bell et al., 2010). An increase in astrocytic coverage of Purkinje cell spines may thus serve as a "cap" for cerebellar synaptogenesis (Lippman Bell et al., 2008; 2010). In Experiment 1, we found an increase in astrocytic coverage of Purkinje cell spines after four days of acrobatic training. Again, at this point rats have nearly mastered the acrobatic course, and, as a result, the synaptogenesis that underlies this motor learning is likely almost complete. Therefore, this increase in astrocytic coverage may be important for terminating synaptogenesis and stabilizing the newly formed synapses. It is also possible that this extra coverage allows Bergmann glia to have enhanced communication with the parallel fiber-Purkinje cell synapses during motor learning. To further test this hypothesis, it will be important to assess astrocytic coverage of Purkinje cell spines even earlier in acrobatic training. If cerebellar astrocytes are regulating synaptogenesis as described, we could expect a decrease in astrocytic coverage of Purkinje cell spines during the first few days of training. In contrast, rather than regulating synaptogenesis, this increase in astrocytic volume and coverage could be related to increased metabolic demands related to motor learning. However, this seems less likely, as astrocytic volume does not increase in this region during more intense aerobic exercise (Anderson et al., 1994; Kleim et al., 2007).

Astrocytic hM4Di DREADD Activation Affects Synaptogenesis and Astrocytic Volume

The astrocytic hM4Di DREADD was activated as indicated by enhanced c-Fos expression colocalizing with the virus. It is becoming clear that this activation of Gi-signaling in astrocytes increases calcium and c-Fos expression in these cells (Durkee et al., 2019; MacDonald et al., 2019; Nagai et al., 2019; Kol et al., 2020), and our results extend this effect to cerebellar astrocytes. We also found that c-Fos was elevated in cells that did not express virus in the hM4Di DREADD group. In hindsight, it would have been helpful to include a neuronal marker, such as NeuN, to verify whether or not those cells expressing c-Fos were neuronal. Nevertheless, it is necessary to consider how the astrocytic hM4Di DREADD also influences neighboring cells that do not express the virus and are most likely neurons. Interestingly, compared to all other groups, the hM4Di DREADD rats that completed acrobatic training had the highest expression of non-colocalized c-Fos, and acrobatic training did not increase c-Fos expression in the mCherry control group after four days. Future experiments could determine if there is a relationship between the poor performance these rats exhibited on the acrobatic course and c-Fos expression. Additionally, activation of the astrocytic hM4Di DREADD has been found to influence local neuronal populations, and one mechanism recently identified by which they do this is through promoting synaptogenesis (Hennes et al., 2020; Nagai et al., 2019; Yu et al., 2020).

Our results indicate one of the primary ultrastructural changes produced by the astrocytic hM4Di DREADD activation is elevated synaptogenesis. The astrocytic hM4Di DREADD group had more excitatory synapses than the mCherry control group, regardless of training condition. This aligns with recent experiments finding hM4Di DREADD activation in striatal astrocytes activates a signaling pathway that leads to the release of thrombospondin-1 (an astrocyte secreted synaptogenic cue) and in turn elevated excitatory synapse formation (Nagai et al., 2019).

Astrocytic hM4Di DREADD activation in this experiment also produced hyperactivity and disturbed attention in mice, and these effects were reversed by blocking the effects of thrombospondin-1 (Nagai et al., 2019). This effect was replicated again in striatal astrocytes in a Huntington's Disease mouse model, and enhanced synaptogenesis due to astrocytic hM4Di DREADD activation corrected synaptic and behavioral dysfunctions in these mice (Yu et al., 2020). Astrocytic hM4Di DREADD activation in a mouse model of vision loss also produced enhanced neuronal plasticity and reactivation in this region, and the authors suggest one parsimonious explanation for this effect is the enhancement of excitatory synapse formation due to Gi-signaling activity in astrocytes (Hennes et al., 2020). It our experiment, it is also possible that these astrocytes expressing hM4Di DREADDs are not secreting factors that directly regulate synaptogenesis, but that synaptogenesis is allowed to go unchecked because activating Gi-signaling in these cells disrupts their ability to regulate parallel fiber-Purkinje cell synaptic activity. We only quantified excitatory synapses, but, in the future, it would be intriguing to analyze whether inhibitory interneuron synapses with Purkinje cells are also impacted by astrocytic hM4Di DREADD activation, or if this phenomenon exclusively affects excitatory synapses. In addition to enhanced synaptogenesis, an increase in astrocytic volume fraction was also detected following the activation of the astrocytic hM4Di DREADD in Experiment 2. Few other studies have analyzed astrocytic structural plasticity following hM4Di DREADD activation, but Yu et al. (2020) also found that hM4Di activation in striatal astrocytes increased the territory size of astrocytes, meaning there was enhanced branching and thus a greater area occupied by these striatal astrocytes. It is also important to note that, although not robust, all rats in our experiment had hM4Di-DREADD expression in inhibitory interneurons in the cerebellar

molecular layer. It will be important to determine whether expression in these cells is contributing to the behavioral and structural effects observed.

A causal role between enhanced synaptogenesis caused by astrocytic hM4Di DREADD activation and motor performance deficits on the rotarod and acrobatic course cannot be gleaned from this experiment. Determining if aberrant synaptogenesis caused by Gi-signaling is responsible for this motor deficit is the next major question to answer. It does seem plausible that enhanced synaptogenesis in the cerebellum would disrupt motor behavior. Purkinje cells, the sole output of the cerebellar cortex, are rapidly integrating information received from parallel and climbing fibers. If the weight of these inputs changes, and arbitrary synapses are added to the system, this could add noise and interfere with processing of parallel fiber inputs necessary for optimal motor coordination. We could also be observing a ceiling effect, where so many parallel fiber-Purkinje synapses have been added via hM4Di DREADD activation that it is more challenging for the system to continue to add the additional synapses necessary for motor-skill learning. Even though the motor control alleyway requires no skilled movement to complete, in the future, it will be important to run home cage control rats to ensure movement itself is not interacting with the astrocytic hM4Di DREADD activation to produce synaptogenesis.

A related future direction is to identify which population of cerebellar astrocytes are driving this behavioral effect. We targeted our virus expression to the entire PML, which includes Bergmann glia in the molecular/Purkinje cell layers and velate astrocytes in the granule cell layer. Of the cerebellar astrocytes, Bergmann glia have been studied most and their influence on motor behavior has been documented (Nimmerjahn et al., 2009; Saab et al., 2012), but so little is known about the velate astrocytes in the granule cell layer that is difficult to hypothesize if one or both groups of astrocytes are responsible for this motor coordination deficit.

Synaptogenesis was quantified only in the molecular layer, but this does not mean astrocytes from other cerebellar layers, that are also part of local cerebellar circuitry, could not be influencing this effect. It is possible that synaptogenesis was also elevated in the granule cell layer. Synaptogenesis following acrobatic training has never been assessed in the granule cell layer, but it will be important for future experiments to examine plasticity in this layer as the result of motor-skill learning and chemogenetic manipulations. Based on their locations in the local cerebellar circuitry alone, it is plausible that both populations of cerebellar astrocytes could be contributing to the observed motor impairment on the acrobatic course. The disruption of velate astrocytes could be influencing what information reaches the molecular layer, and the Bergmann glia could be influencing what information reaches Purkinje cells and in turn the deep cerebellar nuclei cerebellar output channels. The ratio of virus expression between Bergmann glia and velate astrocytes was not quantified in this experiment, but this is an additional analysis that could be completed to gather more information about which population of astrocytes could be contributing most to this deficit.

Conclusions

Acrobatic motor learning produced rapid ultrastructural changes in cerebellar neurons and astrocytes. An increase in parallel fiber-Purkinje cell synapse density and in astrocyte volume was identified after four days of acrobatic training. Cerebellar ultrastructural plasticity happened quickly in this paradigm, and it is probable that these events contribute to the acquisition of new motor-skills. In addition, the expression of astrocytic hM4Di DREADDs impaired performance on the acrobatic course, and this effect was likely driven by motor coordination deficits. Synaptogenesis was also increased by astrocytic hM4Di DREADD activation and exploring if this effect underlies the behavioral deficits observed on the acrobatic

course is an important future direction. Identifying the structural changes associated with motor-skill acquisition, in addition to determining how astrocytic Gi-signaling impacts motor coordination, help us better understand the role of astrocytes in behavior and, clinically, could aid in discerning new therapeutic targets for the treatment of motor impairments present in numerous disorders from autism to stroke.

References

Adamsky, A., Kol, A., Kreisel, T., Doron, A., Ozeri-Engelhard, N., Melcer, T., … Goshen, I. (2018). Astrocytic activation generates de novo neuronal potentiation and memory enhancement. *Cell*, *174*(1), 59-71.e14. https://doi.org/10.1016/j.cell.2018.05.002

Albergaria, C., & Carey, M. R. (2014). All Purkinje cells are not created equal. *ELife*, *3*, e03285. https://doi.org/10.7554/eLife.03285

Albus, J. S. (1971). A theory of cerebellar function. *Mathematical Biosciences*, *10*(1), 25–61. https://doi.org/10.1016/0025-5564(71)90051-4

Anderson, B. J., Li, X., Alcantara, A. A., Isaacs, K. R., Black, J. E., & Greenough, W. T. (1994). Glial hypertrophy is associated with synaptogenesis following motor-skill learning, but not with angiogenesis following exercise. *Glia*, *11*(1), 73–80. https://doi.org/10.1002/glia.440110110

Andreasen, N. C., O'Leary, D. S., Paradiso, S., Cizadlo, T., Arndt, S., Watkins, G. L., … Hichwa, R. D. (1999). The cerebellum plays a role in conscious episodic memory retrieval. *Human Brain Mapping*, *8*(4), 226–234.

Andreasen, Nancy C., O'Leary, D. S., Arndt, S., Cizadlo, T., Rezai, K., Watkins, G. L., … Hichwa, R. D. (1995). I. PET studies of memory: Novel and practiced free recall of complex narratives. *NeuroImage*, *2*(4), 284–295. https://doi.org/10.1006/nimg.1995.1036

Andreasen, Nancy C., O'Leary, D. S., Cizadlo, T., Arndt, S., Rezai, K., Watkins, G. L., … Hichwa, R. D. (1995). II. PET studies of memory: Novel versus practiced free recall of word lists. *NeuroImage*, *2*(4), 296–305. https://doi.org/10.1006/nimg.1995.1037

Andreasen, Nancy C., Paradiso, S., & O'Leary, D. S. (1998). "Cognitive dysmetria" as an integrative theory of schizophrenia: A dysfunction in cortical-subcortical-cerebellar circuitry? *Schizophrenia Bulletin*, *24*(2), 203–218. https://doi.org/10.1093/oxfordjournals.schbul.a033321

Andreasen, Nancy C., & Pierson, R. (2008). The role of the cerebellum in schizophrenia. *Biological Psychiatry*, *64*(2), 81–88. https://doi.org/10.1016/j.biopsych.2008.01.003

Apps, R., Hawkes, R., Aoki, S., Bengtsson, F., Brown, A. M., Chen, G., … Ruigrok, T. J. H. (2018). Cerebellar modules and their role as operational cerebellar processing units. *Cerebellum*, *17*(5), 654–682. https://doi.org/10.1007/s12311-018-0952-3

Araujo, A. P. B., Carpi-Santos, R., & Gomes, F. C. A. (2019). The role of astrocytes in the development of the cerebellum. *Cerebellum, 18*(6), 1017-1035. https://doi.org/10.1007/s12311-019-01046-0

Atkins, M. J., & Apps, R. (1997). Somatotopical organisation within the climbing fibre projection to the paramedian lobule and copula pyramidis of the rat cerebellum. *Journal of Comparative Neurology*, *389*(2), 249–263.

Balakrishnan, S., Jackson, C., Russell, N., & Bellamy, T. C. (2011). Ectopic release sites lack fast vesicle recycling mechanisms, causing long-term depression of neuron-glial transmission in rat cerebellum. *Glia*, *59*(1), 82–93. https://doi.org/10.1002/glia.21078

Barmack, N. H., & Yakhnitsa, V. (2008). Functions of interneurons in mouse cerebellum. *Journal of Neuroscience*, *28*(5), 1140–1152. https://doi.org/10.1523/JNEUROSCI.3942-07.2008

Baumel, Y., Jacobson, G. A., & Cohen, D. (2009). Implications of functional anatomy on information processing in the deep cerebellar nuclei. *Frontiers in Cellular Neuroscience*, *3*. https://doi.org/10.3389/neuro.03.014.2009

Bartling, B., Al-Robaiy, S., Lehnich, H., Binder, L., Hiebl, B., & Simm, A. (2017). Sex-related differences in the wheel-running activity of mice decline with increasing age. *Experimental Gerontology*, *87*(Pt B), 139–147. https://doi.org/10.1016/j.exger.2016.04.011

Behnke, V. K., Stevenson, M. E., & Swain, R. A. (2018). Inactivation of the cerebellar fastigial nuclei alters social behavior in the rat. *Behavioral Neuroscience*, *132*(6), 552–560. https://doi.org/10.1037/bne0000256

Beierlein, M., & Regehr, W. G. (2006). Brief bursts of parallel fiber activity trigger calcium signals in Bergmann glia. *Journal of Neuroscience*, *26*(26), 6958–6967. https://doi.org/10.1523/JNEUROSCI.0613-06.2006

Bellamy, T. C. (2006). Interactions between Purkinje neurones and Bergmann glia. *Cerebellum*, *5*(2), 116–126. https://doi.org/10.1080/14734220600724569

Berry, K. P., & Nedivi, E. (2017). Spine dynamics: Are they all the same? *Neuron*, *96*(1), 43–55. https://doi.org/10.1016/j.neuron.2017.08.008

Black, J. E., Isaacs, K. R., Anderson, B. J., Alcantara, A. A., & Greenough, W. T. (1990). Learning causes synaptogenesis, whereas motor activity causes angiogenesis, in cerebellar cortex of adult rats. *Proceedings of the National Academy of Sciences*, *87*(14), 5568–5572. https://doi.org/10.1073/pnas.87.14.5568

Blizard, D. A., Lippman, H. R., & Chen, J. J. (1975). Sex differences in open-field behavior in the rat: The inductive and activational role of gonadal hormones. *Physiology & Behavior*, *14*(5), 601–608. https://doi.org/10.1016/0031-9384(75)90188-2

Bloedel, J. R., & Bracha, V. (1998). Current concepts of climbing fiber function. *The Anatomical Record*, *253*(4), 118–126. https://doi.org/10.1002/(SICI)1097-0185(199808)253:4<118::AID-AR7>3.0.CO;2-P

Bostan, A. C., Dum, R. P., & Strick, P. L. (2010). The basal ganglia communicate with the cerebellum. *Proceedings of the National Academy of Sciences*, *107*(18), 8452–8456. https://doi.org/10.1073/pnas.1000496107

Bostan, A. C., Dum, R. P., & Strick, P. L. (2013). Cerebellar networks with the cerebral cortex and basal ganglia. *Trends in Cognitive Sciences*, *17*(5), 241–254. https://doi.org/10.1016/j.tics.2013.03.003

Bourne, J., & Harris, K. M. (2007). Do thin spines learn to be mushroom spines that remember? *Current Opinion in Neurobiology*, *17*(3), 381–386. https://doi.org/10.1016/j.conb.2007.04.009

Bower, J. M. (1997). Is the cerebellum sensory for motor's sake, or motor for sensory's sake: The view from the whiskers of a rat? *Progress in Brain Research*, *114*, 463–496. https://doi.org/10.1016/s0079-6123(08)63381-6

Brockett, A. T., Kane, G. A., Monari, P. K., Briones, B. A., Vigneron, P.-A., Barber, G. A., … Gould, E. (2018). Evidence supporting a role for astrocytes in the regulation of cognitive flexibility and neuronal oscillations through the Ca2+ binding protein S100β. *PLoS ONE*, *13*(4). https://doi.org/10.1371/journal.pone.0195726

Buitrago, M. M., Ringer, T., Schulz, J. B., Dichgans, J., & Luft, A. R. (2004). Characterization of motor skill and instrumental learning time scales in a skilled reaching task in rat. *Behavioural Brain Research*, *155*(2), 249–256. https://doi.org/10.1016/j.bbr.2004.04.025

Bröer, S., & Brookes, N. (2001). Transfer of glutamine between astrocytes and neurons. *Journal of Neurochemistry*, *77*(3), 705–719. https://doi.org/10.1046/j.1471-4159.2001.00322.x

Buckner, R. L. (2013). The cerebellum and cognitive function: 25 years of insight from anatomy and neuroimaging. *Neuron*, *80*(3), 807–815. https://doi.org/10.1016/j.neuron.2013.10.044

Burman, K., Darian-Smith, C., & Darian-Smith, I. (2000). Geometry of rubrospinal, rubroolivary, and local circuit neurons in the macaque red nucleus. *Journal of Comparative Neurology*, *423*(2), 197–219. https://doi.org/10.1002/1096-9861(20000724)423:2<197::AID-CNE2>3.0.CO;2-0

Butt, A. M., & Kalsi, A. (2006). Inwardly rectifying potassium channels (Kir) in central nervous system glia: A special role for Kir4.1 in glial functions. *Journal of Cellular and Molecular Medicine*, *10*(1), 33–44. https://doi.org/10.1111/j.1582-4934.2006.tb00289.x

Carrillo, J., Cheng, S.-Y., Ko, K. W., Jones, T. A., & Nishiyama, H. (2013). The long-term structural plasticity of cerebellar parallel fiber axons and its modulation by motor learning. *Journal of Neuroscience*, *33*(19), 8301–8307. https://doi.org/10.1523/JNEUROSCI.3792-12.2013

Carta, I., Chen, C. H., Schott, A. L., Dorizan, S., & Khodakhah, K. (2019). Cerebellar modulation of the reward circuitry and social behavior. *Science*, *363*(6424), eaav0581. https://doi.org/10.1126/science.aav0581

Cervetto, C., Frattaroli, D., Venturini, A., Passalacqua, M., Nobile, M., Alloisio, S., … Marcoli, M. (2015). Calcium-permeable AMPA receptors trigger vesicular glutamate release from Bergmann gliosomes. *Neuropharmacology*, *99*, 396–407. https://doi.org/10.1016/j.neuropharm.2015.08.011

Chen, N., Sugihara, H., Kim, J., Fu, Z., Barak, B., Sur, M., … Han, W. (n.d.). Direct modulation of GFAP-expressing glia in the arcuate nucleus bi-directionally regulates feeding. *ELife*, *5*. https://doi.org/10.7554/eLife.18716

Cheng, F. Y., Fleming, J. T., & Chiang, C. (2018). Bergmann glial Sonic hedgehog signaling activity is required for proper cerebellar cortical expansion and architecture. *Developmental Biology*, *440*(2), 152–166. https://doi.org/10.1016/j.ydbio.2018.05.015

Chrobak, A. A., & Soltys, Z. (2017). Bergmann glia, long-term depression, and autism spectrum disorder. *Molecular Neurobiology*, *54*(2), 1156–1166. https://doi.org/10.1007/s12035-016-9719-3

Clark, B. A., & Barbour, B. (1997). Currents evoked in Bergmann glial cells by parallel fibre stimulation in rat cerebellar slices. *Journal of Physiology*, *502 (Pt 2)*, 335–350. https://doi.org/10.1111/j.1469-7793.1997.335bk.x

Clower, D. M., West, R. A., Lynch, J. C., & Strick, P. L. (2001). The inferior parietal lobule is the target of output from the superior colliculus, hippocampus, and cerebellum. *Journal of Neuroscience*, *21*(16), 6283–6291. https://doi.org/10.1523/JNEUROSCI.21-16-06283.2001

Coesmans, M., Weber, J. T., De Zeeuw, C. I., & Hansel, C. (2004). Bidirectional parallel fiber plasticity in the cerebellum under climbing fiber control. *Neuron*, *44*(4), 691–700. https://doi.org/10.1016/j.neuron.2004.10.031

Coffman, K. A., Dum, R. P., & Strick, P. L. (2011). Cerebellar vermis is a target of projections from the motor areas in the cerebral cortex. *Proceedings of the National Academy of Sciences*, *108*(38), 16068–16073. https://doi.org/10.1073/pnas.1107904108

Colucci-Guyon, E., Giménez Y Ribotta, M., Maurice, T., Babinet, C., & Privat, A. (1999). Cerebellar defect and impaired motor coordination in mice lacking vimentin. *Glia*, *25*(1), 33–43.

Combs, C. M., & Thomas, C. E. (1970). Electrical responses in the paramedian lobule evoked by stimulating various parts of the cat cerebellar cortex. *Experimental Neurology*, *27*(1), 23–33. https://doi.org/10.1016/0014-4886(70)90198-6

Consalez, G. G., & Hawkes, R. (2013). The compartmental restriction of cerebellar interneurons. *Frontiers in Neural Circuits*, *6*. https://doi.org/10.3389/fncir.2012.00123

Courchesne, E., Yeung-Courchesne, R., Hesselink, J. R., & Jernigan, T. L. (1988). Hypoplasia of cerebellar vermal lobules VI and VII in autism. *New England Journal of Medicine*, *318*(21), 1349–1354. https://doi.org/10.1056/NEJM198805263182102

Courville, J., Faraco-Cantin, F., & Diakiw, N. (1974). A functionally important feature of the distribution of the olivo-cerebellar climbing fibers. *Canadian Journal of Physiology and Pharmacology*, *52*(6), 1212–1217. https://doi.org/10.1139/y74-159

Dalla, C., & Shors, T. J. (2009). Sex differences in learning processes of classical and operant conditioning. *Physiology & Behavior*, *97*(2), 229–238. https://doi.org/10.1016/j.physbeh.2009.02.035

D'Angelo, E., Solinas, S., Mapelli, J., Gandolfi, D., Mapelli, L., & Prestori, F. (2013). The cerebellar Golgi cell and spatiotemporal organization of granular layer activity. *Frontiers in Neural Circuits*, *7*. https://doi.org/10.3389/fncir.2013.00093

De Camilli, P., Miller, P. E., Levitt, P., Walter, U., & Greengard, P. (1984). Anatomy of cerebellar Purkinje cells in the rat determined by a specific immunohistochemical marker. *Neuroscience*, *11*(4), 761-IN2. https://doi.org/10.1016/0306-4522(84)90193-3

De Zeeuw, C. I., Hansel, C., Bian, F., Koekkoek, S. K., van Alphen, A. M., Linden, D. J., & Oberdick, J. (1998). Expression of a protein kinase C inhibitor in Purkinje cells blocks cerebellar LTD and adaptation of the vestibulo-ocular reflex. *Neuron*, *20*(3), 495–508. https://doi.org/10.1016/s0896-6273(00)80990-3

De Zeeuw, Chris I., & Hoogland, T. M. (2015). Reappraisal of Bergmann glial cells as modulators of cerebellar circuit function. *Frontiers in Cellular Neuroscience*, *9*. https://doi.org/10.3389/fncel.2015.00246

Desmond, J. E., Gabrieli, J. D. E., Wagner, A. D., Ginier, B. L., & Glover, G. H. (1997). Lobular patterns of cerebellar activation in verbal working-memory and finger-tapping tasks as revealed by functional MRI. *Journal of Neuroscience*, *17*(24), 9675–9685. https://doi.org/10.1523/JNEUROSCI.17-24-09675.1997

Deverett, B., Kislin, M., Tank, D. W., & Wang, S. S.-H. (2019). Cerebellar disruption impairs working memory during evidence accumulation. *Nature Communications*, *10*(1), 1–7. https://doi.org/10.1038/s41467-019-11050-x

DiFeo, G., Curlik, D. M., & Shors, T. J. (2015). The motirod: A novel physical skill task that enhances motivation to learn and thereby increases neurogenesis especially in the female hippocampus. *Brain Research*, *1621*, 187–196. https://doi.org/10.1016/j.brainres.2014.11.045

D'Mello, A. M., Crocetti, D., Mostofsky, S. H., & Stoodley, C. J. (2015). Cerebellar gray matter and lobular volumes correlate with core autism symptoms. *NeuroImage: Clinical*, *7*, 631–639. https://doi.org/10.1016/j.nicl.2015.02.007

Duan, S., Anderson, C. M., Stein, B. A., & Swanson, R. A. (1999). Glutamate induces rapid upregulation of astrocyte glutamate transport and cell-surface expression of GLAST. *Journal of Neuroscience, 19*(23), 10193–10200.

Dum, R. P., Li, C., & Strick, P. L. (2002). Motor and nonmotor domains in the monkey dentate. *Annals of the New York Academy of Sciences*, *978*, 289–301. https://doi.org/10.1111/j.1749-6632.2002.tb07575.x

Durkee, C.A., Covelo, A., Lines, J., Kofuji, P., Aguilar, J., & Araque, A. (2019). Gi/o protein-coupled receptors inhibit neurons but activate astrocytes and stimulate gliotransmission. *Glia, 67*(6), 1076-1093. https://doi.org/10.1002/glia.23589

Eccles, J. C., Ito, M., & Szentágothai, J. (1967). *The cerebellum as a neuronal machine*. https://doi.org/10.1007/978-3-662-13147-3

Enger, M., & Brodal, P. (1985). Organization of corticopontocerebellar connections to the paramedian lobule in the cat. *Anatomy and Embryology*, *172*(2), 227–238. https://doi.org/10.1007/BF00319605

Fatemi, S. H., Halt, A. R., Realmuto, G., Earle, J., Kist, D. A., Thuras, P., & Merz, A. (2002). Purkinje cell size is reduced in cerebellum of patients with autism. *Cellular and Molecular Neurobiology*, *22*(2), 171–175. https://doi.org/10.1023/A:1019861721160

Federmeier, K. D., Kleim, J. A., & Greenough, W. T. (2002). Learning-induced multiple synapse formation in rat cerebellar cortex. *Neuroscience Letters*, *332*(3), 180–184. https://doi.org/10.1016/S0304-3940(02)00759-0

Flumerfelt, B. A., Otabe, S., & Courville, J. (1973). Distinct projections to the red nucleus from the dentate and interposed nuclei in the monkey. *Brain Research*, *50*(2), 408–414. https://doi.org/10.1016/0006-8993(73)90742-7

Galliano, E., Gao, Z., Schonewille, M., Todorov, B., Simons, E., Pop, A. S., … De Zeeuw, C. I. (2013). Silencing the majority of cerebellar granule cells uncovers their essential role in motor learning and consolidation. *Cell Reports*, *3*(4), 1239–1251. https://doi.org/10.1016/j.celrep.2013.03.023

Gallimore, A. R., Kim, T., Tanaka-Yamamoto, K., & De Schutter, E. (2018). Switching on depression and potentiation in the cerebellum. *Cell Reports*, *22*(3), 722–733. https://doi.org/10.1016/j.celrep.2017.12.084

Gao, J. H., Parsons, L. M., Bower, J. M., Xiong, J., Li, J., & Fox, P. T. (1996). Cerebellum implicated in sensory acquisition and discrimination rather than motor control. *Science*, *272*(5261), 545–547. https://doi.org/10.1126/science.272.5261.545

Glickstein, M., Strata, P., & Voogd, J. (2009). Cerebellum: History. *Neuroscience*, *162*(3), 549–559. https://doi.org/10.1016/j.neuroscience.2009.02.054

Glickstein, Mitchell, & Doron, K. (2008). Cerebellum: Connections and functions. *Cerebellum*, *7*(4), 589–594. https://doi.org/10.1007/s12311-008-0074-4

González-Tapia, D., González-Ramírez, M. M., Vázquez-Hernández, N., & González-Burgos, I. (2017). Motor learning induces plastic changes in Purkinje cell dendritic spines in the rat cerebellum. *Neurologia, S0213-4853*(17), 30352-3. https://doi.org/10.1016/j.nrl.2017.10.007

González-Tapia, David, Velázquez-Zamora, D. A., Olvera-Cortés, M. E., & González-Burgos, I. (2015). The motor learning induces plastic changes in dendritic spines of Purkinje cells from the neocerebellar cortex of the rat. *Restorative Neurology and Neuroscience*, *33*(5), 639–645. https://doi.org/10.3233/RNN-140462

Graham, D. J., & Wylie, D. R. (2012). Zebrin-immunopositive and -immunonegative stripe pairs represent functional units in the pigeon vestibulocerebellum. *Journal of Neuroscience*, *32*(37), 12769–12779. https://doi.org/10.1523/JNEUROSCI.0197-12.2012

Grasselli, G., & Hansel, C. (2014). Cerebellar long-term potentiation: Cellular mechanisms and role in learning. *International Review of Neurobiology*, *117*, 39–51. https://doi.org/10.1016/B978-0-12-420247-4.00003-8

Grosche, J., Matyash, V., Möller, T., Verkhratsky, A., Reichenbach, A., & Kettenmann, H. (1999). Microdomains for neuron–glia interaction: Parallel fiber signaling to Bergmann glial cells. *Nature Neuroscience*, *2*(2), 139–143. https://doi.org/10.1038/5692

Groth, J. D., & Sahin, M. (2015). High frequency synchrony in the cerebellar cortex during goal directed movements. *Frontiers in Systems Neuroscience*, *9*. https://doi.org/10.3389/fnsys.2015.00098

Haines, D. E., & Patrick, G. W. (1981). Cerebellar corticonuclear fibers of the paramedian lobule of tree shrew (Tupaia glis) with comments on zones. *Journal of Comparative Neurology*, *201*(1), 99–119. https://doi.org/10.1002/cne.902010108

Hansel, C., Linden, D. J., & D'Angelo, E. (2001). Beyond parallel fiber LTD: The diversity of synaptic and non-synaptic plasticity in the cerebellum. *Nature Neuroscience*, *4*(5), 467–475. https://doi.org/10.1038/87419

Harper, J. W., & Heath, R. G. (1973). Anatomic connections of the fastigial nucleus to the rostral forebrain in the cat. *Experimental Neurology*, *39*(2), 285–292. https://doi.org/10.1016/0014-4886(73)90231-8

Harvey, R. J., & Napper, R. M. (1988). Quantitative study of granule and Purkinje cells in the cerebellar cortex of the rat. *Journal of Comparative Neurology*, *274*(2), 151–157. https://doi.org/10.1002/cne.902740202

Hawkes, R., & Herrup, K. (1995). Aldolase C/zebrin II and the regionalization of the cerebellum. *Journal of Molecular Neuroscience*, *6*(3), 147–158. https://doi.org/10.1007/BF02736761

Heath, R. G., & Harper, J. W. (1974). Ascending projections of the cerebellar fastigial nucleus to the hippocampus, amygdala, and other temporal lobe sites: Evoked potential and histological studies in monkeys and cats. *Experimental Neurology*, *45*(2), 268–287. https://doi.org/10.1016/0014-4886(74)90118-6

Heck, D. H., Thach, W. T., & Keating, J. G. (2007). On-beam synchrony in the cerebellum as the mechanism for the timing and coordination of movement. *Proceedings of the National Academy of Sciences*, *104*(18), 7658–7663. https://doi.org/10.1073/pnas.0609966104

Hennes, M., Lombaert, N., Wahis, J., Van den Haute, C., Holt, M.G., Arckens, L. (2020). Astrocytes shape the plastic response of adult cortical neurons to vison loss. *Glia, 68*(10), 2102-2118. https://doi.org/10.1002/glia.23830

Hoddevik, G. H. (1975). The pontocerebellar projection onto the paramedian lobule in the cat: An experimental study with the use of horseradish peroxidase as a tracer. *Brain Research*, *95*(2), 291–307. https://doi.org/10.1016/0006-8993(75)90108-0

Hoogland, T. M., & Kuhn, B. (2010). Recent developments in the understanding of astrocyte function in the cerebellum in vivo. *Cerebellum*, *9*(3), 264–271. https://doi.org/10.1007/s12311-009-0139-z

Hoogland, T. M., Kuhn, B., Göbel, W., Huang, W., Nakai, J., Helmchen, F., … Wang, S. S.-H. (2009). Radially expanding transglial calcium waves in the intact cerebellum. *Proceedings of the National Academy of Sciences*, *106*(9), 3496–3501. https://doi.org/10.1073/pnas.0809269106

Hoshi, E., Tremblay, L., Féger, J., Carras, P. L., & Strick, P. L. (2005). The cerebellum communicates with the basal ganglia. *Nature Neuroscience*, *8*(11), 1491–1493. https://doi.org/10.1038/nn1544

Hounsgaard, J., & Nicholson, C. (1983). Potassium accumulation around individual Purkinje cells in cerebellar slices from the guinea-pig. *Journal of Physiology*, *340*(1), 359–388. https://doi.org/10.1113/jphysiol.1983.sp014767

Hoxha, E., Tempia, F., Lippiello, P., & Miniaci, M. C. (2016). Modulation, plasticity and pathophysiology of the parallel fiber-Purkinje cell synapse. *Frontiers in Synaptic Neuroscience*, *8*, 35. https://doi.org/10.3389/fnsyn.2016.00035

Iino, M., Goto, K., Kakegawa, W., Okado, H., Sudo, M., Ishiuchi, S., … Ozawa, S. (2001). Glia-synapse interaction through Ca2+-permeable AMPA receptors in Bergmann glia. *Science*, *292*(5518), 926–929. https://doi.org/10.1126/science.1058827

Isaacs, K. R., Anderson, B. J., Alcantara, A. A., Black, J. E., & Greenough, W. T. (1992). Exercise and the brain: Angiogenesis in the adult rat cerebellum after vigorous physical activity and motor skill learning. *Journal of Cerebral Blood Flow and Metabolism*, *12*(1), 110–119. https://doi.org/10.1038/jcbfm.1992.14

Ishikawa, T., Tomatsu, S., Izawa, J., & Kakei, S. (2016). The cerebro-cerebellum: Could it be loci of forward models? *Neuroscience Research*, *104*, 72–79. https://doi.org/10.1016/j.neures.2015.12.003

Ito, M., & Kano, M. (1982). Long-lasting depression of parallel fiber-Purkinje cell transmission induced by conjunctive stimulation of parallel fibers and climbing fibers in the cerebellar cortex. *Neuroscience Letters*, *33*(3), 253–258. https://doi.org/10.1016/0304-3940(82)90380-9

Ito, Masao. (2002). Historical review of the significance of the cerebellum and the role of Purkinje cells in motor learning. *Annals of the New York Academy of Sciences*, *978*(1), 273–288. https://doi.org/10.1111/j.1749-6632.2002.tb07574.x

Ito, Masao, & Itō, M. (1984). *The Cerebellum and Neural Control*. Raven Press.

Ivry, R. (1997). Cerebellar timing systems. *International Review of Neurobiology*, *41*, 555–573.

Ivry, R. B., & Keele, S. W. (1989). Timing functions of the cerebellum. *Journal of Cognitive Neuroscience*, *1*(2), 136–152. https://doi.org/10.1162/jocn.1989.1.2.136

Jansen, J., & Brodal, A. (1940). Experimental studies on the intrinsic fibers of the cerebellum. II. The cortico-nuclear projection. *Journal of Comparative Neurology*, *73*(2), 267–321. https://doi.org/10.1002/cne.900730204

Jörntell, H., & Hansel, C. (2006). Synaptic memories upside down: Bidirectional plasticity at cerebellar parallel fiber-Purkinje cell synapses. *Neuron*, *52*(2), 227–238. https://doi.org/10.1016/j.neuron.2006.09.032

Kawato, M. (1999). Internal models for motor control and trajectory planning. *Current Opinion in Neurobiology*, *9*(6), 718–727. https://doi.org/10.1016/S0959-4388(99)00028-8

Kelly, R. M., & Strick, P. L. (2003). Cerebellar loops with motor cortex and prefrontal cortex of a nonhuman primate. *Journal of Neuroscience*, *23*(23), 8432–8444. https://doi.org/10.1523/JNEUROSCI.23-23-08432.2003

Kleim, J. A., Pipitone, M. A., Czerlanis, C., & Greenough, W. T. (1998). Structural stability within the lateral cerebellar nucleus of the rat following complex motor learning. *Neurobiology of Learning and Memory*, *69*(3), 290–306. https://doi.org/10.1006/nlme.1998.3828

Kleim, J. A., Swain, R. A., Armstrong, K. A., Napper, R. M., Jones, T. A., & Greenough, W. T. (1998). Selective synaptic plasticity within the cerebellar cortex following complex motor skill learning. *Neurobiology of Learning and Memory*, *69*(3), 274–289. https://doi.org/10.1006/nlme.1998.3827

Kleim, J. A., Swain, R. A., Czerlanis, C. M., Kelly, J. L., Pipitone, M. A., & Greenough, W. T. (1997). Learning-dependent dendritic hypertrophy of cerebellar stellate cells: Plasticity of local circuit neurons. *Neurobiology of Learning and Memory*, *67*(1), 29–33. https://doi.org/10.1006/nlme.1996.3742

Kleim, J. A., Vij, K., Ballard, D. H., & Greenough, W. T. (1997). Learning-dependent synaptic modifications in the cerebellar cortex of the adult rat persist for at least four weeks. *Journal of Neuroscience*, *17*(2), 717–721.

Kleim, J. A., Lussnig, E., Schwarz, E. R., Comery, T. A., & Greenough, W. T. (1996). Synaptogenesis and FOS expression in the motor cortex of the adult rat after motor skill learning. *Journal of Neuroscience*, *16*(14), 4529–4535. https://doi.org/10.1523/JNEUROSCI.16-14-04529.1996

Kleim, J. A., Markham, J. A., Vij, K., Freese, J. L., Ballard, D. H., & Greenough, W. T. (2007). Motor learning induces astrocytic hypertrophy in the cerebellar cortex. *Behavioural Brain Research*, *178*(2), 244–249. https://doi.org/10.1016/j.bbr.2006.12.022

Klintsova, A. Y., Cowell, R. M., Swain, R. A., Napper, R. M. A., Goodlett, C. R., & Greenough, W. T. (1998). Therapeutic effects of complex motor training on motor performance deficits induced by neonatal binge-like alcohol exposure in rats: I. Behavioral results. *Brain Research*, *800*(1), 48–61. https://doi.org/10.1016/S0006-8993(98)00495-8

Klintsova, A. Y., Scamra, C., Hoffman, M., Napper, R. M. A., Goodlett, C. R., & Greenough, W. T. (2002). Therapeutic effects of complex motor training on motor performance deficits induced by neonatal binge-like alcohol exposure in rats: II. A quantitative stereological study of synaptic plasticity in female rat cerebellum. *Brain Research*, *937*(1), 83–93. https://doi.org/10.1016/S0006-8993(02)02492-7

Kol, A., Adamsky, A., Groysman, M., Kreisel, T., London, M., & Goshen, I. (2020). Astrocytes contribute to remote memory formation by modulating hippocampal-cortical communication during learning. *Nature Neuroscience*, *23,* 1229-1239. https://doi.org/10.1038/s41593-020-0679-6

Korbo, L., Andersen, B. B., Ladefoged, O., & Møller, A. (1993). Total numbers of various cell types in rat cerebellar cortex estimated using an unbiased stereological method. *Brain Research*, *609*(1–2), 262–268. https://doi.org/10.1016/0006-8993(93)90881-m

Koziol, L. F., Budding, D., Andreasen, N., D'Arrigo, S., Bulgheroni, S., Imamizu, H., … Yamazaki, T. (2014). Consensus paper: The cerebellum's role in movement and cognition. *Cerebellum*, *13*(1), 151–177. https://doi.org/10.1007/s12311-013-0511-x

Krupa, D. J., & Thompson, R. F. (1997). Reversible inactivation of the cerebellar interpositus nucleus completely prevents acquisition of the classically conditioned eye-blink response. *Learning & Memory*, *3*(6), 545–556. https://doi.org/10.1101/lm.3.6.545

Lalonde, R., & Strazielle, C. (2003). The effects of cerebellar damage on maze learning in animals. *Cerebellum*, *2*(4), 300–309. https://doi.org/10.1080/14734220310017456

Larsall, O. & Jansen, J. (1972). *The comparative anatomy and histology of the cerebellum*. St. Paul, MN: University of Minnesota Press.

Lee, J.-M., Kim, C.-J., Park, J.-M., Song, M. K., & Kim, Y.-J. (2018). Effect of treadmill exercise on spatial navigation impairment associated with cerebellar Purkinje cell loss following chronic cerebral hypoperfusion. *Molecular Medicine Reports*, *17*(6), 8121–8128. https://doi.org/10.3892/mmr.2018.8893

Lee, K. J., Park, I. S., Kim, H., Greenough, W. T., Pak, D. T. S., & Rhyu, I. J. (2013). Motor skill training induces coordinated strengthening and weakening between neighboring synapses. *Journal of Neuroscience*, *33*(23), 9794–9799. https://doi.org/10.1523/JNEUROSCI.0848-12.2013

Leggio, M. G., Molinari, M., Neri, P., Graziano, A., Mandolesi, L., & Petrosini, L. (2000). Representation of actions in rats: The role of cerebellum in learning spatial performances by observation. *Proceedings of the National Academy of Sciences*, *97*(5), 2320–2325.

Leto, K., Carletti, B., Williams, I. M., Magrassi, L., & Rossi, F. (2006). Different types of cerebellar GABAergic interneurons originate from a common pool of multipotent progenitor cells. *Journal of Neuroscience*, *26*(45), 11682–11694. https://doi.org/10.1523/JNEUROSCI.3656-06.2006

Leung, A. W., & Li, J. Y. H. (2018). The molecular pathway regulating Bergmann glia and folia generation in the cerebellum. *Cerebellum*, *17*(1), 42–48. https://doi.org/10.1007/s12311-017-0904-3

Lev-Ram, V., Wong, S. T., Storm, D. R., & Tsien, R. Y. (2002). A new form of cerebellar long-term potentiation is postsynaptic and depends on nitric oxide but not cAMP. *Proceedings of the National Academy of Sciences*, *99*(12), 8389–8393. https://doi.org/10.1073/pnas.122206399

Lippman Bell, J. J., Lordkipanidze, T., Cobb, N., & Dunaevsky, A. (2010). Bergmann glial ensheathment of dendritic spines regulates synapse number without affecting spine motility. *Neuron Glia Biology*, *6*(3), 193–200. https://doi.org/10.1017/S1740925X10000165

Lippman, J. J., Lordkipanidze, T., Buell, M. E., Yoon, S. O., & Dunaevsky, A. (2008). Morphogenesis and regulation of Bergmann glial processes during Purkinje cell dendritic spine ensheathment and synaptogenesis. *Glia*, *56*(13), 1463–1477. https://doi.org/10.1002/glia.20712

Llinas, R., Walton, K., Hillman, D., & Sotelo, C. (1975). Inferior olive: Its role in motor learning *Science*, *190*(4220), 1230-1231.

López-Bayghen, E., Espinoza-Rojo, M., & Ortega, A. (2003). Glutamate down-regulates GLAST expression through AMPA receptors in Bergmann glial cells. *Brain Research. Molecular Brain Research*, *115*(1), 1–9. https://doi.org/10.1016/s0169-328x(03)00136-0

Lu, X., Miyachi, S., & Takada, M. (2012). Anatomical evidence for the involvement of medial cerebellar output from the interpositus nuclei in cognitive functions. *Proceedings of the National Academy of Sciences*, *109*(46), 18980–18984. https://doi.org/10.1073/pnas.1211168109

Lynch, J. C., Hoover, J. E., & Strick, P. L. (1994). Input to the primate frontal eye field from the substantia nigra, superior colliculus, and dentate nucleus demonstrated by transneuronal transport. *Experimental Brain Research*, *100*(1), 181–186. https://doi.org/10.1007/BF00227293

MacDonald, A.J., Holmes, F.E., Beall, C., Pickering, A.E., & Ellacott, K.L.J. (2019). Regulation of food intake by astrocytes in the brainstem dorsal vagal complex. *Glia, 68,* 1241-1254. https://doi.org/10.1002/glia.23774

Macher, K., Böhringer, A., Villringer, A., & Pleger, B. (2014). Cerebellar-parietal connections underpin phonological storage. *Journal of Neuroscience*, *34*(14), 5029–5037. https://doi.org/10.1523/JNEUROSCI.0106-14.2014

MacLaren, D. A. A., Browne, R. W., Shaw, J. K., Krishnan Radhakrishnan, S., Khare, P., España, R. A., & Clark, S. D. (2016). Clozapine n-oxide administration produces behavioral effects in Long-Evans rats: Implications for designing DREADD experiments. *ENeuro*, *3*(5). https://doi.org/10.1523/ENEURO.0219-16.2016

Magnotta, V. A., Adix, M. L., Caprahan, A., Lim, K., Gollub, R., & Andreasen, N. C. (2008). Investigating connectivity between the cerebellum and thalamus in schizophrenia using diffusion tensor tractography: A pilot study. *Psychiatry Research: Neuroimaging*, *163*(3), 193–200. https://doi.org/10.1016/j.pscychresns.2007.10.005

Mandolesi, L., Leggio, M. G., Graziano, A., Neri, P., & Petrosini, L. (2001). Cerebellar contribution to spatial event processing: Involvement in procedural and working memory components. *European Journal of Neuroscience*, *14*(12), 2011–2022. https://doi.org/10.1046/j.0953-816x.2001.01819.x

Manto, M., Bower, J. M., Conforto, A. B., Delgado-García, J. M., da Guarda, S. N. F., Gerwig, M., … Timmann, D. (2012). Consensus paper: Roles of the cerebellum in motor Control—The diversity of ideas on cerebellar involvement in movement. *Cerebellum*, *11*(2), 457–487. https://doi.org/10.1007/s12311-011-0331-9

Marek, S., Siegel, J. S., Gordon, E. M., Raut, R. V., Gratton, C., Newbold, D. J., … Dosenbach, N. U. F. (2018). Spatial and temporal organization of the individual human cerebellum. *Neuron*, *100*(4), 977-993.e7. https://doi.org/10.1016/j.neuron.2018.10.010

Marr, D., & Thach, W. T. (1991). A Theory of Cerebellar Cortex. In L. Vaina (Ed.), *From the Retina to the Neocortex: Selected Papers of David Marr* (pp. 11–50). https://doi.org/10.1007/978-1-4684-6775-8_3

Martínez, D., García, L., Aguilera, J., & Ortega, A. (2014). An acute glutamate exposure induces long-term down regulation of GLAST/EAAT1 uptake activity in cultured Bergmann glia cells. *Neurochemical Research*, *39*(1), 142–149. https://doi.org/10.1007/s11064-013-1198-6

Matsui, K., Jahr, C. E., & Rubio, M. E. (2005). High-concentration rapid transients of glutamate mediate neural-glial communication via ectopic release. *Journal of Neuroscience*, *25*(33), 7538–7547. https://doi.org/10.1523/JNEUROSCI.1927-05.2005

Matyash, V., Filippov, V., Mohrhagen, K., & Kettenmann, H. (2001). Nitric oxide signals parallel fiber activity to Bergmann glial cells in the mouse cerebellar slice. *Molecular and Cellular Neurosciences*, *18*(6), 664–670. https://doi.org/10.1006/mcne.2001.1047

Mauk, M. D., Medina, J. F., Nores, W. L., & Ohyama, T. (2000). Cerebellar function: Coordination, learning or timing? *Current Biology*, *10*(14), R522–R525. https://doi.org/10.1016/S0960-9822(00)00584-4

Miall, R. C., & Wolpert, D. M. (1996). Forward models for physiological motor control. *Neural Networks*, *9*(8), 1265–1279. https://doi.org/10.1016/S0893-6080(96)00035-4

Micheva, K. D., Busse, B., Weiler, N. C., O'Rourke, N., & Smith, S. J. (2010). Single-synapse analysis of a diverse synapse population: Proteomic imaging methods and markers. *Neuron*, *68*(4), 639–653. https://doi.org/10.1016/j.neuron.2010.09.024

Middleton, F. A., & Strick, P. L. (1994). Anatomical evidence for cerebellar and basal ganglia involvement in higher cognitive function. *Science*, *266*(5184), 458–461. https://doi.org/10.1126/science.7939688

Middleton, Frank A., & Strick, P. L. (1997). Chapter 32 Dentate output channels: Motor and cognitive components. In C. I. De Zeeuw, P. Strata, & J. Voogd (Eds.), *Progress in Brain Research* (pp. 553–566). https://doi.org/10.1016/S0079-6123(08)63386-5

Middleton, Frank A, & Strick, P. L. (1998). Cerebellar output: Motor and cognitive channels. *Trends in Cognitive Sciences*, *2*(9), 348–354. https://doi.org/10.1016/S1364-6613(98)01220-0

Middleton, Frank A., & Strick, P. L. (2001). Cerebellar projections to the prefrontal cortex of the primate. *Journal of Neuroscience*, *21*(2), 700–712. https://doi.org/10.1523/JNEUROSCI.21-02-00700.2001

Miyazaki, T., Yamasaki, M., Hashimoto, K., Kohda, K., Yuzaki, M., Shimamoto, K., … Watanabe, M. (2017). Glutamate transporter GLAST controls synaptic wrapping by Bergmann glia and ensures proper wiring of Purkinje cells. *Proceedings of the National Academy of Sciences*, 201617330. https://doi.org/10.1073/pnas.1617330114

Mottolese, C., Richard, N., Harquel, S., Szathmari, A., Sirigu, A., & Desmurget, M. (2013). Mapping motor representations in the human cerebellum. *Brain*, *136*(1), 330–342. https://doi.org/10.1093/brain/aws186

Müller, T., Möller, T., Neuhaus, J., & Kettenmann, H. (1996). Electrical coupling among Bergmann glial cells and its modulation by glutamate receptor activation. *Glia*, *17*(4), 274–284. https://doi.org/10.1002/(SICI)1098-1136(199608)17:4<274::AID-GLIA2>3.0.CO;2-%23

Nagai, J., Rajbhandari, A.K., Gangawani, M.R., Hachisuka, A., Coppola, G., Masmanidis, S.C., Fanselow, M.S., & Khakh, B.S. (2019). Hyperactivity with disrupted attention by activation of an astrocyte synaptogenic cue. *Cell, 177*(5), 1280-1292.e20 https://doi.org/10.1016/j.cell.2019.03.2019

Ng, H. B. T., Kao, K.-L. C., Chan, Y. C., Chew, E., Chuang, K. H., & Chen, S. H. A. (2016). Modality specificity in the cerebro-cerebellar neurocircuitry during working memory. *Behavioural Brain Research*, *305*, 164–173. https://doi.org/10.1016/j.bbr.2016.02.027

Nimmerjahn, A., Mukamel, E. A., & Schnitzer, M. J. (2009). Motor behavior activates Bergmann glial networks. *Neuron*, *62*(3), 400–412. https://doi.org/10.1016/j.neuron.2009.03.019

Noblett, K. L., & Swain, R. A. (2003). Pretraining enhances recovery from visuospatial deficit following cerebellar dentate nucleus lesion. *Behavioral Neuroscience*, *117*(4), 785–798. https://doi.org/10.1037/0735-7044.117.4.785.

Nopoulos, P. C., Ceilley, J. W., Gailis, E. A., & Andreasen, N. C. (1999). An MRI study of cerebellar vermis morphology in patients with schizophrenia: Evidence in support of the cognitive dysmetria concept. *Biological Psychiatry*, *46*(5), 703–711. https://doi.org/10.1016/S0006-3223(99)00093-1

Okugawa, G., Sedvall, G. C., & Agartz, I. (2003). Smaller cerebellar vermis but not hemisphere volumes in patients with chronic schizophrenia. *American Journal of Psychiatry*, *160*(9), 1614–1617. https://doi.org/10.1176/appi.ajp.160.9.1614

Padmashri, R., Suresh, A., Boska, M. D., & Dunaevsky, A. (2015). Motor-skill learning is dependent on astrocytic activity. *Neural Plasticity, 938023.* https://doi.org/10.1155/2015/938023

Pakaprot, N., Kim, S., & Thompson, R. F. (2009). The role of the cerebellar interpositus nucleus in short and long term memory for trace eyeblink conditioning. *Behavioral Neuroscience*, *123*(1), 54–61. https://doi.org/10.1037/a0014263

Pakhotin, P., & Verkhratsky, A. (2005). Electrical synapses between Bergmann glial cells and Purkinje neurones in rat cerebellar slices. *Molecular and Cellular Neurosciences*, *28*(1), 79–84. https://doi.org/10.1016/j.mcn.2004.08.014

Palay, S.L., & Chan-Palay, V. (1974). *Cerebellar cortex—cytology and organization.* Berlin/Heidelberg, Germany: Springer-Verlag Bergin Heidelberg.

Pardoe, J., & Apps, R. (2002). Structure-function relations of two somatotopically corresponding regions of the rat cerebellar cortex: Olivocortico-nuclear connections. *Cerebellum*, *1*(3), 165. https://doi.org/10.1080/14734220260418402

Park, J.-S., Onodera, T., Nishimura, S., Thompson, R. F., & Itohara, S. (2006). Molecular evidence for two-stage learning and partial laterality in eyeblink conditioning of mice. *Proceedings of the National Academy of Sciences*, *103*(14), 5549–5554. https://doi.org/10.1073/pnas.0601150103

Parker, K. L., Narayanan, N. S., & Andreasen, N. C. (2014). The therapeutic potential of the cerebellum in schizophrenia. *Frontiers in Systems Neuroscience*, *8*. https://doi.org/10.3389/fnsys.2014.00163

Piet, R., & Jahr, C. E. (2007). Glutamatergic and purinergic receptor-mediated calcium transients in Bergmann glial cells. *Journal of Neuroscience*, *27*(15), 4027–4035. https://doi.org/10.1523/JNEUROSCI.0462-07.2007

Pijpers, A., Apps, R., Pardoe, J., Voogd, J., & Ruigrok, T. J. H. (2006). Precise spatial relationships between mossy fibers and climbing fibers in rat cerebellar cortical zones. *Journal of Neuroscience*, *26*(46), 12067–12080. https://doi.org/10.1523/JNEUROSCI.2905-06.2006

Prevosto, V., Graf, W., & Ugolini, G. (2017). The control of eye movements by the cerebellar nuclei: Polysynaptic projections from the fastigial, interpositus posterior and dentate nuclei to lateral rectus motoneurons in primates. *European Journal of Neuroscience*, *45*(12), 1538–1552. https://doi.org/10.1111/ejn.13546

Reeber, S. L., Arancillo, M., & Sillitoe, R. V. (2018). Bergmann glia are patterned into topographic molecular zones in the developing and adult mouse cerebellum. *Cerebellum*, *17*(4), 392–403. https://doi.org/10.1007/s12311-014-0571-6

Rochefort, C., Lefort, J. M., & Rondi-Reig, L. (2013). The cerebellum: A new key structure in the navigation system. *Frontiers in Neural Circuits*, *7*. https://doi.org/10.3389/fncir.2013.00035

Rondi-Reig, L., Paradis, A.-L., Lefort, J. M., Babayan, B. M., & Tobin, C. (2014). How the cerebellum may monitor sensory information for spatial representation. *Frontiers in Systems Neuroscience*, *8*. https://doi.org/10.3389/fnsys.2014.00205

Rosas-Hernández, R., Bastián, Y., Juárez Tello, A., Ramírez-Saíto, Á., Escobar García, D. M., Pozos-Guillén, A., & Mendez, J. A. (2019). AMPA receptors modulate the reorganization of F-actin in Bergmann glia cells through the activation of RhoA. *Journal of Neurochemistry*, *149*(2), 242–254. https://doi.org/10.1111/jnc.14658

Saab, A. S., Neumeyer, A., Jahn, H. M., Cupido, A., Šimek, A. A. M., Boele, H.-J., … Kirchhoff, F. (2012). Bergmann glial AMPA receptors are required for fine motor coordination. *Science*, *337*(6095), 749–753. https://doi.org/10.1126/science.1221140

Sasaki, T., Beppu, K., Tanaka, K. F., Fukazawa, Y., Shigemoto, R., & Matsui, K. (2012). Application of an optogenetic byway for perturbing neuronal activity via glial photostimulation. *Proceedings of the National Academy of Sciences*, *109*(50), 20720–20725. https://doi.org/10.1073/pnas.1213458109

Schmahmann, J. D., MacMore, J., & Vangel, M. (2009). Cerebellar stroke without motor deficit: Clinical evidence for motor and non-motor domains within the human cerebellum. *Neuroscience*, *162*(3), 852–861. https://doi.org/10.1016/j.neuroscience.2009.06.023

Schmahmann, J. D., & Sherman, J. C. (1998). The cerebellar cognitive affective syndrome. *Brain*, *121*(4), 561–579. https://doi.org/10.1093/brain/121.4.561

Schmahmann, Jeremy D. (1998). Dysmetria of thought: Clinical consequences of cerebellar dysfunction on cognition and affect. *Trends in Cognitive Sciences*, *2*(9), 362–371. https://doi.org/10.1016/S1364-6613(98)01218-2

Schmahmann, Jeremy D. (2000). The role of the cerebellum in affect and psychosis. *Journal of Neurolinguistics*, *13*(2), 189–214. https://doi.org/10.1016/S0911-6044(00)00011-7

Schmahmann, Jeremy D. (2019). The cerebellum and cognition. *Neuroscience Letters*, *688*, 62–75. https://doi.org/10.1016/j.neulet.2018.07.005

Schonewille, M., Belmeguenai, A., Koekkoek, S. K., Houtman, S. H., Boele, H. J., van Beugen, B. J., … De Zeeuw, C. I. (2010). Purkinje cell-specific knockout of the protein phosphatase PP2B impairs potentiation and cerebellar motor learning. *Neuron*, *67*(4), 618–628. https://doi.org/10.1016/j.neuron.2010.07.009

Schonewille, Martijn, Gao, Z., Boele, H.-J., Veloz, M. F. V., Amerika, W. E., Simek, A. A. M., … De Zeeuw, C. I. (2011). Reevaluating the role of LTD in cerebellar motor learning. *Neuron*, *70*(1), 43–50. https://doi.org/10.1016/j.neuron.2011.02.044

Shibuki, K., Gomi, H., Chen, L., Bao, S., Kim, J. J., Wakatsuki, H., … Itohara, S. (1996). Deficient cerebellar long-term depression, impaired eyeblink conditioning, and normal motor coordination in GFAP mutant mice. *Neuron*, *16*(3), 587–599. https://doi.org/10.1016/S0896-6273(00)80078-1

Shipman, M. L., & Green, J. T. (2019). Cerebellum and cognition: Does the rodent cerebellum participate in cognitive functions? *Neurobiology of Learning and Memory*. https://doi.org/10.1016/j.nlm.2019.02.006

Sotelo, C. (2015). Molecular layer interneurons of the cerebellum: Developmental and morphological aspects. *Cerebellum*, *14*(5), 534–556. https://doi.org/10.1007/s12311-015-0648-x

Spacek, J. (1985). Three-dimensional analysis of dendritic spines. III. Glial sheath. *Anatomy and Embryology*, *171*(2), 245–252. https://doi.org/10.1007/bf00341419

Stein, J. (2009). Cerebellar forward models to control movement. *The Journal of Physiology*, *587*(Pt 2), 299. https://doi.org/10.1113/jphysiol.2008.167627

Stoodley, C. J. (2012). The cerebellum and cognition: Evidence from functional imaging studies. *Cerebellum*, *11*(2), 352–365. https://doi.org/10.1007/s12311-011-0260-7

Stoodley, C. J., D'Mello, A. M., Ellegood, J., Jakkamsetti, V., Liu, P., Nebel, M. B., … Tsai, P. T. (2017). Altered cerebellar connectivity in autism spectrum disorders and rescue of autism-related behaviors in mice. *Nature Neuroscience*, *20*(12), 1744–1751. https://doi.org/10.1038/s41593-017-0004-1

Stoodley, C. J., & Schmahmann, J. D. (2009). Functional topography in the human cerebellum: A meta-analysis of neuroimaging studies. *NeuroImage*, *44*(2), 489–501. https://doi.org/10.1016/j.neuroimage.2008.08.039

Stoodley, C. J., & Schmahmann, J. D. (2010). Evidence for topographic organization in the cerebellum of motor control versus cognitive and affective processing. *Cortex; a Journal Devoted to the Study of the Nervous System and Behavior*, *46*(7), 831–844. https://doi.org/10.1016/j.cortex.2009.11.008

Stoodley, C. J., Valera, E. M., & Schmahmann, J. D. (2012). Functional topography of the cerebellum for motor and cognitive tasks: An fMRI study. *NeuroImage*, *59*(2), 1560–1570. https://doi.org/10.1016/j.neuroimage.2011.08.065

Strata, P., & Rossi, F. (1998). Plasticity of the olivocerebellar pathway. *Trends in Neurosciences*, *21*(9), 407–413. https://doi.org/10.1016/s0166-2236(98)01305-8

Strata, P. (2009). David Marr's theory of cerebellar learning: 40 years later. *Journal of Physiology*, *587*(Pt 23), 5519–5520. https://doi.org/10.1113/jphysiol.2009.180307

Strata, P., Provini, L., & Redman, S. (2012). On the concept of spinocerebellum. *Proceedings of the National Academy of Sciences*, *109*(11), E622; author reply E623. https://doi.org/10.1073/pnas.1121224109

Strick, P. L., Dum, R. P., & Fiez, J. A. (2009). Cerebellum and nonmotor function. *Annual Review of Neuroscience*, *32*(1), 413–434. https://doi.org/10.1146/annurev.neuro.31.060407.125606

Suzuki, L., Coulon, P., Sabel-Goedknegt, E. H., & Ruigrok, T. J. H. (2012). Organization of cerebral projections to identified cerebellar zones in the posterior cerebellum of the rat. *Journal of Neuroscience*, *32*(32), 10854–10869. https://doi.org/10.1523/JNEUROSCI.0857-12.2012

Swain, R. A., Kerr, A. L., & Thompson, R. F. (2011). The cerebellum: A neural system for the study of reinforcement learning. *Frontiers in Behavioral Neuroscience*, *5*. https://doi.org/10.3389/fnbeh.2011.00008

Takayasu, Y., Iino, M., Kakegawa, W., Maeno, H., Watase, K., Wada, K., … Ozawa, S. (2005). Differential roles of glial and neuronal glutamate transporters in Purkinje cell synapses. *Journal of Neuroscience*, *25*(38), 8788–8793. https://doi.org/10.1523/JNEUROSCI.1020-05.2005

Tiburcio-Félix, R., Escalante-López, M., López-Bayghen, B., Martínez, D., Hernández-Kelly, L. C., Zinker, S., … Ortega, A. (2018). Glutamate-dependent translational control of glutamine synthetase in Bergmann glia cells. *Molecular Neurobiology*, *55*(6), 5202–5209. https://doi.org/10.1007/s12035-017-0756-3

Tucker, L. B., Fu, A. H., & McCabe, J. T. (2016). Performance of male and female C57BL/6J mice on motor and cognitive tasks commonly used in pre-clinical traumatic brain injury research. *Journal of Neurotrauma*, *33*(9), 880–894. https://doi.org/10.1089/neu.2015.3977

Tuscher, J. J., Taxier, L. R., Schalk, J. C., Haertel, J. M., & Frick, K. M. (2019). Chemogenetic suppression of medial prefrontal-dorsal hippocampal interactions prevents estrogenic enhancement of memory consolidation in female mice. *ENeuro*, *6*(2). https://doi.org/10.1523/ENEURO.0451-18.2019

van der Steen, M. C. M., Schwartze, M., Kotz, S. A., & Keller, P. E. (2015). Modeling effects of cerebellar and basal ganglia lesions on adaptation and anticipation during sensorimotor synchronization. *Annals of the New York Academy of Sciences*, *1337*, 101–110. https://doi.org/10.1111/nyas.12628

Van Swearingen, A. E. D., Walker, Q. D., & Kuhn, C. M. (2013). Sex differences in novelty- and psychostimulant-induced behaviors of C57BL/6 mice. *Psychopharmacology*, *225*(3), 707–718. https://doi.org/10.1007/s00213-012-2860-4

Võikar, V., Kõks, S., Vasar, E., & Rauvala, H. (2001). Strain and gender differences in the behavior of mouse lines commonly used in transgenic studies. *Physiology & Behavior*, *72*(1), 271–281. https://doi.org/10.1016/S0031-9384(00)00405-4

Voogd, J. (1969). The importance of fiber connections in the comparative anatomy of the mammalian cerebellum. *Neurology of Cerebellar Evolution and Development,* 493–514.

Voogd, J., Gerrits, N. M., & Ruigrok, T. J. (1996). Organization of the vestibulocerebellum. *Annals of the New York Academy of Sciences*, *781*, 553–579. https://doi.org/10.1111/j.1749-6632.1996.tb15728.x

Voogd, J., & Ruigrok, T. J. H. (1997). Chapter 2 Transverse and longitudinal patterns in the mammalian cerebellum. In C. I. De Zeeuw, P. Strata, & J. Voogd (Eds.), *Progress in Brain Research* (pp. 21–37). https://doi.org/10.1016/S0079-6123(08)63356-7

Voogd, Jan. (2014). What we do not know about cerebellar systems neuroscience. *Frontiers in Systems Neuroscience*, *8*. https://doi.org/10.3389/fnsys.2014.00227

Voogd, Jan, & Glickstein, M. (1998). The anatomy of the cerebellum. *Trends in Cognitive Sciences*, *2*(9), 307–313. https://doi.org/10.1016/S1364-6613(98)01210-8

Voogd, Jan, Pardoe, J., Ruigrok, T. J. H., & Apps, R. (2003). The distribution of climbing and mossy fiber collateral branches from the copula pyramidis and the paramedian lobule: Congruence of climbing fiber cortical zones and the pattern of zebrin banding within the rat cerebellum. *Journal of Neuroscience*, *23*(11), 4645–4656. https://doi.org/10.1523/JNEUROSCI.23-11-04645.2003

Wagner, M. J., Kim, T. H., Savall, J., Schnitzer, M. J., & Luo, L. (2017). Cerebellar granule cells encode the expectation of reward. *Nature*, *544*(7648), 96–100. https://doi.org/10.1038/nature21726

Wagner, J. L., Klintsova, A. Y., Greenough, W. T., & Goodlett, C. R. (2013). Rehabilitation training using complex motor learning rescues deficits in eyeblink classical conditioning in female rats induced by binge-like neonatal alcohol exposure. *Alcoholism, Clinical and Experimental Research*, *37*(9), 1561–1570. https://doi.org/10.1111/acer.12122

Wang, F., Xu, Q., Wang, W., Takano, T., & Nedergaard, M. (2012). Bergmann glia modulate cerebellar Purkinje cell bistability via Ca2+-dependent K+ uptake. *Proceedings of the National Academy of Sciences*, *109*(20), 7911–7916. https://doi.org/10.1073/pnas.1120380109

Whiting, B. A., & Barton, R. A. (2003). The evolution of the cortico-cerebellar complex in primates: Anatomical connections predict patterns of correlated evolution. *Journal of Human Evolution*, *44*(1), 3–10. https://doi.org/10.1016/s0047-2484(02)00162-8

Yamada, K., Fukaya, M., Shibata, T., Kurihara, H., Tanaka, K., Inoue, Y., & Watanabe, M. (2000). Dynamic transformation of Bergmann glial fibers proceeds in correlation with dendritic outgrowth and synapse formation of cerebellar Purkinje cells. *Journal of Comparative Neurology*, *418*(1), 106–120. https://doi.org/10.1002/(SICI)1096-9861(20000228)418:1<106::AID-CNE8>3.0.CO;2-N

Yang, L., Qi, Y., & Yang, Y. (2015). Astrocytes control food intake by inhibiting AGRP neuron activity via adenosine A1 receptors. *Cell Reports*, *11*(5), 798–807. https://doi.org/10.1016/j.celrep.2015.04.002

Yu, X., Nagai, J., Marti-Solano, M., Soto, J.S., Coppola, G., Madan Babu, M., & Khakh, B.S. (2020). Context-specific striatal astrocyte molecular responses are phenotypically exploitable. *Neuron,* In Press. https://doi.org/10.1016/j.neuron.2020.09.021

Zang, Y., & De Schutter, E. (2019). Climbing fibers provide graded error signals in cerebellar learning. *Frontiers in Systems Neuroscience*, *13*. https://doi.org/10.3389/fnsys.2019.00046

Zepeda, R. C., Barrera, I., Castelán, F., Suárez-Pozos, E., Melgarejo, Y., González-Mejia, E., … Ortega, A. (2009). Glutamate-dependent phosphorylation of the mammalian target of rapamycin (mTOR) in Bergmann glial cells. *Neurochemistry International*, *55*(5), 282–287. https://doi.org/10.1016/j.neuint.2009.03.011

Zhang, X.-Y., Wang, J.-J., & Zhu, J.-N. (2016). Cerebellar fastigial nucleus: From anatomic construction to physiological functions. *Cerebellum & Ataxias*, *3*. https://doi.org/10.1186/s40673-016-0047-1

Zhou, H., Lin, Z., Voges, K., Ju, C., Gao, Z., Bosman, L. W., … Schonewille, M. (2014). Cerebellar modules operate at different frequencies. *ELife*, *3*, e02536. https://doi.org/10.7554/eLife.02536

MORGAN E. STEVENSON
Curriculum Vitae

EDUCATION

Ph.D. *Expected:* December 2020
University of Wisconsin- Milwaukee
Experimental Psychology (Neuroscience)
Advisor: Rodney A. Swain, Ph.D.
Dissertation: The role of cerebellar structural plasticity and astrocytic activity in motor-skill learning.

M.S.
December 2016
University of Wisconsin- Milwaukee
Experimental Psychology (Neuroscience)
Advisor: Rodney A. Swain, Ph.D.
Thesis: The effects of exercise pattern and intensity on Flk-1 and Flt-1 expression in the hippocampus and cerebellum.

B.A.
May 2012
Wartburg College
Major: Psychology
Minors: Biology, Leadership
Graduated *Magna Cum Laude*
Capstone*:* The role of emotion and learning in facial recognition.

HONORS AND AWARDS

R1 Distinguished Dissertation Fellowship, University of Wisconsin-Milwaukee, 2020
Distinguished Dissertation Fellowship, University of Wisconsin-Milwaukee, 2019
UWM Association for Graduate Students in Psychology Travel Grant, 2018
UWM Graduate Student Excellence Fellowship, 2018
Sigma Xi Grant-in-Aid of Research, 2018
Sigma Xi Grant-in-Aid of Research, 2017
Departmental Summer Fellowship, University of Wisconsin- Milwaukee, 2017
Distinguished Graduate Student Fellowship, University of Wisconsin- Milwaukee, 2017
Graduate Student Travel Award, University of Wisconsin- Milwaukee, 2016 & 2018
Chancellor's Graduate Student Award, University of Wisconsin- Milwaukee, 2014 & 2015
John and Lynn Schiek Stipend Recipient, University of Wisconsin- Milwaukee, 2013
Who's Who Among American College Students, Inducted 2012
Psi Chi Honor Society, Inducted 2011
Regents Scholar, Wartburg College, 2008- 2012
Dean's List, Wartburg College, 2009-2012

PUBLICATIONS

Stevenson, M.E., Behnke, V.B., & Swain, R.A. (2018). Exercise pattern and distance differentially affect hippocampal and cerebellar expression of FLK-1 and FLT-1 receptors in astrocytes and blood vessels. *Behavioural Brain Research*, *337*, 8-16. doi:10.1016/j.bbr.2017.09.037

Behnke, V.B., **Stevenson, M.E.**, & Swain, R.A. (2018). Inactivation of the cerebellar fastigial nuclei alters social behavior in the rat. *Behavioral Neuroscience, 132*(6), 552-560. doi:10.1037/bne0000256

Stevenson, M.E., Lensmire, N.L., & Swain, R.A. (2018). Astrocytes and radial glia-like cells, but not neurons, display a non-apoptotic increase in caspase-3 expression following exercise. *Brain and Behavior, 8*(10), e01110. doi:10.1002/brb2/1110

Zhang, Q., Lee, S.B., Chen, X., **Stevenson, M.E.**, Pan, J., Zhou, Y., Miller, M., Lubet, R., Wang, Y., Mirza, S., & You, M. (2019). Optimized bexarotene aerosol formulation inhibits major subtypes of lung cancer in mice. *Nano Letters, 19*(4), 2231-2241. doi:10.1021/acs.nanolett.8b04309

Stevenson, M.E, Kay, J.J.M., Atry, F., Wickstrom, A.T., Krueger, J.R., Pashaie, R.E., & Swain, R.A. (2020). Wheel running for 26 weeks is associated with sustained vascular plasticity in the rat motor cortex. *Behavioural Brain Research, 380*, 112447, doi:10.1016/j.bbr.2019.112447

Stevenson, M.E., Miller, C.C., Owen, H.A., & Swain, R.A. (2020). Aerobic exercise increases sprouting angiogenesis in the male rat motor cortex. *Brain Structure and Function, 225,* 2301-2314. doi:10.1007/s00429-020-02100-y

Stevenson, M.E., Nazario, A.S., Czyz, A.M., Owen, H.A., Swain, R.A. (In Press). Motor learning rapidly increases synaptogenesis and astrocytic structural plasticity in the rat cerebellum. *Neurobiology of Learning and Memory.* doi:10.1016/j.nlm.2020.107339

Research in Progress

Stevenson, M.E., Taxier, L.R., Czyz, A.M., Owen, H.A., & Swain, R.A. The behavioral and structural contributions of cerebellar astrocytes to motor behavior.
Description: This study will determine whether cerebellar astrocytes contribute to motor-skill learning by using chemogenetic techniques (DREADDs) to disrupt astrocytic activity while rats train on a complex acrobatic course. Astrocytic involvement in synaptogenesis will be assessed.

Nazario, A.S., **Stevenson, M.E**., Lensmire, N.L., & Swain, R.A. Deep cerebellar nuclei contributions to deficits in motivated responding on an operant conditioning task using a rat model of ADHD.
Description: This study aims to elucidate whether abnormalities in the deep cerebellar nuclei contribute to deficits in motivation on an operant conditioning task, in a rat model of ADHD.

PRESENTATIONS

Stevenson, M.E., Behnke, V.K., Swain, R.A. (March, 2016). *The effects of exercise pattern and intensity on Flk-1 and Flt-1 expression in the hippocampus.* Poster presented at the Mini-Neuroscience Symposium at the University of Wisconsin-Milwaukee, Milwaukee, WI.

Behnke, V.K., **Stevenson, M.E**., Hobson H.E., Beltrone, V.G., & Nazario, A. (November, 2016). *The effects of fastigial nuclei inactivation on social behavior in the rat.* Poster presented at the Society for Neuroscience annual meeting in San Diego, CA.

Stevenson, M.E., Behnke, V.K., Hobson, H.E., Beltrone, V.G., & Swain, R.A. (November, 2016). *The effects of exercise pattern and intensity on Flk-1 and Flt-1 expression in the hippocampus.* Poster presented at the Society for Neuroscience annual meeting in San Diego, CA.

Stevenson, M.E. & Swain, R.A. (March, 2017). *Exercise-induced apoptotic cell death in the hippocampus.* Poster presented at the Mini-Neuroscience Symposium at the University of Wisconsin-Milwaukee, Milwaukee, WI.

Stevenson, M.E. (March, 2017). *Brain angiogenesis and exercise.* Invited guest lecture at Wartburg College, Waverly, IA.

Nazario, A.S., Lensmire, N.L., **Stevenson, M.E.**, & Swain, R.A. (March, 2017). *The effects of exercise sequence on learning and memory.* Poster presented at the chapter Society for Neuroscience annual meeting in Chicago, IL.

Stevenson, M.E. & Swain, R.A. (March, 2017). *Exercise-induced apoptotic cell death in the hippocampus.* Poster presented at the chapter Society for Neuroscience annual meeting, Chicago, IL.

Guthrie, M.L., Zahn, N., Li, G., Kodali, R., Forkuo, G., **Stevenson, M.E.**, Mirza, S., Cook, J.M., Stafford, D., & Arnold, L.A. (September, 2017). *Imaging the distribution of selective $GABA_A$ receptor modulators in the asthmatic lung using MALDI assisted mass spectrometry.* Poster presented at the UW System Faculty Meeting at the University of Wisconsin-Milwaukee, Milwaukee, WI.

Guthrie, M.L., Zahn, N., Li, G., Kodali, R., Forkuo, G., **Stevenson, M.E.**, Mirza, S., Cook, J.M., Stafford, D., & Arnold, L.A. (April, 2017). *Imaging the distribution of selective $GABA_A$ receptor modulators in the asthmatic lung using MALDI assisted mass spectrometry.* Poster presented at the 253rd American Chemical Society national meeting, San Francisco, CA.

Guthrie, M.L., Zahn, N., Li, G., Kodali, R., Forkuo, G., **Stevenson, M.E.**, Mirza, S., Cook, J.M., Stafford, D., & Arnold, L.A. (May, 2017). *Imaging the distribution of selective $GABA_A$ receptor modulators in the asthmatic lung using MALDI assisted mass spectrometry.* Poster presented at the Chemistry and Biochemistry Research Symposium at the University of Wisconsin-Milwaukee, Milwaukee, WI.

Stevenson, M.E. (April, 2017). *The effects of exercise pattern and intensity on angiogenesis in the cerebellum.* Presented at the Association of Graduate Students in Psychology's 19th Annual Research Symposium at the University of Wisconsin-Milwaukee, Milwaukee, WI.

Stevenson, M.E. & Swain, R.A. (November, 2017). *Exercise-induced caspase-3 expression (apoptotic cell death) in the hippocampus.* Poster presented at the Society for Neuroscience annual meeting in Washington, DC.

Stevenson, M.E. (April, 2018). *Exercise-induced caspase-3 expression in the hippocampus.* Selected in abstract competition for oral presentation at the 2018 Neuroscience Research Symposium at the University of Wisconsin-Milwaukee, Milwaukee, WI.

Stevenson, M.E., Lensmire, N.L., & Swain R.A. (November, 2018). *Exercise-induced caspase-3 expression in the hippocampus.* Poster presented at the Society for Neuroscience annual meeting in San Diego, CA.

Stevenson, M.E., Mirza, S.P., & Swain, R.A. (January, 2019). *Deciphering markers of exercise-induced brain plasticity using MALDI-TOF IMS.* Poster presented at the Milwaukee Analytical Chemistry Conference, Milwaukee, WI.

Stevenson, M.E. (March, 2019). *The effects of exercise on vascular morphology in the rat primary motor cortex.* Presented at the 2019 Neuroscience Research Symposium at the University of Wisconsin-Milwaukee, Milwaukee, WI.

Stevenson, M.E. (April, 2019). *The effects of exercise on vascular morphology in the rat primary motor cortex.* Presented at the Association of Graduate Students in Psychology's 21st Annual Research Symposium at the University of Wisconsin-Milwaukee, Milwaukee, WI.

Stevenson, M.E., Miller, C.C., Nazario, A.S., Larsen, B.S., Greenberg, Y.S., Owen, H.A., & Swain, R.A. (October, 2019). *Three-dimensional imaging reveals exercise-induced alteration of vascular morphology in the rat primary motor cortex.* Poster presented at the Society for Neuroscience annual meeting in Chicago, IL.

Nazario, A.S., **Stevenson, M.E.**, Greenberg, Y.S., Larson, B.L., Miller, C.C., & Swain, R.A. (October, 2019). *Motivation is deficient in the spontaneously hypertensive rat (SHR), a rodent model of ADHD: Evidence from an operant breakpoint paradigm.* Poster presented at the Society for Neuroscience annual meeting in Chicago, IL.

LABORATORY SKILLS

Cryosectioning, Stereology, Immunohistochemistry, Immunofluorescence, MALDI-TOF mass spectrometry, Stereotaxic surgery and viral infusion, Behavioral training and testing, Scanning and transmission electron microscopy

PROFESSIONAL EXPERIENCE

Teaching Assistant
University of Wisconsin- Milwaukee, Milwaukee, WI, Fall 2014- Spring 2017; Fall 2018- Spring 2019
Courses taught include: Social Psychology, Experimental Social Psychology, Physiological Psychology, and Psychological Statistics

PROFESSIONAL AFFILIATIONS

American Psychological Association (Student Affiliate), 2013- Present
Society for Neuroscience (Student Member), 2015- Present

CIVIC ENGAGEMENT AND LEADERSHIP

Co-Organizer, Glia Journal Club
University of Wisconsin-Milwaukee, Milwaukee, WI, September 2019- Present
Description: Select papers and co-lead monthly meetings focused on discussing all aspects of glial neurobiology.

Treasurer**,** Association of Graduate Students in Psychology (AGSIP)
University of Wisconsin-Milwaukee, Milwaukee, WI, September 2014- May 2017
Description: Managed funds, wrote grant proposals, organized annual symposium.

ADDITIONAL TRAINING

Advanced Mass Spectrometry (AIMS)
Vanderbilt University, Nashville, TN, September 28- October 2, 2015
Description: This short course provided hands-on workshops focused on MALDI imaging, including demonstration of sample preparation and instrumentation.